

**THE PRESERVATION, DISTRIBUTION, AND DETECTABILITY OF
LIPID BIOMARKERS IN THE ATACAMA DESERT AND
IMPLICATIONS FOR MARS**

A Dissertation
Presented to
The Academic Faculty

By

Mary Beth Wilhelm

In Partial Fulfillment
of the Requirements for the Degree
Doctor of Philosophy in the
School of Earth and Atmospheric Sciences

Georgia Institute of Technology

August 2017

Copyright © Mary Beth Wilhelm 2017

THE PRESERVATION, DISTRIBUTION, AND DETECTABILITY OF
LIPID BIOMARKERS IN THE ATACAMA DESERT AND
IMPLICATIONS FOR MARS

Approved by:

Dr. James J. Wray, Advisor
School of Earth and Atmospheric
Sciences
Georgia Institute of Technology

Dr. Eric Gaucher
School of Biological Sciences
Georgia Institute of Technology

Dr. Amanda Stockton
School of Chemistry and Bio-
chemistry
Georgia Institute of Technology

Dr. Britney E. Schmidt
School of Earth and Atmospheric
Sciences
Georgia Institute of Technology

Dr. Roger E. Summons
Department of Earth, Atmo-
spheric and Planetary Sciences
*Massachusetts Institute of Tech-
nology*

Date Approved: June 20, 2017

“The desert could not be claimed or owned—it was a piece of cloth carried by winds, never held down by stones, and given a hundred shifting names...”

Michael Ondaatje

“ ‘This desert,’ Scott had told me, ‘is two hundred million years old and the Earth is four and a half billion years old and me... I’m thirty.’ ”

Ariel Dorfman

This dissertation is dedicated to my grandmothers, Mary Paun Inglese and Bernice Wilhelm, two of the strongest people I have ever known. Their vision set my family on the trajectory toward the pursuit of higher education. For Mary, who always encouraged me to “feed your brain,” to read, and to believe in my dreams. And for Bernice, who taught me the value of having a sense of humor, especially in the face of hardship.

ACKNOWLEDGEMENTS

The work presented here would not have been possible without the generous support of mentors and collaborators at Georgia Tech, NASA, MIT, and CAB.

I would like to thank my advisor, James Wray, for his unwavering advocacy, absolute optimism about my future, and for providing me a platform on which I was encouraged to pursue the research topics of greatest interest to me. I look forward to sharing ideas and new discoveries with him in the long careers that lie ahead of us. I was happy to share in his inspiration and vision over the past five years, and will always be glad to share a heritage (Cornell and Georgia Tech) with him.

At MIT, I benefitted greatly from the support of Roger Summons and his excellent team of lipid experts, especially Xiao-Lei Liu and Shane O'Reilly. I thank him and his team for welcoming me into their laboratory and collaborating on the lipid preservation work presented in Chapter 3.

At NASA Ames Research Center, there are many people who have greatly supported me and my graduate work. Firstly, I would like to thank Niki Parenteau for the numerous hours she spent in training me in laboratory techniques and analysis, discussing project results, and providing excellent feedback on writing. She has helped to shape me into the scientist I am today and taught me the power of patience and constructive scientific skepticism. Linda Jahnke is truly one of the most incredible scientists I know, and I appreciate the time she took to help me develop techniques for lipid extraction in spite of challenging samples, for broadening my perspective on the utility of lipid biomarkers, and welcoming me into her laboratory group. I am grateful to Alfonso Davila for including me on his field expeditions to the Atacama, arming me with the contextual environmental information related to my dissertation work, providing me with the opportunity to collaborate internationally, and for helping me shape my results into a compelling story relevant to the Atacama and beyond.

Thanks to George Cooper, Mastewal Abate, and Taylor Kelly for sharing their technical expertise, especially related to amino acid analyses. And a special thanks to my NASA supervisor, Jeff Hollingsworth for supporting me throughout my graduate career and helping me to navigate the beginning of my career at NASA ARC. I would also like to thank John Karcz, Yvonne Ibarra, Tim Lee, Sandra Owen, Carol Stoker, Chris McKay, Darryl Waller, Dale Andersen for their support throughout my graduate career. I could not ask for a better sounding board.

At NASA Goddard Space Flight Center, I would like to thank Jennifer Eigenbrode for her mentorship and technical training. I feel indebted to her for support and advice at a time when I felt discouraged. I hope that someday I will be able to provide the same opportunities that she gave to me to another student. I appreciate her support on all three chapters of my dissertation: helping to provide supplies and guidance for sampling, training and access to instrumentation, and providing critical feedback on manuscripts.

At the Centro de Astrobiología, I thank Victor Parro García, Miriam García-Villadangos, Juan Manuel Manchado, Antonio Sansano Caramazana, and Aurelio Sanz Arranz for their support. I am grateful for the opportunity to work with them and use future Mars flight instrumentation at their incredible facilities.

At Georgia Tech, I am grateful for the support and camaraderie with fellow graduate students Luju Ojha and George McDonald. I am also appreciative of the help that Eric Gaucher gave me at the beginning of my graduate education in helping me to steer my career in the direction of greatest interest to me.

There are a few others I would like to thank for their input, feedback, field assistance, and guidance on dissertation work including Brian Stamos (Ch. 3), Amy Williams (Ch. 3), Raechel Harnoto (Ch. 2), Terry Jordan (Ch. 3), Paul Mahaffy (Ch. 3), Pablo Sobron (Ch. 4), Richard Quinn (Ch. 4), Andy Mattioda (Ch. 4), Tori Hoehler (Ch. 2) Brian Glass (Ch. 2), Kimberly Warren-Rhodes (Ch. 2), Carolyn

Colonero (Ch. 3), Jonathan Garca Araya (Ch. 2 and 3), Jocelyne DiRugierro (Ch. 2), Beth Shapiro, and Ruth Nichols.

I would like to acknowledge my very first mentors Jennifer Heldmann, Max Bernstein, and Yvonne Pendleton for their continued support over the last decade. I feel extremely lucky to have first learned about astrobiology and space science through their perspectives and for the opportunities that they gave me, especially early on in my career. I am happy to still call them my mentors.

This work was supported primarily by the National Science Foundation Graduate Research Fellowship Program under Grant No. DGE-1148903. Additional support was provided by the NASA Pathways Program, a 2016 P.E.O. International Scholar Award, a 2015 and 2016 NASA Mars Exploration Program Student Travel Grant, a 2014 NASA Astrobiology Institute Early Career Collaboration Award, a 2013 Lunar and Planetary Institute Career Development Award, a 2012-2015 Georgia Tech President's Fellowship. Other programmatic support was provided by a 2016 NASA Ames Science Innovation Fund (SIF), a 2015 NASA Astrobiology Institute Director's Discretionary Fund (DDF), the ARADS project under NASA's Planetary Science and Technology from Analog Research (PSTAR) program, and a Spanish Ministry of Economy and Competitiveness (MINECO) grant No. ESP2015-69540-R.

Finally, but most importantly, I thank my family. To my parents, Clarence and Amy Wilhelm for their guidance, love, and eternal support, my little sisters, Sarah and Rachel Wilhelm, without whom I would never feel whole, and my godparents Sandra Johnson and Curt Wilhelm for their encouragement along my path. My family has given me the greatest gift of all, the foundation on which I am able to pursue my dreams, and for that I am truly grateful.

TABLE OF CONTENTS

Acknowledgments	v
List of Tables	xii
List of Figures	xiii
Chapter 1: Introduction and Background	1
1.1 Biomarkers: Preservation Pathways and Survival in the Terrestrial Fossil Record	1
1.2 Planetary Analog Research	4
1.3 The Yungay Region of the Atacama Desert: Hyperaridity, Age, Soil Properties, and Aridity Gradient	6
1.4 Scope of Dissertation	10
1.4.1 Chapter 2	10
1.4.2 Chapter 3	11
1.4.3 Chapter 4	12
1.4.4 Chapter 5	13
Chapter 2: Declining Trends of Microbial Activity in Atacama Desert Soils with Increasing Dryness Inferred from Biomarker Content	14
2.1 Introduction	14

2.2	Biomarker Proxies for Metabolic Activity	16
2.3	Field Site	17
2.4	Methods	18
2.4.1	Sample Collection	18
2.4.2	Lipid Extractions and Analysis	20
2.4.3	Monounsaturated Fatty Acid Double-Bond Position and Cyclo- propane Fatty Acid Determination	22
2.4.4	Bound Amino Acid Extraction and Analysis	22
2.4.5	Immunoassays	24
2.5	Results	25
2.5.1	Lipids and Amino Acids	25
2.5.2	LDChip Immunoassay	27
2.6	Discussion	27
2.7	Conclusion	34
 Chapter 3: Xeropreservation of Functionalized Lipid Biomarkers in Hyperarid Soils in the Atacama Desert		 40
3.1	Introduction	40
3.1.1	Study Site	41
3.2	Methods	43
3.2.1	Sample Collection	43
3.2.2	Lipid Analyses	44
3.2.3	Anion Analysis	47
3.3	Results	48

3.4	Discussion	59
3.4.1	Anion Distribution with Depth in Yungay	59
3.4.2	Biomarker Preservation Under Prolonged Hyperarid Conditions	60
3.4.3	Microbial Diversiy and Paleoenvironmental Reconstruction Based on Lipid Biomarkers	64
Chapter 4: Detectability of Lipid Biomarkers in Atacama Soils by Mars Flight Instrumentation: Raman Spectroscopy and Evolved Gas Analysis		69
4.1	Critical Assessment of Biomarker Detection with Raman Laser Spec- troscopy on Biomass-Poor Soils	70
4.1.1	Introduction	70
4.1.2	Methods	72
4.1.3	Results and Discussion	75
4.1.4	Conclusion	83
4.2	Organic Ions Detected in Yungay Soils through Evolved Gas Analysis (EGA) Despite Low Biomass Abundance and Perchlorate Presence	83
4.2.1	Introduction	83
4.2.2	Methods	86
4.2.3	Results and Discussion	87
4.2.4	Conclusion	92
Chapter 5: Conclusions and Implications for Mars		95
5.1	Future Work	97
References		116

Vita	117
-----------------------	------------

LIST OF TABLES

3.1	Free Fatty Acids in Yungay Pit Soils Detected through Derivatization with a Silylation Agent (ng free fatty acid/ g of sample): Note these values do not represent the total amount of free fatty acid present in the soils, but instead reflects free fatty acids that remained after acid methanolysis. Some of the FAME content is comprised of what were free fatty acids prior to analysis. N.d. is not detected.	50
3.2	Monohydroxy Monocarboxylic Fatty Acids in Yungay Pit Soils in ng hydroxy fatty acid per g sample N.d. is not detected. . . .	52
3.3	Saturated α- ω- Dicarboxylic Fatty Acids in Yungay Pit Soils in ng DCA per g sample N.d. is not detected. DCAs not detected in samples analyzed from units above 100 cm	55
3.4	The occurrence of glycerol tetraethers (GDGTs) in Yungay Pit Soils (pg GDGT per g sample).	57
4.1	Table of organic byproducts released via EGA and typical m/z values from common biomolecules based off of Valdivia-Silva et al., (2009); Navarro-González et al. (2003); Simmonds et al., (1969), but is not an exhaustive list of byproducts.	85

LIST OF FIGURES

1.1	Flow chart of the typical pathway of biomarker preservation from living organism through early degradation processes to incorporation into the geological record. The focuses of the three thesis chapters are highlighted in yellow.	5
1.2	Map of the driest region in the Atacama Desert from 22°S to 26°S. Study sites shown with stars.	8
1.3	Panoramic photo of study site in the Yungay region showing general lack of colonization by macroscopic organisms. The soil pit (discussed in Chapter 3), in the right-center part of the photograph, is about 1 meter across.	10
2.1	Changes in biomarker content and aridity are plotted with latitude. A. Map of the Atacama Desert with soil sites marked with stars. B. Annual precipitation values are written at latitudinal locations. Red color indicates region experiencing only mm-decadal rain events, Orange and yellow indicates regions that receive 5-10 mm precip./yr. Based on Navarro-González et al., (2003). C. Aridity Index values,(AI), mean annual precipitation/potential evapotranspiration. This entire region, with AI <0.05 is hyperarid. D. The total LDChip antibody microarray florescence of proteins and peptides, the sum of florescence of 242 spots. E. Total number of unique fatty acids 12-30 carbons (normal and saturated, dicarboxylic, branched, and unsaturated fatty acids), a proxy for organism diversity. F. The total concentration of normal, saturated FAMES n -C _{12:0} - n -C _{30:0} . Values indicate the amount of common membrane lipids of living, dormant, and dead organisms. G. Cyclopropane fatty acids (CFA) were only detected in Altamira and Chaaral soils. Values of 0 at the drier sites indicate that CFAs were not detected. The presence of CFA indicates membrane modulation under stress, and thus metabolic activity. H. D/L ratios of aspartic acid from hydrolyzed proteins, peptides, and humic complexes. Increased racemization indicates that organic material is older.	19

2.2	Ratio of <i>Trans</i>/<i>Cis</i> Confirmation of the Double Bond of Unsaturated Fatty Acid $n\text{-C}_{16:1\Delta 9}$ in Atacama Soils Along Aridity Transect. The unsaturated fatty acid $n\text{-C}_{16:1\Delta 9}$ was the only unsaturated fatty acid in detected in all Atacama samples in which both <i>cis</i> and <i>trans</i> isomers of the double bond on C ₉ were present. The ratio of <i>trans</i> to <i>cis</i> for $n\text{-C}_{16:1\Delta 9}$ was found to decrease with increasing dryness. Bacteria modulate membrane fluidity in response to environmental stressors by converting the <i>cis</i> isomer to <i>trans</i> . Although we might expect this ratio to decrease with increasing dryness, the opposite is observed, perhaps indicating a lack of detectable metabolic activity in the driest soils along the transect.	29
2.3	Normal Monounsaturated Fatty Acid and Bond Position Detected in Transect Samples.	33
2.4	Total Number of Unique Fatty Acids Detected in Atacama Soils Along Aridity Transect. A positive linear correlation is found between the total number of unique fatty acids and aridity index. The number of unique fatty acids in soils decreases approximately 3 times with an order of magnitude decline in aridity index value. Fatty acids containing 12-30 carbons including normal and saturated, dicarboxylic, branched, multi-branched, mono and polyunsaturated fatty acids are included in this total number, and can be used as a proxy for diversity of organisms contained within the soil.	35

- 2.5 **Immunoprofiling the aridity gradient in Atacama Soils with LDChip.** Each antibody on the plot is represented by the 3 bars obtained by quantifying the fluorescence of spots on LDChip. Different compounds in the samples reacted with the antibodies on the chip produced the following immunogens: 1, *Leptospirillum ferrooxidans*; 2, 3, *Acidithiobacillus ferrooxidans*; 4, *Halothiobacillus neapolitanus*; 5, *Tumebacillus* sp.; 6, *Planococcus*; 7, *Psychroserpens burtonensis*; 8, *Pyrococcus furiosus*; 9, *Synechocystis* sp.; 10, *Dechloromonas aromatica*; 11, DhnaA, fructose-bisphosphate aldolase from cyanobacteria. Dehydrin protein related with plants and induced under dessication stress; 12, FdhF, formate dehydrogenase H; 13, HtpG, the heat shock protein HtpG, which is a homolog of HSP90, is essential for basal and acquired thermotolerances in cyanobacteria. HtpG is involved in the acclimation to low temperatures in cyanobacteria; 14, IsiA, photosystem II chlorophyll a-binding protein induced under desiccation in cyanobacteria; 15, PhaC1 and PhaC2, class II poly(R)-hydroxyalkanoic acid synthase. Polyhydroxyalkanoate (PHA) synthase genes C1 and C2 from *Pseudomonas putida*. PHAs are produced under nutrient limitations as N and P; 16, PufM, which encodes the M subunit of the photosynthetic reaction centers of most known anoxygenic phototrophs as *Rhodospirillum rubrum*; 17, SodA, SodF, Iron superoxide dismutase involved in desiccation resistance in *Nostoc*; 18, WshR, water stress hypersensitive response protein *Pseudomonas*; 19, Bacterial ferritin; 20, Cells from iron/sulfur environment; 21, *Acidocella aminolytica*; 22, *Sulfobacillus acidophilus*; 23, *Salinibacter ruber*; 24, *Streptomyces* sp.; 25, *Shewanella oneidensis*; 26, *Bacillus subtilis*; 27, *Haloferax mediterranei*; 28, *Anabaena* type strain; 28+, Other cyanobacteria as *Chroococcidiopsis* sp.; 29, 29+, Peptidoglycan (2 Mabs); 30, Perchlorate reductase; 31, Iron reductase; 32, *P. furiosus* ferritin; 33, *Psychrobacter frigidicola*; 34, *Streptomyces* spores; 35, *Desulfosporosinus meridiei*; 36, *Azotobacter vinelandii*; 37, *Halorubrum* sp.; 38, OppA transporter component. . . 36
- 2.6 **Proteins Indicated by LD Chip in Atacama Soils Along Aridity Transect.** Only 8 proteins out of 73 screened for were detected in all hyperarid Atacama soils analyzed by the LDChip immunoassay. In general, these proteins are synthesized under physiological stressful conditions such as nutrient limitation, desiccation, oxidative stress, high temperature, and irradiation. Protein names and functions are included in the Discussion. These 8 proteins were found to decrease in abundance by a factor of 2-13 with increasing dryness along the aridity transect from Chañaral soils to Yungay. The florescence intensity plotted is the average of three spots on the LDChip. 37

2.7	Conceptual Figure Showing Differences in Biomarker Content of Soils Under Increasingly Dry Conditions. Key differences are observed in soils biomarker content along the Atacama's aridity transect including lipids, amino acid racemization, and peptides (this paper), and hypolithic colonization (Warren-Rhodes et al., 2006) that suggest that biological activity may not be occurring or negligible in the driest soils. In light of these differences, we propose a new ecoregion demarcation (Olson et al., 2001) and suggest that it's warranted to reflect the biological inactivity of soils that is imposed by extreme hyperaridity.	39
3.1	Yungay Soil Pit Stratigraphy and Key Lipid Abundances: a) The soil pit contains three major units: gypsiferous soils (0-90 cm depth), clay-rich units (> 90 cm depth), and a 10 cm-thick halite unit that interrupts clay units at 150 cm depth. Gypsiferous soils are matrix-supported and contain angular lithics. A clay unit at 100 cm depth contains centimeter-sized laminations composed of coarse sand. A clay unit at 140 cm depth contains fine sub-cm sized laminations (Fig. 3.6). The massive, well-cemented halite unit (~140-150 cm) has two major morphologies: vertical, crystalline structures and mottled halite. Beneath are alternating bands of well-sorted clay units and contain fibrous plant fragments (cm-size) that become more concentrated with depth. A more detailed description of the stratigraphic profile is provided by (Ewing et al., 2006; 2008). b, c, d) Total abundances of FAME, DCA, and Isoprenoidal GDGT were found to increase with depth with the exception of the halite unit (150 cm). Isoprenoidal GDGT and DCA were absent from upper gypsiferous soil. Isoprenoidal GDGTs are plotted on a logarithmic scale due to the presence of a high relative abundance of Archaeol in the halite unit.	49
3.2	Fatty Acid Methyl Ester (FAME) Profiles for Representative Yungay Pit Samples: Upper gypsiferous soils were dominated by <i>n</i> -C _{16:0} and <i>n</i> -C _{18:0} FAMES. On the other hand, clay units were dominated by <i>n</i> -C _{22:0} and greater chain length FAMES and contain a greater diversity in FAME content. The deepest clay unit had the greatest total FAME abundance. The well-cemented halite unit was dominated by <i>n</i> -C _{16:0} and <i>n</i> -C _{18:0} FAMES. The vertical scale changes between plots.	51
3.3	<i>n</i>-Alkane Content in Yungay Pit Soils: The straight chain <i>n</i> -alkane content of Yungay soils reveals two distinct patterns. Clay rich units exhibit an odd-over-even chain length preference. Conversely, gypsiferous soils and the halite unit exhibit a slight even-over-odd chain length preference.	53

3.4	Glycerol Ether Lipids Detected in Atacama Samples: Glycerol ether lipids detected in the Atacama samples. Archaeol and C20-C25 extended archaeol are archaeal diethers. Isoprenoidal and branched GDGTs are archaeal and bacterial tetraethers, respectively.	56
3.5	Anion Profiles in the Yungay Soil Column: Anion profiles of chloride, perchlorate, nitrate and sulfate with depth in the Yungay. The point at 150 cm was taken from the massive, well-cemented halite unit.	58
3.6	Finely Laminated Soil Unit at 140 cm depth: Image of a perchlorate and nitrate-rich soil unit located at 140 cm depth, 10 cm above the massive, well-cemented halite unit. This unit is comprised of silt to fine sand-sized particles that form undisrupted, fine sub-cm sized laminations and contains cm-sized voids. Such laminations are diagnostic of quiescent deposition in a sustained aqueous environment, such as a perennial pond.	61
3.7	Centimeter-Sized Fragments of Fibrous Plant Material Found at 215 cm Depth: An image taken of sample collected from the unit at 215 cm. The arrow points to one of the fibrous cm-sized plant fragments present interspersed throughout this unit, and a likely source for some of the plant lipid biomarkers detected.	66
4.1	RLS spectra of four fatty acid standards.	76
4.2	RLS spectra of two geolipid standards.	77
4.3	RLS spectra of one pure alkane and two alkane mixtures.	78
4.4	RLS spectra of five polycyclic aromatic hydrocarbon standards with various configurations and number of rings.	79
4.5	RLS spectra of 10 points along a surface soil sample from the Yungay region. Mineral and organic peaks are labeled.	81
4.6	RLS spectra of 10 points along an ancient clay-rich soil from 215 cm depth in Yungay. The two peaks indicative of carbon are labeled. . .	82
4.7	SAM-like EGA of Yungay surface soil. Red traces are organic m/z values may indicate the breakdown of a lipid membrane followed by green traces of organic m/z values that may be sourced from breakdown of sugars and nucleobases.	90

4.8	SAM-like EGA of clay-rich soil from 215 cm depth in Yungay. Traces of organic ions are suggestive of the presence of fatty acids bound in a different way than the original cellular state as was indicated in the surface soil.	91
4.9	SAM-like EGA of halite and perchlorate-rich sample from 1.5 m depth in Yungay may show evidence of halogen-chemistry occurring within the instrument. Potential fluid inclusions bearing organics in the halite (sharp peaks) are released at 850-900°C.	93

SUMMARY

Desert environments on Earth are colonized by organisms adapted to desiccation. However, the limits of adaptation are not known. We hypothesized that extreme and prolonged dryness might impart too great a challenge for microbial survival. To test this, we surveyed biomolecular proxies for soil microorganism activity across a steep rainfall gradient from the driest region within the Atacama Desert in Chile that receives just a few millimeters of precipitation per decade to a few millimeters a year. Lipid biomarker proxies for membrane response to environmental stress, degree of amino acid racemization, integrity of stress proteins suggest that organisms in the driest soils in the Atacama are not or very minimally metabolically active. This suggests that the dry threshold for soil habitability has been crossed in the driest hyperarid regions in the Atacama, and implies that it may also have been crossed on the surface of Mars, which is 100-1000 times drier.

While dry Atacama soils in this region might not be habitable, dryness could lead to greater preservation of biomarkers generated during a wetter epoch. Our understanding of long-term organic matter preservation comes mostly from studies in aquatic systems. In contrast, taphonomic processes in extremely dry environments are relatively understudied and are poorly understood. We investigated the accumulation and preservation of lipid biomarkers in hyperarid soils in the Yungay region of the Atacama Desert where microbial activity might not exist. Lipids from seven soil horizons in a 2.5 m vertical profile were extracted and analyzed using GC-MS and LC-MS. Diagnostic functionalized lipids and geolipids were detected and increased in abundance and diversity with depth. Deeper clay units contained fossil organic matter (radiocarbon dead) that has been protected from rainwater since the onset of hyperaridity. We showed that these clay units contain lipids in an excellent state of structural preservation with functional groups and unsaturated bonds in carbon

chains. This indicates that minimal degradation of lipids has occurred in these soils since the time of their deposition between >40,000 and 2 million years ago. The exceptional structural preservation of biomarkers is likely due to the long-term hyperaridity that has minimized microbial and enzymatic activity, a taphonomic process we term xeropreservation (i.e. preservation by drying). The degree of biomarker preservation allowed us to reconstruct major changes in ecology in the Yungay region that reflect a shift in hydrological regime from wet to dry since the early Quaternary. Our results suggest that hyperarid environments, which comprise 7.5% of the continental landmass, could represent a rich and relatively unexplored source of paleobiological information on Earth, and potentially Mars.

Greater characterization of the organic material contained in ancient and/or modern martian sediments will be one of the primary astrobiological goals in the next few decades. Life detection on other planets rests on the ability to interpret positive or negative results as well as contextualization with naturally-occurring terrestrial samples. We took advantage of the above-mentioned characterized Atacama soil samples which contain both viable and fossil biomass, and are biomarker-poor and perchlorate-rich to assess the organic detection capability of current and future Mars mission flight-instrumentation. Firstly, Raman laser spectroscopy, slated to fly on both ESA and NASA Mars rovers, was not able to identify the most abundant biogenic lipid or hydrocarbon compounds contained in Yungay soils. Instead, only two non-specific carbon bands were detected in ~75% of sample points. These bands are commonly observed in non-biologic carbon-bearing samples. However, evolved gas analysis (EGA) techniques similar to what is being employed currently on the Curiosity Rover revealed organic ions in all samples analyzed. Organics contained in Yungay surface soils had the strongest indication of bioenicity. However, analysis of million-year-old buried halite revealed the presence of organic-bearing water inclusions. Our study suggests that sample acquisition and handling which includes

preparation leads to increased quality of organic information.

CHAPTER 1

INTRODUCTION AND BACKGROUND

1.1 Biomarkers: Preservation Pathways and Survival in the Terrestrial Fossil Record

“Biosignature” is a general term that encompasses many types of evidence for life such as morphological (e.g. stromatolites), isotopic, or molecular. The term *biomarker* is more specific, referring to organic compounds that retain biological heritage in their molecular structure through geologic time (Meyers and Ishiwatari, 1993). Molecular biomarkers can be useful in understanding the identity and/or activity of organisms in a diversity of environmental settings, and particularly in geological deposits where only a small fraction of the original biomass remains (e.g. Peters et al., 2005). Biomarkers are targets for life detection on Earth and on planets and moons in the Solar System, particularly on Mars where widespread habitable conditions at the surface might have existed only during the first billion years of the planet’s history (Ehlmann et al., 2011; Grotzinger et al., 2015), and molecular evidence for early forms of life might have decayed significantly since its deposition (Brocks and Summons, 2003).

On Earth, preservation of biomarkers in the fossil record is not the norm, as approximately 99.9% of organic material in the biosphere is recycled (Des Marais, 2001). Some environments are more conducive to longterm preservation: for example, when fast sedimentation or mineral encapsulation occurs (Farmer and Des Marais, 1999; Van Veen and Kuikman, 1990), or low temperatures and low humidity limit microbial activity (Rethemeyer et al., 2010). When it comes to preservation, not all biomarkers are equal. Biomolecules follow chemical decay pathways (Collins and

Riley, 2000), which can provide estimates of time since death (Miller et al., 2000; Penkman et al., 2011). Different classes of biomarkers have different timespans of stability in the fossil record. Typically, the more information-rich biomarkers (e.g., DNA) decay at the fastest rates. It has been estimated that DNA can maximally survive less than one million years in the fossil record (Coolen et al., 2004; Allentoft et al., 2012). The oldest synergistic recovery age of proteins is 70 Ma, about an order of magnitude or two longer than DNA (Muyzer et al., 1992). Amino acids are useful biomarkers for determining the biogenicity and age of organics. This is due to their chiral properties as biology primarily utilizes L-enantiomer amino acids, and to the observation that there are a few proteinogenic amino acids not detected in exogenous organic material (Burton et al., 2012; Cobb and Pudritz, 2014). For these reasons and the fact that they can be detected at low concentrations by spacecraft-based analyses (Skelley et al., 2005), amino acids have been proposed as targets for life detection extraterrestrially (e.g., Europa Lander Study, 2016). However, in most surface environments (particularly ones with transient liquid water), complete racemization occurs after only 10 Ma (Bada and McDonald, 1995; Bada, 1999), which limits the utility of using amino acid chirality in the search for evidence of life in ancient martian geologic deposits. Furthermore, in marine systems, D-amino acids are found to accumulate due to biological processing (Bada and Hoopes, 1979; McCarthy et al., 1998), which would complicate the interpretation of D- and L- amino acids detected on ocean worlds.

Lipids are among the most stable organic molecules over geological time and have a long history in biogeochemical analyses of past and present life (Peters et al., 2005). While some lipids, such as labile fatty acids, are susceptible to microbial recycling (e.g. Klein et al., 1971), others are more robust and long-lived in the fossil record, retaining a biogenic hallmark either in their structure (e.g. 2-methylhopane hydrocarbon derivatives of 2-methyl-bacteriohopanepolyols) or patterns in chain-length preference

(e.g. higher relative abundances of even carbon chain lengths over odd in fatty acids). Some polycyclic isoprenoid lipid biomarkers (i.e., hopanes and steranes) are resistant to diagenetic degradation processes and can be preserved for billions of years recording the presence and activity of microorganisms (Summons et al., 1999; Brocks and Summons, 2003; Eigenbrode, 2008; Summons et al., 2008; Summons et al., 2011). Additionally, lipid biomarkers have a long history in analyses and investigations of present microbial life (Kates 1978; Volkman et al., 1998; Volkman 2006; Rashby et al., 2007; Jahnke et al., 2004; Parenteau et al., 2014). The ubiquity of lipids in life and their longevity in the terrestrial fossil record makes them excellent targets for the search for evidence of life on Mars. For these reasons, I focused my dissertation research topics on lipid biomarker preservation and detection.

Determining the initial (modern) preservation state of biomolecules is critical in understanding the long-term (geologic) preservation of organic material (Keil and Mayer, 2014), particularly for diagnostic biomolecules such as certain classes of lipid compounds. Biomarkers undergo a predictable pathway of degradation and subsequent preservation in sediments (Fig. 1.1). The preservation of biomarkers is dictated by a primary biotic forcing and subsequent environmental parameters including temperature, overburden pressure, radiation, mineralogy, oxidizing conditions, and dryness. When a living organism dies, its intact cellular material is degraded by the action of other microbes and enzymatic material (Skopintsev, 1981; Kuzyakov, 2010). After microbial degradation, remaining degraded biomolecules may be subjected to special circumstances such as fast sedimentation and shallow burial that lead to initial geologic preservation (Burdige, 2007; Farmer and Des Marais, 1999). Material will undergo diagenesis and may be preserved over geologic time if deep burial or other processes occur (Eglinton and Logan, 1991; Knoll et al., 2007). Finally, remaining biomarkers will have to survive exhumation (e.g. Banerjee et al., 2006) and, on Earth, microbially mediated degradation at the surface (Petsch et al., 2001) before they can

be collected and analyzed. On Mars, surface exposure results in even faster rates of degradation of organics and putative biomarkers due to the radiative environment (Pavlov et al., 2012) and oxidizing conditions of soils (Benner et al., 2000).

To date, many biomarker investigations have focused on end-stages of biomarker degradation, typically in marine or lacustrine environments with a high concentration of biomass. Instead, my dissertation research focuses on the comparatively less understood earlier stages of degradation (Fig. 1.1) in a unique terrestrial environment, the hyperarid core of the Atacama Desert in Chile in near-surface soils with extremely low concentration of biomass. In Chapter 2, I use lipid, protein, and amino acid biomarkers of living and dead organisms as indicators of microbial activity to understand the habitability of surface soils under increasingly dry climatological conditions. In Chapter 3, given the nearly negligible levels of microbial activity in the driest soils in the Atacama, I assess preservation of lipid biomarkers under extremely dry conditions as a means of exploring how dryness may influence preservation processes of lipid biomarkers may operate on the martian surface. Finally, in Chapter 4, relying on biomarker data collected by standard laboratory techniques reported in the previous chapters, I assess the detectability of biomarkers in biomass-poor, oxidant-rich soils with current and future Mars flight instrumentation.

1.2 Planetary Analog Research

The goal of “planetary analog research” is to study processes occurring in terrestrial environments in order to understand and predict how those processes might be occurring in analogous extraterrestrial environments. Much of the field focuses on understanding the limits of terrestrial life in “extreme environments” on Earth, and applying that knowledge to better understand how to “seek, identify, and characterize life and life-related chemistry that may exist or have existed on other solar system bodies,” (NASA PSTAR Solicitation, 2016). The Atacama Desert in Chile is consid-

Preservation Pathways of Biomarkers

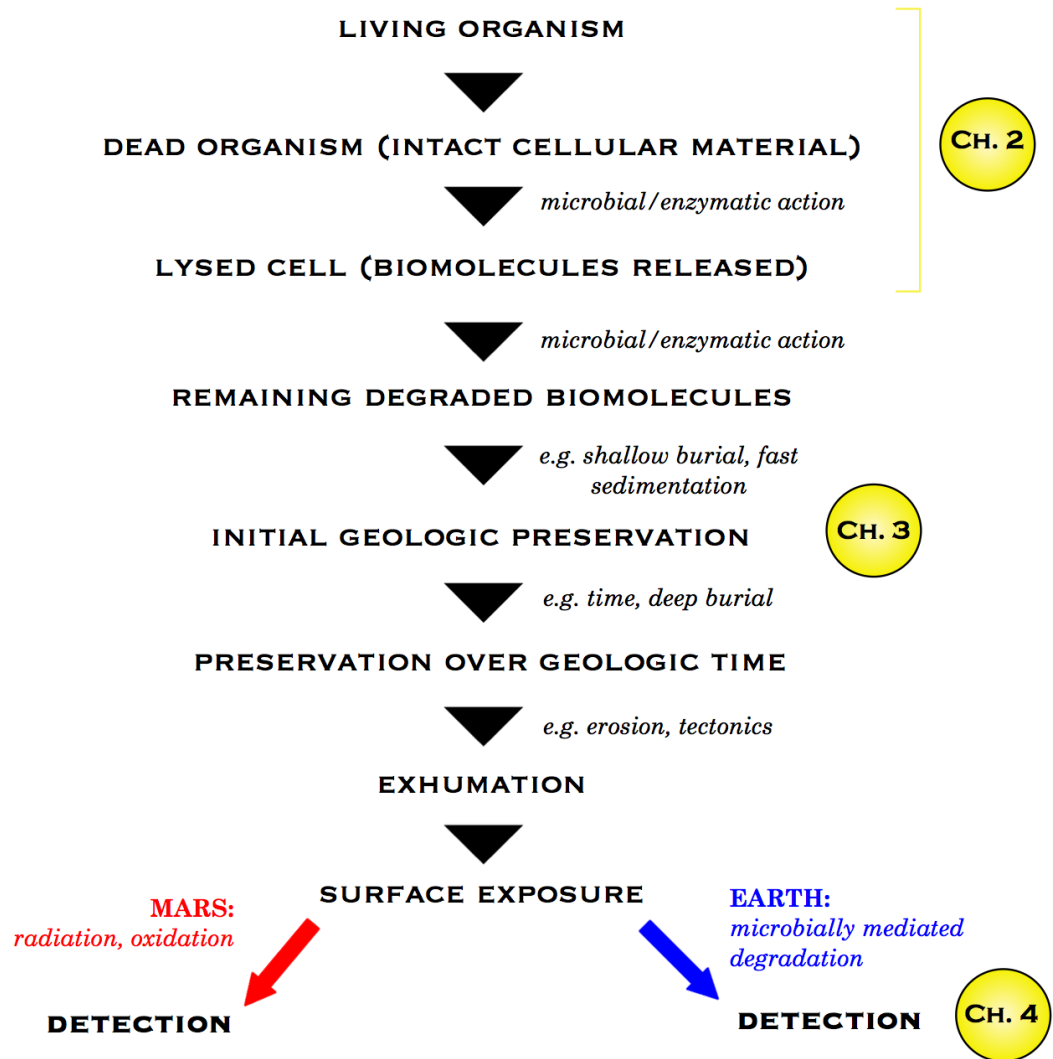


Figure 1.1: Flow chart of the typical pathway of biomarker preservation from living organism through early degradation processes to incorporation into the geological record. The focuses of the three thesis chapters are highlighted in yellow.

ered by many to be a Mars analog environment (e.g., Navarro-Gonzalez et al., 2003; McKay et al., 2003). For my dissertation research, I have primarily focused on how the effects of extreme and prolonged dryness alter processes of biomarker preservation and distribution.

1.3 The Yungay Region of the Atacama Desert: Hyperaridity, Age, Soil Properties, and Aridity Gradient

The Atacama Desert in Chile is an old, temperate desert about 1000 kilometers in length running parallel to the Pacific Ocean (Warren-Rhodes et al., 2006). It is possibly the driest region on the planet as well as one of the longest-lived deserts (McKay et al., 2003). The desert has been arid to semi-arid for about 150 million years (Hartley et al., 2005), and has experienced extreme aridity for the last 10-15 million years (Hartley and Chong, 2002). It is believed that this most recent period of extreme aridity has been punctuated by short-lived periods of increased wetness (e.g. Jordan et al., 2014). The active subduction zone in Chile has created many mountain ranges, including the Andes and the coastal ranges (e.g. the Vacuña Makenna Mountains near the Yungay region) that have acted as natural barriers against precipitation in the central depression of the Atacama, shielding the region from the prevailing stable and long-lived south-east trade winds through a rainshadow effect that results in warm dry air descending upon the desert (Houston and Hartley, 2003). Additionally, the north-flowing cold Humboldt ocean current (Garreaud et al., 2010) offshore is unable to pick up much moisture. The confluence of these factors has resulted in the extreme dryness of the central depression of the Atacama, so much so that seismicity has played a noticeable role in erosion in this region (Quade et al., 2012), and ventifacts such as pyramidal rocks can be abundantly observed. Prolonged and extreme dryness has led to an “extraordinarily uncommon” landscape (Jordan et al., 2014), and to development of unusual soil properties as described below, including

the accumulation of rare salts and low concentrations of aged biomass.

The Yungay region (Fig. 1.2), located within the driest region in the Atacama between $\sim 22^{\circ}\text{S}$ to 26°S latitude (Börgel, 1973), is considered to be hyperarid according to the United Nations Environment Programme (UNEP) definition with an aridity index value of 0.001 (Davila and Schulze-Makuch, 2016). This region is 100 times drier than the Mojave Desert. Even the nearby coastal city of Antofagasta is 30 times drier than the Mojave. The mean annual temperature in Yungay is 19°C , with temperatures ranging from -10° to 40°C . The mean annual precipitation is $<< 2\text{mm}$ per year, with rain events only occurring about once per decade (McKay et al., 2003; Warren-Rhodes et al., 2006). The last two times rain has fallen in Yungay were in 2015 and 2006, with $<4\text{ mm}$ falling on both occasions. Additionally, it has been shown that more than a few millimeters of rainfall is required in order for water to percolate through the top soil in Yungay (Davis et al., 2010).

The prolonged dryness has caused rare salts to accumulate in Yungay, such as nitrates, sulfates, chlorides, and perchlorates. Much of this salt has been mined over the last 100 years and has contributed significantly to the Chilean economy (Dorfman, 2004). Accumulated salts act as a barrier to moisture at deeper points in the soil column. A 10 cm thick gypsum/anhydrite layer located at about 10 cm depth throughout the region can expand by approximately 700% when wetted by the decadal rain event (Ewing et al., 2006), causing meter-scale polygonal fracturing to form in the upper surface layer. At a depth of 150 cm there is a $\sim 10\text{-}20\text{ cm}$ thick halite unit which also acts as an “aquiclude” against percolating water (Ewing et al., 2006 & 2008). These units undoubtedly have had an influence on how material is able to move around in the upper portion of the soil column, as well as acted to prevent the flow of the small amounts of rainwater to deeper, buried clay units since the onset of hyperaridity in this region about 2-6 million years ago. The water table is currently at about 100 m below the study site of interest in Yungay. The role of groundwater

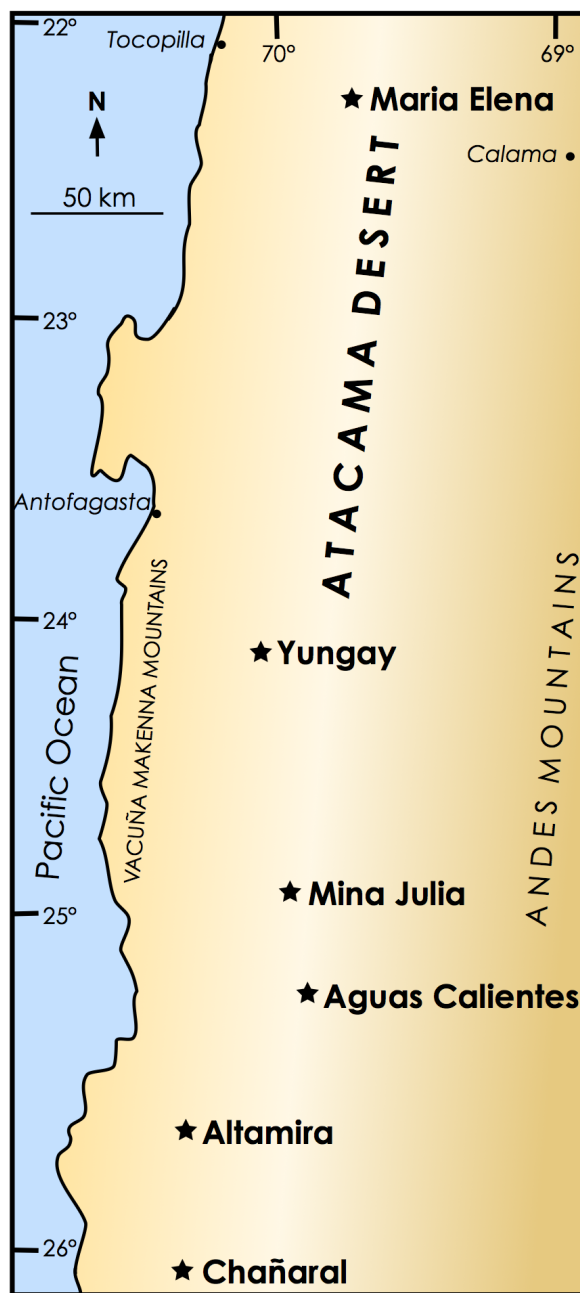


Figure 1.2: Map of the driest region in the Atacama Desert from 22°S to 26°S. Study sites shown with stars.

in the formation of the halite unit should be explored in future studies of the region.

Surface age exposure at Yungay is dated to be >2 My based on cosmogenic radionuclide concentrations in boulders and Ar isotopes in interbedded volcanic ash (Ewing et al., 2006). The stratigraphic sequence in this region spans 2-6.6 My (Wang et al., 2015) based on ^{10}Be concentrations in the soil column down to approximately 2 m depth. Skelley et al., (2007) found organics in the surface soil to be $\sim 1,000$ to 100,000 years old based on the racemization of amino acids. Organic material contained within the soil is radiocarbon dead below about 1 m (Ewing et al., 2008), meaning that it is older than 40,000 years.

The extended periods of extreme dryness have also resulted in low concentrations of biomass in Yungay surface soils, the lowest reported on Earth, with cell counts estimated to be between 10 and 10,000 cells per gram of soil (Navarro-Gonzales et al., 2003; Crits-Christoph et al., 2013). In this region, there is also a general lack of habitation by plants (Fig. 1.3), lichens, archaea, endolithic and hypolithic communities, and soil microorganisms (Navarro-González et al., 2003; Warren Rhodes et al., 2006). Surface bacterial composition is more consistent with deposition of organisms contained in atmospheric aerosols rather than an in-situ population (Lester et al., 2007; Cannon et al., 2007). The lack of colonization by organisms, especially plants, which are active recyclers and distributors of organic carbon in the majority of terrestrial environments, allows an opportunity to look at the distribution, preservation, and transport of organic carbon with primarily abiotic processes occurring (Ewing et al., 2008). In this unique system, organic carbon is deposited by atmospheric processes where it then undergoes photolysis at the surface, limited dissolved transport within only the upper meter of the soil column, and limited decomposition (Ewing et al., 2008).

To the south of Yungay, moisture increases marginally from $<<2$ mm/year to about 10 mm/year within about 200 km near Chañ (from 24° to $\sim 26^\circ\text{S}$, Fig. 1.2).



Figure 1.3: Panoramic photo of study site in the Yungay region showing general lack of colonization by macroscopic organisms. The soil pit (discussed in Chapter 3), in the right-center part of the photograph, is about 1 meter across.

This aridity gradient is a useful and well-studied feature of the Atacama (Navarro-Gonzalez et al., 2003; Warren-Rhodes et al., 2006), and has primarily been used to understand the response of the biological system to increasingly dry conditions. Significant ecological changes are observed to occur with increasing dryness over this short distance, including a decrease of cultural heterotrophic colony forming units (Navarro-Gonzalez et al., 2003), a decrease in the amount of benzene and formic acid detected by pyrolysis GC-MS of soils (Navarro-Gonzalez et al., 2003), a decrease in bacterial diversity (Navarro-Gonzalez et al., 2003; Crits-Christoph et al., 2013), a decrease in hypolithic colonization of cyanobacteria of quartz stones (Warren-Rhodes et al., 2006), and an increase of radiocarbon age of hypolithic communities (Warren-Rhodes et al., 2006). This has led some to conclude that the “dry limit of life” had been crossed in the driest parts of the Atacama, although this remains a point of contention in the literature (Crits-Christoph et al., 2013; Azua-Bustos et al., 2015).

1.4 Scope of Dissertation

1.4.1 Chapter 2

While the majority of the Earth’s surface is habitable by organisms adapted to the imposed set of environmental conditions, extreme and prolonged dryness may produce too great a challenge for microbial survival. While DNA and other organic material has been identified in the driest soils in the Atacama Desert, it is still un-

clear whether or not microorganisms are capable of growth when a few millimeters of rainwater are available only once per decade. In this chapter, I measure a suite of molecular biosignatures over increasingly dry climatological conditions along the Atacama's aridity gradient in the driest region of the desert to test the hypothesis that soils organisms are active in-situ. This includes analysis of lipid biomarkers that are proxies for microbial activity, degree of racemization of amino acids, and proteins/peptides that are typically found in organisms under stressful environmental conditions. Results suggest that organisms are not active in the driest soils in the Atacama, as indicators of metabolic activity are either not present (some lipids), fragmented (protein/peptides), and/or have been excluded from metabolic activity for tens of thousands of years (amino acids). Thus, my data suggests that organisms are not adapted to the extreme and prolonged dry conditions in the driest part of the Atacama. The inactivity of the majority of microorganisms in these soils allows me to assess the preservation of lipid biomarkers primarily due to abiotic degradation processes in the following chapter. These findings are significant in assessing the habitability of the surface of modern Mars, which is many orders of magnitude drier than the driest parts of the Atacama.

1.4.2 Chapter 3

Understanding the preservation or taphonomy of organic matter in the geologic record has been critical for reconstructing the evolutionary history of life on Earth, and for developing strategies to search for evidence of life elsewhere. Microbes are incredibly efficient at metabolizing organic matter to CO_2 , and are responsible for the decomposition of 99.9% of biomass produced by primary productivity. Environments in which microbial activity is greatly limited may enhance the preservation of organic compounds, even over long periods of time. This chapter describes the preservation state of labile biomarkers in extremely dry environments where microbial activity is

limited by low water potential. To my knowledge, this study is the first examination of taphonomic processes in hyperarid settings. Specifically, we characterize the preservation of lipids in soils that have experienced extreme dryness for 10-15 million years. Analysis of clay layers containing fossil organic matter between >40,000 years (carbon dead) and ~2 million years old reveals exceptional structural preservation of functionalized fatty acids and other labile lipids. Due to the hyperaridity, protection from rainwater, and subsequent suspension of microbial degradative activity, these fragile lipids have not been significantly degraded or transformed since their synthesis, a taphonomic process termed ‘xeropreservation.’ These findings are significant in revealing the stability of labile, functionalized lipids under hyperarid conditions, and point to the possible preservation of other labile biomolecules. Despite the low productivity of deserts, xeropreservation of biomolecules in hyperarid settings, which comprise 7.5% of the continental landmass, could represent a rich, but relatively unexplored source of paleobiological information. These results are also important for the search for evidence of life on Mars, where hyperarid conditions have prevailed for most of the planet’s history.

1.4.3 Chapter 4

Utilizing the measurements of biomarker content in Atacama soils in the previous two chapters using traditional laboratory techniques as a baseline, the ability of Mars flight-instrumentation to detect organics and biomarkers is tested. This includes a prototype for a Raman instrument slated to fly on the ExoMars mission in 2020, similar to that to be used by NASA’s Mars 2020 mission, as well as an Evolved Gas Analyzer similar to that currently being employed onboard the Mars Science Laboratory. Both techniques are significantly more operationally simple than standard laboratory organic analysis. Results reveal that only two non-specific carbon bands are detectable by the Raman flight technique in biomass-poor Atacama soils.

On the contrary, evolved gas analysis reveals an abundance of organic ions despite low concentration of organics and high concentrations of oxidizing salts in soils such as perchlorate. Furthermore, this technique is suggestive of the breakdown of fatty acids and other cellular contents in surface soils, as well as informative about the relationship between organic and inorganic material contained within older soil samples. Both techniques reveal only basic information about organic and putative biomarker content of samples, suggesting that operational simplicity comes at a great scientific cost.

1.4.4 Chapter 5

I close this dissertation with a discussion of broad conclusions and implications of this work, particularly as it pertains to the conditions on the martian surface. I also recommend directions of future investigations in the Atacama and other planetary analog environments such as the Antarctic Dry Valleys.

CHAPTER 2

DECLINING TRENDS OF MICROBIAL ACTIVITY IN ATACAMA DESERT SOILS WITH INCREASING DRYNESS INFERRED FROM BIOMARKER CONTENT

2.1 Introduction

Desert environments are colonized by desiccation-tolerant organisms capable of enduring severe dehydration and resuming metabolic activity shortly after rehydration (Noy-Meir, 1973; Potts, 1994; Alpert, 2005; Proctor et al., 2007; Pointing and Belnap, 2012; Lebre et al., 2017). The physiological and ecological adaptations involved in desiccation-tolerance have been studied for decades (e.g., Noy-Meir, 1973; Potts, 1994; Alpert, 2005; Pointing and Belnap, 2012; Wierzbos et al., 2012), but the actual limits of desiccation-tolerance are still poorly constrained across the three domains of life (Alpert, 2005). Beyond the implications for terrestrial ecosystems, a better understanding of the environmental limits of desiccation-tolerance would be relevant to habitability models of Mars, today and in the past (Davila and Schulze-Makuch, 2016).

Desiccation stress is particularly severe in hyperarid soils of the Atacama Desert in northern Chile (Rundel et al. 1991; McKay et al., 2003; Navarro-González et al., 2003). The extreme dryness has resulted in some of the lowest levels of biomass observed in any surface environment on Earth (Ewing et al., 2008; Crits-Christoph et al., 2013), and past investigations have largely focused on determining whether extant microorganisms are present in the soils, with variable success (Navarro-González et al., 2003; Cannon et al., 2007; Lester et al., 2007; Crits-Christoph et al., 2013; Azabustos et al., 2015). Labeled release experiments, similar to those performed by

the Viking Landers on Mars, showed no biological response in hyperarid Atacama soils (Navarro-Gonzalez et al., 2003); but follow-up studies demonstrated that viable microorganisms are in fact present (Connon et al., 2007; Lester et al., 2007; Crits-Christoph et al., 2013; Azúa-Bustos et al., 2015). It remains to be determined whether these microorganisms have an acute tolerance to extreme desiccation (Azúa-Bustos et al., 2015); whether they represent a native soil population surviving on rare and sporadic rain events (Crits-Christoph et al., 2013); or whether they are merely wind-transported organisms from other, more active regions; and/or they reflect a soil population preserved from a wetter epoch in the Atacama's history (Connon et al., 2007).

We conducted a survey of biomolecular proxies for metabolic activity in soils of the Atacama Desert across a steep rainfall gradient from about 10 mm/year to <2 mm/year (Navarro-González et al., 2003; Warren-Rhodes et al., 2006). We hypothesized that soil microbial activity levels would change along the gradient in response to increasing dryness, and these changes would be reflected in the type and abundance of metabolic markers. Markers of metabolic activity could decline in abundance along the gradient due to diminishing levels of biomass, but stress-response markers from desiccation-tolerant strains ought to still be present in the driest soils. This would hold even if metabolic activity was limited to episodic spurts, especially given the excellent conditions for lipid biomarker preservation over tens to hundreds of thousands of years (see Chapter 3). Instead, our results suggest that organisms in the driest soils in the Atacama are not metabolically active, or so few organisms are active that the abundances of potential molecular biomarkers that would have been generated would be too low for detection even by the sensitive laboratory techniques utilized.

2.2 Biomarker Proxies for Metabolic Activity

The presence of cyclopropane fatty acids (CFA) is a proxy for microbial activity and stress response, because many bacteria modify their existing membrane unsaturated fatty acids into CFA in response to environmental stressors, which include exposure to oxidants, starvation, desiccation, and large temperature fluctuations (Marr and Ingraham 1962; Guckert et al., 1986; Grogan and Cronan, 1997; Annous et al., 1999; Chen and Gnzle, 2016). CFA enhance the stability of membranes under environmental stress, decrease membrane permeability against toxic compounds (Poger and Mark, 2015), and aid in bacteria revival after freeze-drying (Muoz-Rojas et al., 2006). In Atacama soils, the presence of CFA could be a proxy for soil microbial activity, with an expected higher relative abundance of CFA with increasing dryness. In addition, CFA could also be a proxy for past episodes of metabolic activity because there is no microbial known mechanism to reverse the cyclopropanation of phospholipid fatty acids within the membrane (Zhang and Rock, 2008). Abiotic and biotic degradation of CFA is not expected in this hyperarid setting, given that that fatty acids, including those with unsaturations, are well-preserved in these hyperarid soils (Chapter 3). Additionally, cyclopropane functionality is more stable than unsaturation (Zhang and Rock, 2008).

The ratio of *trans* to *cis* unsaturation fatty acid isomers is another metabolic stress marker in bacteria. The conversion of *cis* unsaturated fatty acids to *trans* is an adaptive mechanism that can be used by bacteria to modulate membrane fluidity in response to environmental changes (Heipieper et al., 2003). A few bacteria have been shown to increase the ratio of *trans/cis* unsaturated fatty acids in response to stressors such as nutrient deprivation, low temperatures, and osmotic stress (Guckert et al., 1986; Okuyama et al., 1991; Heipieper et al., 1995; Heipieper et al., 1996). Therefore, an increase in this ratio with increasingly dry conditions could be interpreted as an

indication of a metabolic adaptation.

Additionally, there are a number of proteins that are expressed when organisms are exposed to environmental stressors (Shirkey et al., 2000) such as heat shock proteins; IsiA protein for iron deficiency (Chen et al., 2005; Wilson et al., 2007); superoxide dismutase for oxidative stress (Shirkey et al., 2000); or sodA protein involved in resistance to radiation (Markillie et al., 1999). Hence, the presence and structural integrity of these proteins could be an indicator of current or past metabolic activity in desert soils.

Most organisms utilize only L-enantiomer amino acids to synthesize proteins. In microbially active soils, if proteins are continuously synthesized, the D/L ratio of amino acids ought to be low. However, in the absence of active metabolic processes, amino acids racemize; i.e., L- and D- enantiomers interconvert until they are present in equal amounts. For that reason, the D/L ratio of amino acids is commonly used to assess the approximate age of organic material contained in the fossil record (Bada et al., 1999). Aspartic acid has one of the highest rates of racemization (Poinar et al., 1996), which makes it a useful proxy for suspended metabolic activity in samples that have ages of a few thousand to tens of thousands of years. An important caveat is that bridging peptides in peptidoglycan, the main structural component of bacterial cell walls, contain D-amino acids (Schleifer and Kandler, 1972), which can lead to biological enhancement of D/L ratios where cell walls preferentially accumulate in the environment (McCarthy et al., 1998).

2.3 Field Site

Sampling sites were selected based on previously published studies of the Atacama’s microbial ecology in order to have comparable datasets (Navarro-González et al., 2003; Warren-Rhodes et al., 2006; Ewing et al., 2008; Crits-Christoph et al., 2013; Azúa-Bustos et al., 2015). Sites were located along a south to north transect from

latitudes of 26° to 24°S, centered at 70°W. Mean annual precipitation along the transect decreases from about 10 mm/year to <<2 mm/year (Navarro-González et al., 2003). While the totality of this particular transect is considered hyperarid based on the United Nations Environmental Program (UNEP) Aridity Index (AI) definition ($AI < 0.05$), AI values decline by an order of magnitude from 0.01 to 0.001 over these latitudes (Davila and Schulze-Makuch, 2016). Samples were collected on post-Miocene alluvial fan deposits to minimize geological variation and exposure ages and to simplify interpretation of ecological results. From south to north these sites include Chañaral (26° 9'50.34"S, 70°17'6.30"W), Altamira (25° 41'6.84"S, 70° 16'30.96"W), Aguas Calientes (25° 14'38.50"S, 69° 51'42.40"W), Mina Julia (24° 53'37.74"S, 69° 53'55.38"W), Yungay/Yungay South (24° 6'5.16"S, 70° 1'5.04"W), Yungay North (24° 5'30.54"S, 70° 0'2.52"W) and Maria Elena (22°16'5.82"S, 69°43'18.48"W) and are plotted in Figure 2.1a.

2.4 Methods

2.4.1 Sample Collection

Samples were collected for laboratory analyses in September 2014. In addition, immunoassays (see below) were performed on-site in the Atacama in February 2017 on samples collected at selected sites along the transect. Due to the extremely low inventory of biomass in Atacama soils (Ewing et al., 2006), samples were collected by scientists wearing full-body, sterile, clean-room suits (<1 colony forming unit per 10,000 garments), masks, glasses, and gloves to minimize the introduction of anthropogenic biological contaminants (Meadow et al., 2015) during sampling. Soil samples from the surface (0 cm) to 5 cm depth were excavated from each sample site. A solvent-cleaned spoon was used to scoop samples into three 8 oz glass jars (holding approximately 300 g of soil each) that had been heated to 500°C for greater than 8 hours to combust all traces of organic material. Each sample was collected using

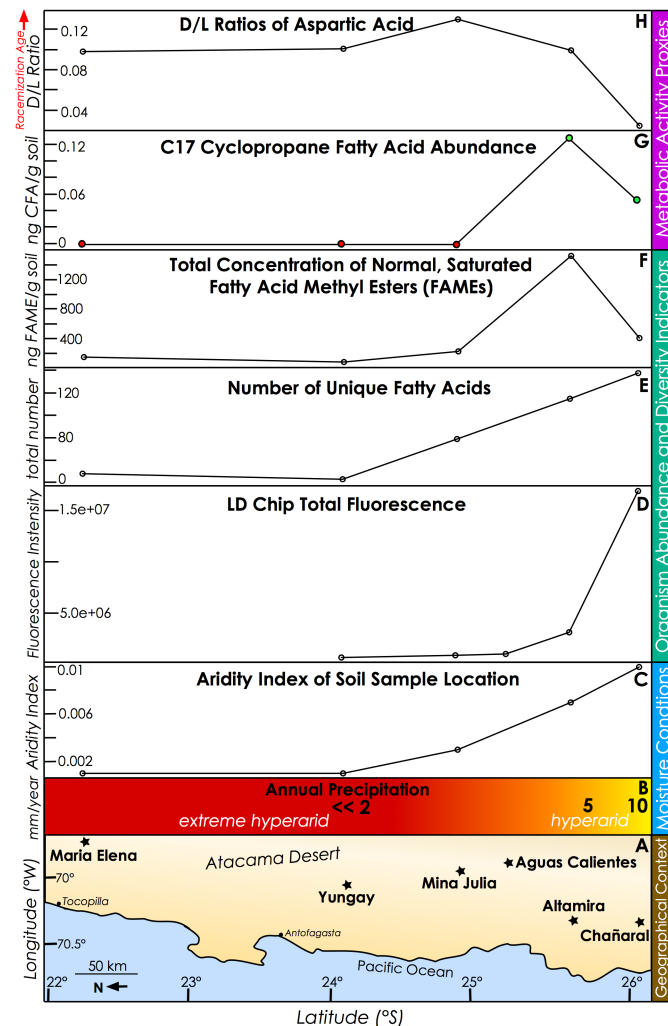


Figure 2.1: **Changes in biomarker content and aridity are plotted with latitude.** A. Map of the Atacama Desert with soil sites marked with stars. B. Annual precipitation values are written at latitudinal locations. Red color indicates region experiencing only mm-decadal rain events, Orange and yellow indicates regions that receive 5-10 mm precip./yr. Based on Navarro-González et al., (2003). C. Aridity Index values, (AI), mean annual precipitation/potential evapotranspiration. This entire region, with AI < 0.05 is hyperarid. D. The total LDChip antibody microarray florescence of proteins and peptides, the sum of florescence of 242 spots. E. Total number of unique fatty acids 12-30 carbons (normal and saturated, dicarboxylic, branched, and unsaturated fatty acids), a proxy for organism diversity. F. The total concentration of normal, saturated FAMEs n -C_{12:0}- n -C_{30:0}. Values indicate the amount of common membrane lipids of living, dormant, and dead organisms. G. Cyclopropane fatty acids (CFA) were only detected in Altamira and Chañaral soils. Values of 0 at the drier sites indicate that CFAs were not detected. The presence of CFA indicates membrane modulation under stress, and thus metabolic activity. H. D/L ratios of aspartic acid from hydrolyzed proteins, peptides, and humic complexes. Increased racemization indicates that organic material is older.

a unique spoon to minimize cross contamination. Samples were kept frozen during transport and then stored at -20°C until analysis.

2.4.2 Lipid Extractions and Analysis

Glass jars containing samples were removed from the -20°C freezer and kept for 30 minutes to 1 hour at room temperature to prevent condensation of moisture onto the soil. Soils were not lyophilized in order to reduce the exposure time to the laboratory environment and minimize contamination risk; this step was not considered critical given their extremely low water content. Preliminary samples that were lyophilized to estimate water content in soil showed only 1.4% reduction in mass due to water loss.

Hundreds of grams of soil were removed from the glass jars and then homogeneously powdered with a ceramic mortar and pestle that had been previously solvent-rinsed and combusted (550°C, 12 hours). Soil mass was scaled based on previously measured lipid abundances in soils to ensure detection lipids of low relative abundance such as C17 cyclopropane fatty acids (Ewing et al., 2006; Wilhelm et al., 2017): [88.8 g of Chañaral soil to 221.7 g of biomass-lean Yungay soil].

Soil samples were extracted using a modified Bligh and Dyer protocol (Bligh and Dyer, 1959; Jahnke et al., 1992). The protocol was modified primarily to minimize transfer steps and contamination and loss of biomass during extraction (Wilhelm et al., 2017). Three extractions were performed on powdered sample: 40 mL of HPLC-grade water, 100 mL of pesticide-grade methanol, and 50 mL of pesticide grade-methylene chloride (DCM). After the addition of solvents, the resultant slurry was sonicated, stirred, and left to settle until solvent became mostly clear, at which point it was poured into a new previously combusted flask.

Solvent extracts were then added to a solvent-washed Teflon separatory funnel with 180 mL of extract and 47 mL of methylene chloride and inverted two times

to mix. Water (47 mL) was then added to drive the methanol into the aqueous phase, and the mixture was gravimetrically separated. The methylene chloride layer was slowly drained into a new flask; the methanol and water phase discarded. The resulting extract was evaporated under a stream of N₂ and transferred into smaller previously combusted vials until ~100 μ L remained. Care was taken to minimize the number of containers used in the evaporation process and to thoroughly rinse and sonicate the sides of all vessels after draining to recover any lipid left behind. This evaporation process concentrated the extract by roughly 3 orders of magnitude.

Thirty percent of the total lipid extract (TLE) was used for analysis by gas chromatography-mass spectrometry (GC-MS). The TLE was derivatized via a medium acid hydrolysis using commercial methanolic HCl 0.5N (Supelco, LC08137B) following the Kates (1986) procedure, which adds a methyl group to the carboxyl moiety of any free fatty acids present (Wilhelm et al., 2017), and also transesterifies complex lipids (membrane-bound fatty acids, such as phospholipids and glycolipids) to generate fatty acid methyl esters (FAME). This acid methanolysis treatment generates a ‘total’ solvent-extractable fatty acid pool present as FAME. An unsaturated *n*-C_{22:1} FAME standard (Sigma-Aldrich) (40 μ l of a 25 ng/l standard) was then added to the TLE for a mass of 25 ng per 1 μ l injection into the GC-MS.

The final volume of 30% of the derivatized TLE in DCM was 40 μ L, which contained 30% of the derivatized total lipid extract. 1/40th of this volume was then injected into the GC-MS. GC-MS of lipids was performed on an Agilent 7890B GC-5977A MSD system equipped with an Agilent DB-5MS column (60 m x 250 μ m x 0.25 μ m, Agilent, Santa Clara, CA, USA) with high purity helium as carrier gas at 1mL/min. The inlet temperature was 280°C. Initial oven temperature was 50°C, ramped to 120°C at 10°C/min, then increased from 120°C to 320°C at 4°C/min and held at this temperature for 5 min. The MS source temperature was 280°C. Our instrument is capable of detecting 1 picogram of a C23 FAME standard using the

same 60 m DB-5MS column and heating protocol as was used in analysis.

2.4.3 Monounsaturated Fatty Acid Double-Bond Position and Cyclopropane Fatty Acid Determination

Because it is difficult to distinguish unsaturated fatty acids from CFA due to similar elution and mass spectral patterns, the unsaturated fatty acids were derivatized using dimethyl disulfide (DMDS) to determine the double bond positions (Yamamoto et al., 1991), as well as chromatographically separate these compounds from the CFA. The FAME fraction (30% of the TLE) was added to a reaction vial and treated with 300 μ L DMDS and 4 mg iodine and heated to 35°C for 30 minutes and cooled. 1 mL of hexane-diethyl ether (1:1) was added to this mixture and then it was titrated with 10% aqueous $\text{Na}_2\text{S}_2\text{O}_3$. The FAME-DMDS adducts, as well as un-reacted saturated FAME and the CFA, were extracted with hexane:dichloromethane (4:1, v:v), and concentrated to a final volume of 20 μ L. 1/20 μ L of this final volume was injected on the GC-MS using the previously described chromatographic conditions. Mono- and diunsaturated FAMES form DMDS adducts with distinct spectra that elute at later points in the chromatogram, whereas CFA are unaffected by this treatment and remain at the same elution time as in the previous FAME chromatogram.

FAME are described using the nomenclature “number of carbons:number of unsaturations,” followed by double-bond locations referenced from the delta (Δ), or carboxylic, end of the molecule.

2.4.4 Bound Amino Acid Extraction and Analysis

Only previously unopened jars of soil samples were used for amino acid analyses. All extraction steps were done in a Labconco B2 Biosafety Cabinet that intakes air and passes it through a HEPA filtration system, substantially lowering the risk of contaminating biomass-poor samples. The interior filtered environment of this

Biosafety Cabinet is certified as a Class 100 clean room). Scientists wore clean-room suit sleeves while working with the samples inside the biosafety cabinet in order to further reduce the risk of anthropogenic contamination of samples. Samples were first ground in a unique mortar and pestle that was previously heated to 550°C for 12 hours. An acid hydrolysis extraction protocol was utilized to liberate bound amino acids (i.e., proteins, humic complexes, peptides) from soils. It is estimated that in typical soils, 99.5% of amino acids are in a bound (polymeric) form and the remainder are “free” (Stevenson, 1982). These proportions, estimations of the concentration of amino acids relative to other biomarker classes already measured in Yungay soils (Wilhelm et al., 2017), and instrument detection limits were taken into account to determine the approximate mass of soil required for extraction. 2.5 mL of 6M HCl in amino acid-free H₂O (Sigma-Aldrich) was added to approximately 3 g of ground soil in heat-cleaned (550°C for 12 hr) glass reaction vials. Vials were then sealed and heated for 24 hours at 100°C (Bada et al., 1999, filtered through combusted silica filters to remove solid particles, and dried on a rotary evaporator.

In preparation for chiral analysis by GC-MS, each sample was acidified and de-salted with a column of ion exchanging resin: AG 50W-X4, 100-200. After drying, the carboxyl and amine moieties on the amino acids were derivatized with a mixture of (+)-2-butanol/acetyl chloride to form (+)butyl esters (on carboxyl groups) and a mixture of trifluoroacetic anhydride (TFAA)/ethyl acetate to add trifluoroacetyl groups to amino nitrogens: the resulting compounds are “(+)-butyl/TFA” derivatives. After complete drying, each sample was brought to a final volume of 40 μ L with ethyl acetate: this represented 30% of the derivatized amino-acid extract. 1 μ L of each was injected into a GC-MS. This GC-MS was an Agilent 6890N GC coupled to a 5975 MS (Agilent, Santa Clara, CA, USA). The GC oven was equipped with an Agilent DB-17MS column (60 m x 0.250 mm x 0.25 μ m, with helium as carrier gas at 1mL/min. The inlet temperature was 230°C; initial oven temperature was 35°C;

oven was ramped to 70°C at 3°C/min and held 30 min, temperature then increased to 90°C at 2°C/min, then increased to 230°C at 3°C/min and held for 60 min; MS source temperature was 280°C. In this configuration the GC-MS is capable of detecting low femtomole quantities of amino acids. Laboratory blanks were found to be free of amino acids.

2.4.5 Immunoassays

Antibody microarrays: printing LDChip and fluorescent sandwich immunoassay

The Life Detector Chip (LDChip) is a powerful analytical technique that can be performed in the field immediately after sample collection to avoid any alteration of biomarker degradation during transportation and storage. All samples were analyzed in the field a few hours after collection.

LD Chip is an antibody microarray-based biosensor (Rivas et al., 2008; Parro et al., 2011; 2016) that contains over 200 antibodies with broad specificities produced against biological polymers including lipo/exo-polysaccharides; bacterial strains belonging to main taxonomic groups (Alpha-, Beta-, Gamma-, Delta-Proteobacteria; Cyanobacteria, Actinobacteria, Firmicutes, Bacteroidetes); and Archaea, among others (Rivas et al., 2008; Parro et al., 2011; 2016). Antibodies showing positive immuno-recognition are shown in Figure 2.5.

The Immunoglobulin (IgG) fraction of each antibody (after protein A affinity purification) was printed on epoxy-activated glass slides (Arrayit, CA, USA) using a MicroGrid II TAS arrayer (Biorobotics, Genomic Solutions, UK) as reported previously (Rivas et al., 2008; Parro et al., 2011). For the fluorescent multiplex sandwich immunoassay, all protein A-purified antibodies were fluorescently labeled with Alexa 647 fluorochrome (Molecular Probes, OR, USA) following vendor recommendations, checked, titrated and used as described (Rivas et al., 2008; Blanco et al., 2017).

Sample preparation and Immunoassays with LDChip

Up to 0.5 g of soil samples were suspended in 2 mL of TBSTRR buffer (0.4 M Tris-HCl pH 8, 0.3 M NaCl, 0.1% Tween 20) and sonicated using a manual and portable ultrasonicator (Dr. Hielscher 50 W DRH-UP50H sonicator, Hielscher Ultrasonics, Berlin, Germany) for 3x 1 minute cycles, with 30-second pauses on ice. Then, samples were filtered through 5 μ m nitrocellulose filters to remove sand and coarse material. The filtrates were used as a multianalyte-containing sample for the fluorescent sandwich microarray immunoassays (FSMI) as described in previous works (Parro et al., 2011; Blanco et al., 2017; Parro et al., 2016).

LDChip image processing and quantification

The LDChip microarray images were analyzed and quantified by GenePix Pro Software (Molecular Devices, Sunnyvale, CA, USA). The local background (B) as quantified by GenePix software was subtracted. Then, the final fluorescence intensity A of each antibody spot was calculated following the equation: $A = (F_{635} - B)_{\text{sample}} - (F_{635} - B)_{\text{blank}}$, where F_{635} is the median of the fluorescence of all the spot pixels at 635 nm, either from the sample or the blank assay (only buffer instead of sample), as previously reported (Parro et al., 2011; Rivas et al., 2008). An additional 2.5 times the average of A was applied as cutoff value to all spots of the array to minimize false positives.

2.5 Results

2.5.1 Lipids and Amino Acids

The abundance and diversity of free and membrane-bound fatty acids analyzed as FAME were generally found to decrease along the transect (Fig. 2.1). The number of unique fatty acids detected was found to decrease from 138 in the Chañaral surface

soils to less than 50 in Yungay and Maria Elena soils (Fig. 2.1e). These FAMES included chain lengths between C₁₂ and C₃₀ and the alkyl chains included terminal and mid-chain methyl branches, mono- and polyunsaturated bonds, and, sometimes, a second carboxyl function. The lowest total abundance of normal, straight-chain saturated fatty acids (SFAs) measured along the aridity transect were in Yungay and Maria Elena soils (Fig. 2.1f). Yungay soils had 0.089 μg of *n*-C_{12:0} - *n*-C_{30:0} SFAs per g of soil. Chañaral and Altamira soils contained 5 — 20 times more normal SFAs than Yungay soils: 0.4 and 1.5 $\mu\text{g/g}$ soil, respectively. Yungay also contained the fewest distinct monounsaturated fatty acids, with only two detected in soils collected at the “Yungay North” site. Altamira and Chañaral had much higher monounsaturated fatty acid content, exhibiting similar diversity to each other (Fig. 2.3).

Only the *n*-C_{16:1 Δ 9} and *n*-C_{18:1 Δ 9} monounsaturated fatty acids were detected in all samples along the transect (Fig. 2.3). Both *cis* and *trans* *n*-C_{16:1 Δ 9} were detected at all sites, and this unsaturated fatty acid was the only one to have detectable *cis* and *trans* isomers. The ratio of *trans* to *cis* *n*-C_{16:1 Δ 9} decreased with increasing dryness (Fig. 2.2). All ratios were less than or equal to 0.01. The highest *trans/cis* value measured was in Chañaral samples at 0.012, and the lowest value was 0.003 in Maria Elena soils.

The C₁₇ cyclopropane fatty acids (CFA) were only detected in Chañaral and Altamira soils at abundances of 0.05 and 0.12 $\mu\text{g/g}$ soil, respectively (Fig. 2.1g). CFA were not detected in Mina Julia, Yungay and Maria Elena soils. The ratio of CFA to SFAs was 0.12 in Chañaral, and 0.07 in Altamira. However, CFA were not detected in surface soils in Yungay, Maria Elena, and Mina Julia (Fig. 2.1g). In Yungay soils, the concentration of SFAs was 0.089 $\mu\text{g/g}$ soil, which was 4 — 17 times lower than Chañaral and Altamira, respectively. Assuming a similar ratio of CFA to SFAs (~ 0.1), the expected abundance of CFA in Yungay would still have been well above the detection limit of the instrument (<1 picogram C₁₇ CFA per gram of soil) given the

increased mass of soil extracted (88.8 g of Chañaral soil vs. 221.7 g of Yungay soil). Therefore, the absence of CFA in Yungay cannot be attributed to signal dilution due to lower biomass.

The D/L ratios of hydrolyzed aspartic acid were found to increase 5 times with decreasing aridity along the transect (Fig. 2.1h), indicating that greater racemization had occurred at drier sites. Specifically, Chañaral soils were found to have D/L ratios of 0.02, versus 0.10 in Yungay soils.

2.5.2 LDChip Immunoassay

The total immunoassay fluorescence significantly decreased from Chañaral to Yungay by a factor of 24 (Fig. 2.1d). A large fraction (>75%) of the antibody spots showed positive fluorescence in Chañaral soils (Fig. 2.5), indicating the presence of abundant polymeric biological material. By contrast, only 7% (18/242) were positive in Yungay, Mina Julia, and Aguas Calientes soils, mainly corresponding to antibodies to proteins and peptides and Cyanobacteria from the *Synechocystis* genus. The LDChip fluorescence indicates the presence of proteins through screening for the antibody binding to immunogenic peptides that are located at the most external part of the protein structure of interest. There were 8 peptides detected out of 73 tested in all soils along the transect (Fig. 2.6), but the immunoassay signal for these peptides decreased by up to an order of magnitude towards the driest sites. As the aridity decreased, the number of antibodies recognizing microbial markers increased, particularly those corresponding to Gram-positive bacteria (*Firmicutes* and *Actinobacteria*).

2.6 Discussion

CFA were present in Chañaral and Altamira surface soils, but were not detected in the drier surface soils in Yungay, Maria Elena, and Mina Julia (detection limit pg/g; see Results section) (Fig. 2.1g). The lack of detectable CFA in the driest

soils along the aridity gradient appears to be at odds with the trends in rainfall. Chañaral and Altamira experience 5-10 mm of rainfall on average every year (Warren-Rhodes et al., 2006), whereas Yungay, Maria Elena, and Mina Julia experience <2 mm of rainfall on average every year, with consecutive rainfall events interspaced by ten years or more (McKay et al., 2003). The difference in rainfall abundance and recurrence ought to induce a bigger stress response in active soil communities in the driest sites, resulting in a higher ratio of CFA to saturated fatty acids, or at least a measurable CFA signal. Instead, our results suggest that microorganisms in these extremely dry soils do not generate CFA in response to environmental stress. This possibly reflects very low or nonexistent metabolic activity. The alternative explanation that microorganisms in the driest soils are less stressed is unlikely given that other than aridity, physicochemical conditions like temperature, mineral content, and geologic terrain are similar between all sample sites analyzed (Warren-Rhodes et al., 2006). Our results are consistent with previous reports of the absence of cyclopropyl phospholipid fatty acids in Yungay soils (Connon et al., 2007).

It was expected that the ratio of *trans* to *cis* unsaturated fatty acids would increase with increasingly dry conditions. Yet the opposite trend is observed along the transect: the *trans/cis* ratio of the fatty acid $n\text{-C}_{16:1\Delta 9}$, the only unsaturated fatty acid with detectable *trans* and *cis* isomers in all Atacama soils analyzed, decreased with increasing dryness (Fig. 2.2). This trend also indicates a lack of bacterial activity in the driest soils, or that the active portion of the microbial population is greatly outnumbered by the inactive portion (i.e., signal dilution).

We observed an increase in the D/L ratio of aspartic acid liberated from proteins, peptides, and humic complexes in soils with increasing dryness (Fig. 2.1h). The highest value observed was 0.13 in Mina Julia soils, and the lowest was 0.02 in Chañaral soils. Yungay soils showed a D/L ratio of 0.10, lower than the previously observed value of 0.4 (Skelley et al., 2007). In all samples, there is undoubtedly some contribu-

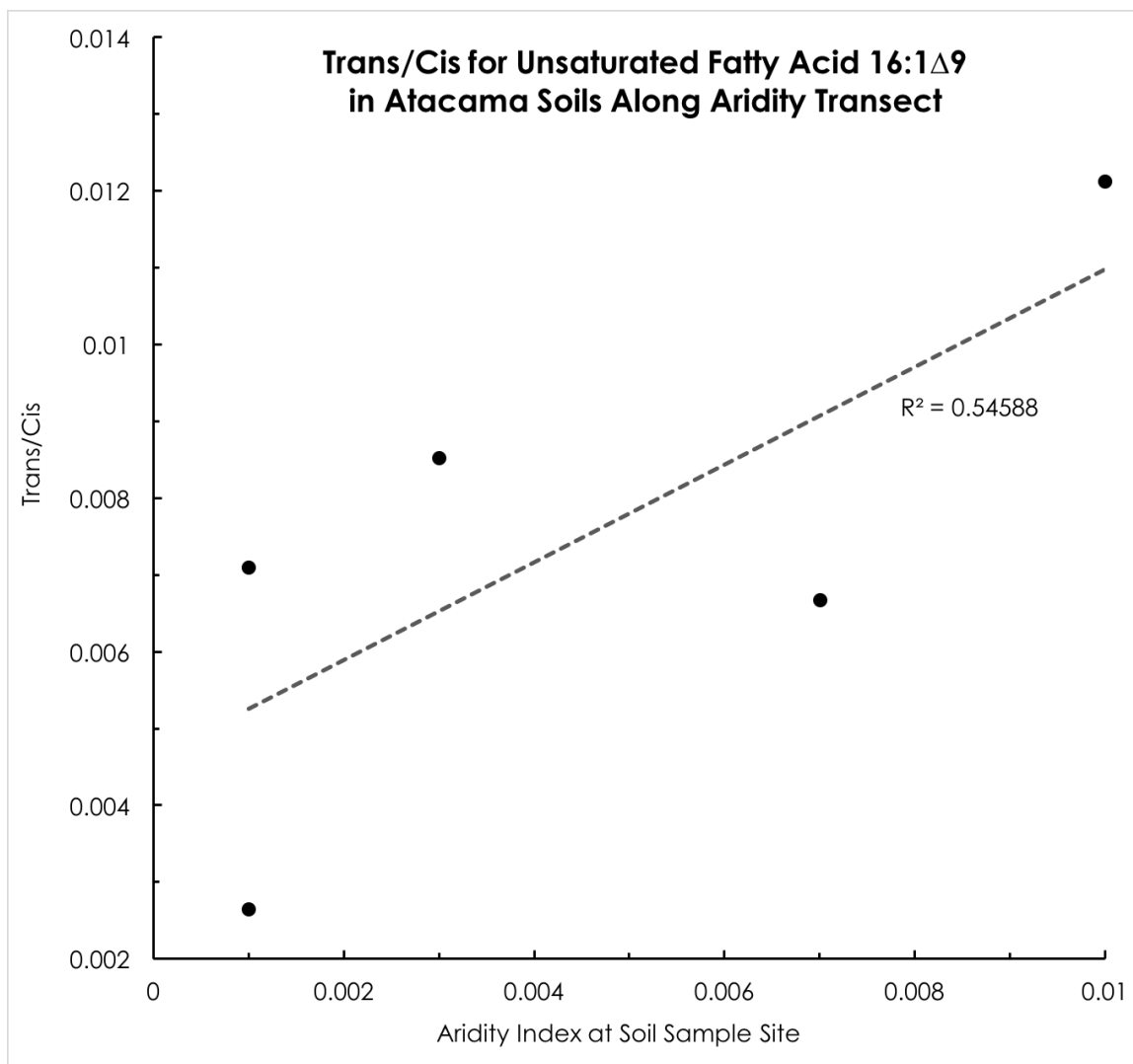


Figure 2.2: **Ratio of *Trans/Cis* Confirmation of the Double Bond of Unsaturated Fatty Acid $n\text{-C}_{16:1\Delta 9}$ in Atacama Soils Along Aridity Transect.** The unsaturated fatty acid $n\text{-C}_{16:1\Delta 9}$ was the only unsaturated fatty acid in detected in all Atacama samples in which both *cis* and *trans* isomers of the double bond on C_9 were present. The ratio of *trans* to *cis* for $n\text{-C}_{16:1\Delta 9}$ was found to decrease with increasing dryness. Bacteria modulate membrane fluidity in response to environmental stressors by converting the *cis* isomer to *trans*. Although we might expect this ratio to decrease with increasing dryness, the opposite is observed, perhaps indicating a lack of detectable metabolic activity in the driest soils along the transect.

tion of D-enantiomers from Gram-positive bacteria. However, given the age of these soils (Ewing et al., 2006), the order-of-magnitude differences in the D-enantiomer relative abundances between sites is likely primarily due to higher racemization in drier soils. Using a previously reported expression for calculating the “dry” sample age based on D/L ratios of aspartic acid in the Atacama (Skelley et al., 2007), our measured ratio returns a “dry” age of ~14,000 years in Yungay. This age is likely affected by both the viable and non-viable biomass. The viable population of organisms would contribute mostly enantiomerically pure amino acids, whereas dead organisms would contain more racemized amino acids. As such, the derived age of amino acids in hyperarid soils must be taken as an approximation rather than an absolute value. The derived age of amino acids in the driest soils supports the notion of limited, if any, metabolic recycling of organic matter over long periods of time.

While the data show no evidence of microbial growth in samples in the driest locations, we cannot rule out the synthesis of CFA at levels below detection limits (<1 pg/g soil), equivalent to a few active cells (assuming an average cell dry weight of 1 pg). Additionally, our results do not account for possible patchiness in microbial growth at spatial scales larger than the sampling scale (roughly 20 x 20 cm). Collectively, our data suggest that even after episodic rain events (McKay et al., 2003) or fogs (Cáceres et al., 2007) that occasionally saturate surface soils at the driest locations, microbial growth might not be possible because the duration of liquid water in the soils (Davis et al., 2010) might be too short to overcome the energetic demands of many years of complete desiccation (Noy-Meir, 1973).

The LDChip immunoassays revealed the presence of some peptides (8 out of 73 screened for) whose proteins are usually involved in desiccation and oxidative stresses. Their relative abundance, measured as immunofluorescence signal, decreases by about 2-13 times from Chanaral to Yungay (Fig. 2.6). Several lines of evidence may indicate that the observed peptides/proteins are not being synthesized *in situ* in the

driest soils. First, in the case of HtpG and DhnA, two epitopes in each protein were searched for with the LDChip, but only one was detected in Yungay, Mina Julia, and Aguas Calientes soils. This may imply that the protein is not intact, or a portion of the protein is not able to interact with the antibody. Second, the detection of peptides associated with the cyanobacterial IsiA, SodA, and SodF proteins in Yungay soils is at odds with the absence of cyanobacterial DNA (Connon et al., 2007; Crits-Christoph et al., 2013). However, this lack of detection of cyanobacterial DNA could be a result of the heterogeneous distribution of communities. This scenario is consistent with the immunodetection of cyanobacterial LDChip markers from a thousand-year-old Antarctic microbial mat in which no amplifiable cyanobacterial DNA could be detected (Blanco et al., 2017). The IsiA protein is synthesized in cyanobacteria when under iron deficiency (Chen et al., 2005; Wilson et al., 2007); the superoxide dismutase protein SodF is abundant in the cyanobacteria *Nostoc commune* after prolonged desiccation (Shirkey et al., 2000); and HtpG has been found to be essential in cyanobacteria acclimation to low temperature (Hossain and Nakamoto, 2002) and oxidative stress (Hossain and Nakamoto, 2003). It is possible that either cyanobacterial DNA is present at very low levels in Yungay and has eluded detection by PCR amplification, or these peptides are derived from other types of organisms. It is also possible that these proteins, or their fragments, reflect transport of cyanobacteria from other regions of the Atacama (Patzelt et al., 2014), with a better degree of preservation than DNA. Whether grown locally or wind transported, the LDChip detected the presence of *Synechocystis*-like cyanobacterial markers in Yungay, Mina Julia and Aguas Calientes (Fig. 2.5). Finally, DhnA, Hsp90, a homolog of HtpG, and a homolog of WshR could have been sourced from plants. Dehydrin protein DhnA is found in plants under desiccation stress (Saavedra et al., 2006). HtpG is a heat shock protein found in *Escherichia coli* (Spence and Georgopoulos, 1989), 42% identical to the hsp90 protein found in some plants (Krishna and Gloor, 2001). And the HR ho-

molog of WshR is used by plants in defense against bacterial pathogens (Wright and Beattie, 2004). Given that plants are not present in the extreme hyperarid soils and may have been absent for up to 2 million years (Ewing et al., 2008), these proteins or peptides were likely not synthesized *in situ*.

Taken together, the association of some of the detected peptides/proteins with plants or cyanobacteria in the extreme hyperarid soils, the decrease in abundance with increasing dryness, and singular peptide representation of a few proteins in extreme hyperarid soils strongly suggest that these peptides were not synthesized *in situ*, and instead have either been sourced from more active regions in the Atacama and/or preserved from a more active time period in the Atacama’s history. Based on the LDChip data alone, it is difficult to tell which of these two hypotheses are more likely. However, previous studies have suggested that the sparse microbial population in Yungay surface soils is primarily derived from atmospheric inputs (Connon et al., 2007; Lester et al., 2007), and atmospheric deposition dominates the input of organics into Yungay soils (Ewing et al., 2008). Additionally, the lack of CFA adds further credibility to the wind-blown hypothesis for the origin of biomass, given that if CFA were synthesized *in situ*, they are likely to be well preserved, especially in Yungay soils (Zhang and Rock, 2008; Wilhelm et al. 2017). Furthermore, the unsaturated fatty acid $n\text{-C}_{18:1\Delta 9}$, one of only two detected in all transect samples analyzed (Fig. 2.3), is known to occur in spores (Graham et al., 1995; Ruess et al., 2002; Sakamoto et al., 2004) which are easily blown by wind. Large quantities of $n\text{-C}_{18:1\Delta 9}$ have been reported in some soil spores (Madan et al., 2002). The ubiquity of $n\text{-C}_{18:1\Delta 9}$ along the aridity transect may indicate that organisms and biomolecules that are transported by aeolian processes on aerosols in this region are dominated by spores. This is consistent with the detection of spore-forming saprobes in hyperarid sands in the Atacama that are readily dispersed by wind (Conley et al., 2006).

Finally, microbial diversity and abundance were found to decrease with increasing

	Chañaral	Altamira	Mina Julia	Yungay North	Yungay South	Maria Elena
$n\text{-C}_{14:1\Delta 7}$	x					
$n\text{-C}_{15:1\Delta 4}$		x				
$n\text{-C}_{15:1\Delta 7}$	x	x			x	x
$n\text{-C}_{15:1\Delta 9}$	x	x	x		x	x
$n\text{-C}_{15:1\Delta 9}$			x			
$n\text{-C}_{16:1\Delta 9}$	x	x	x	x	x	x
$n\text{-C}_{16:1\Delta 11}$	x	x	x			
$n\text{-C}_{17:1\Delta 9}$	x	x	x		x	x
$n\text{-C}_{17:1\Delta 11}$	x	x	x			x
$n\text{-C}_{18:1\Delta 9}$	x	x	x	x	x	x
$n\text{-C}_{18:1\Delta 11}$	x	x	x		x	x
$n\text{-C}_{18:1\Delta 13}$	x		x			
$n\text{-C}_{19:1\Delta 9}$	x	x	x			x
$n\text{-C}_{19:1\Delta 11}$			x			
$n\text{-C}_{20:1\Delta 11}$	x	x	x			
$n\text{-C}_{22:1\Delta 13}$		x	x			x

Figure 2.3: Normal Monounsaturated Fatty Acid and Bond Position Detected in Transect Samples.

dryness. We used the number of unique fatty acids as a general proxy for microbial diversity (e.g., White et al., 1993). A positive linear correlation ($R^2 > 0.97$) was observed between aridity index and the number of unique fatty acids in surface soils (Fig. 2.4). Chañaral had >3 times the number of unique fatty acids as Yungay. This trend is consistent with DNA sequence data (Crits-Christoph et al., 2013). The total abundance of normal saturated fatty acids also decreased with increasing dryness. Altamira soils had the highest fatty acid abundances, >17 times the 88.8 ng/g abundance of normal fatty acids detected in Yungay soils. The decline in diversity and abundance of fatty acids with increasing dryness is consistent with LDChip total fluorescence data and unique detections of antibodies (Figs. 1d, 4, 5). Total fluorescence decreased by a factor of 24 between Chañaral and Yungay. Furthermore, a large fraction of unique antibodies tested showed positive immunodetection in Chañaral, whereas Yungay soils only rendered 18 unique immunodetections (Fig. 2.5). Low abundance and diversity of biomarkers does not necessarily indicate that metabolic activity is not occurring, but when considered along with the lack of CFA, unsaturated fatty acid *trans/cis* ratio trends, peptide/protein content and fragmentation, and high aspartic acid D/L ratios, the low abundance and diversity of organisms could indeed be a hallmark of a lack of significant biological activity in the driest Atacama soils. The presence of biomarkers even in the driest Atacama soils demonstrates that soils can be non-sterile, but also generally not habitable under the current climate regime. We propose that an additional aridity classification is needed to distinguish these regions as “extreme hyperarid” (Fig. 2.1b).

2.7 Conclusion

Our novel use of an array of biochemical markers such as lipids, amino acids, and peptides along the aridity transect reveals that biological activity is either not occurring or extremely low in the driest Atacama soils. Lipid and peptide data point to

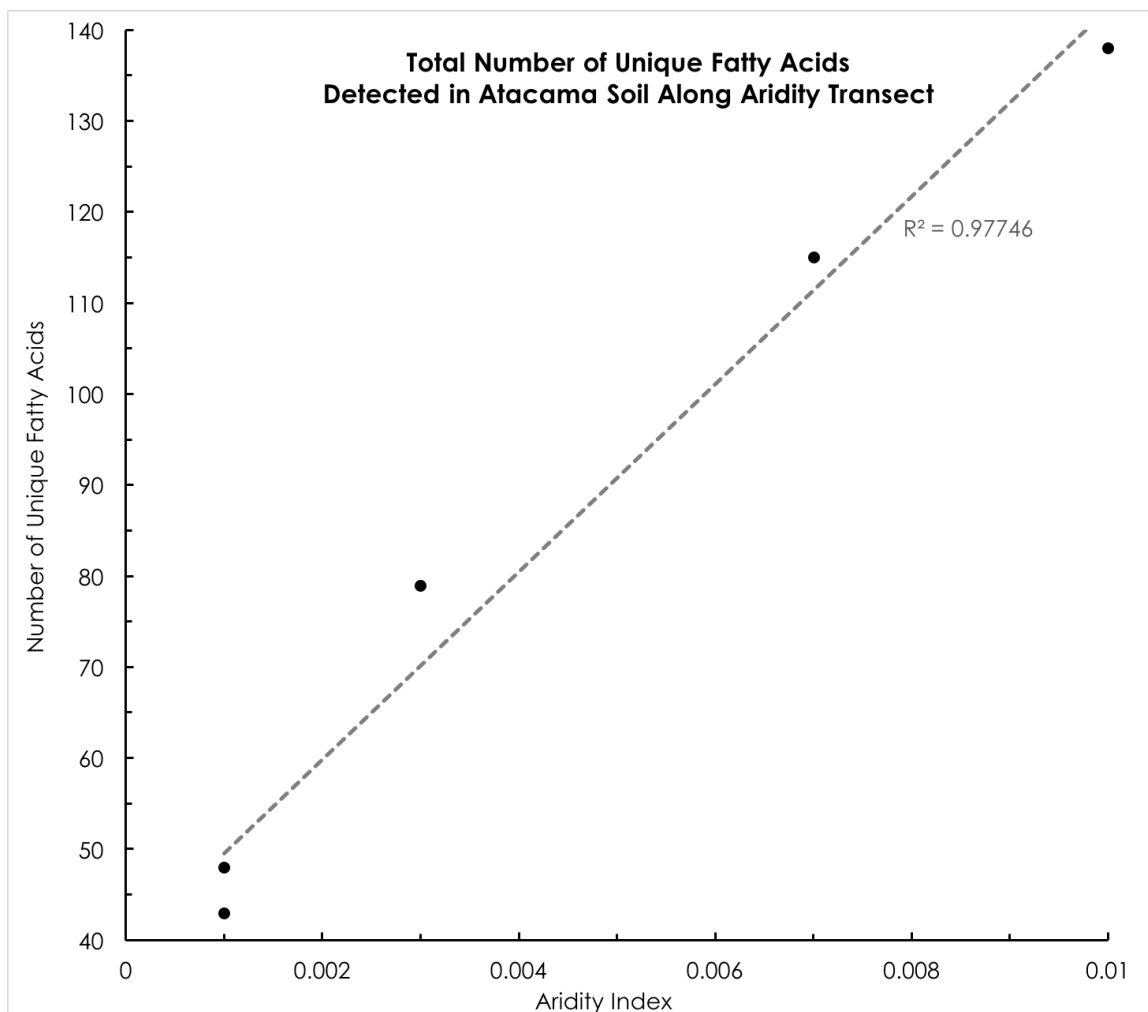


Figure 2.4: Total Number of Unique Fatty Acids Detected in Atacama Soils Along Aridity Transect. A positive linear correlation is found between the total number of unique fatty acids and aridity index. The number of unique fatty acids in soils decreases approximately 3 times with an order of magnitude decline in aridity index value. Fatty acids containing 12-30 carbons including normal and saturated, dicarboxylic, branched, multi-branched, mono and polyunsaturated fatty acids are included in this total number, and can be used as a proxy for diversity of organisms contained within the soil.

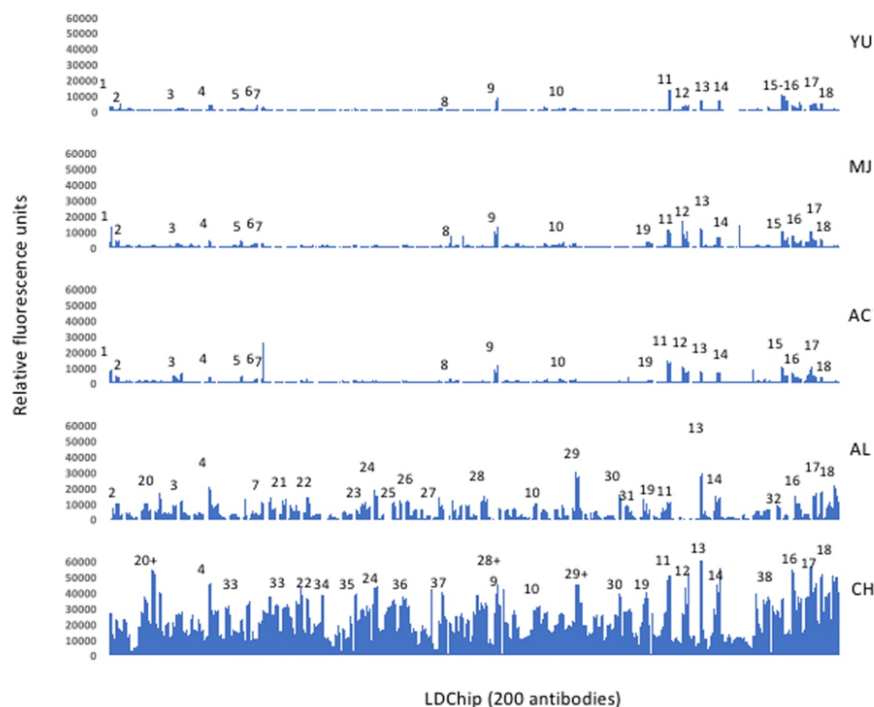


Figure 2.5: Immunoprofiling the aridity gradient in Atacama Soils with LD-Chip. Each antibody on the plot is represented by the 3 bars obtained by quantifying the fluorescence of spots on LDChip. Different compounds in the samples reacted with the antibodies on the chip produced the following immunogens: 1, *Leptospirillum ferrooxidans*; 2, 3, *Acidithiobacillus ferrooxidans*; 4, *Halothiobacillus neapolitanus*; 5, *Tumebacillus* sp.; 6, *Planococcus*; 7, *Psychroserpens burtonensis*; 8, *Pyrococcus furiosus*; 9, *Synechocystis* sp.; 10, *Dechloromonas aromatica*; 11, DhnA, fructose-bisphosphate aldolase from cyanobacteria. Dehydrin protein related with plants and induced under dessication stress; 12, FdhF, formate dehydrogenase H; 13, HtpG, the heat shock protein HtpG, which is a homolog of HSP90, is essential for basal and acquired thermotolerances in cyanobacteria. HtpG is involved in the acclimation to low temperatures in cyanobacteria; 14, IsiA, photosystem II chlorophyll a-binding protein induced under desiccation in cyanobacteria; 15, PhaC1 and PhaC2, class II poly(R)-hydroxyalkanoic acid synthase. Polyhydroxyalkanoate (PHA) synthase genes C1 and C2 from *Pseudomonas putida*. PHAs are produced under nutrient limitations as N and P; 16, PufM, which encodes the M subunit of the photosynthetic reaction centers of most known anoxygenic phototrophs as *Rhodospirillum rubrum*; 17, SodA, SodF, Iron superoxide dismutase involved in desiccation resistance in *Nostoc*; 18, WshR, water stress hypersensitive response protein *Pseudomonas*; 19, Bacterial ferritin; 20, Cells from iron/sulfur environment; 21, *Acidocella aminolytica*; 22, *Sulfobacillus acidophilus*; 23, *Salinibacter ruber*; 24, *Streptomyces* sp.; 25, *Shewanella oneidensis*; 26, *Bacillus subtilis*; 27, *Haloferax mediterranei*; 28, *Anabaena* type strain; 28+, Other cyanobacteria as *Chroococcidiopsis* sp.; 29, 29+, Peptidoglycan (2 Mabs); 30, Perchlorate reductase; 31, Iron reductase; 32, *P. furiosus* ferritin; 33, *Psychrobacter frigidicola*; 34, *Streptomyces* spores; 35, *Desulfosporosinus meridiei*; 36, *Azotobacter vinelandii*; 37, *Halorubrum* sp.; 38, OppA transporter component.

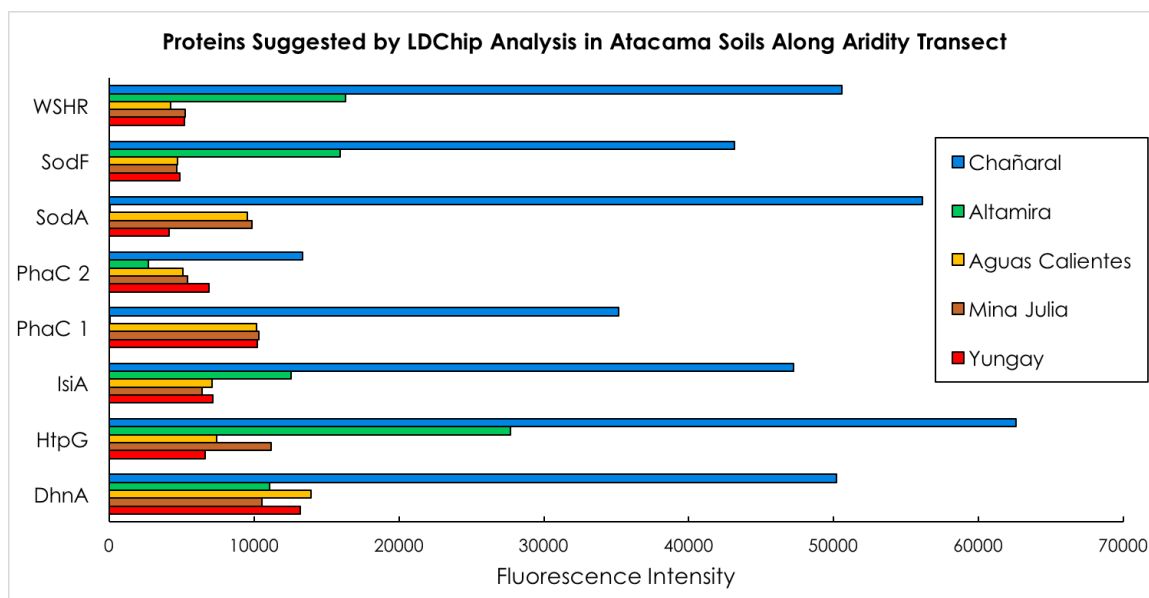


Figure 2.6: **Proteins Indicated by LD Chip in Atacama Soils Along Aridity Transect.** Only 8 proteins out of 73 screened for were detected in all hyperarid Atacama soils analyzed by the LDChip immunoassay. In general, these proteins are synthesized under physiological stressful conditions such as nutrient limitation, desiccation, oxidative stress, high temperature, and irradiation. Protein names and functions are included in the Discussion. These 8 proteins were found to decrease in abundance by a factor of 2-13 with increasing dryness along the aridity transect from Chañaral soils to Yungay. The florescence intensity plotted is the average of three spots on the LDChip.

biomolecules not currently being synthesized *in situ*, and perhaps transported from more active regions in the Atacama and deposited in extreme hyperarid soils. Amino acid racemization data suggest that this biological material is then left to slowly degrade over timescales of tens of thousands of years in surface soils. Despite the non-habitability of the driest Atacama soils under the current climatic conditions, clearly biogenic biomarkers and biomolecular trends are well-preserved.

In the driest region of one of the driest deserts on Earth, water availability is too low to allow the majority of a soil microbial population to grow. This presents a unique set of trends in biomarker content of soils that distinguishes it from other, only slightly wetter parts of the desert (Fig. 2.7). These features include a lack of (1) colonization by plants and lichens, (2) a lack of lipids that indicate membrane modulation in response to deleterious environmental conditions (such as cyclopropane fatty acids and *trans/cis* ratios of unsaturated fatty acids), (3) significant racemization of amino acids contained in surface soils, (4) a relatively low abundance and diversity of biomass/TOC (this study; Ewing et al., 2008; Crits-Christoph et al., 2013), and (5) a <1% colonization of stones by hypolithic organisms (Warren-Rhodes et al., 2006). As such, we propose that a new ecoregion demarcation (Olson et al., 2001) is warranted to reflect this general biological inactivity of extremely hyperarid regions. These biomarker characteristics would be worth exploring in other hyperarid terrestrial regions that experience similarly low levels of water activities, such as the University Valley portion of the McMurdo Dry Valleys in Antarctica (Goordial et al., 2016), where water availability to organisms is limited by cold temperatures.

Differences in Biomarker Content of Soils Under Increasingly Dry Conditions

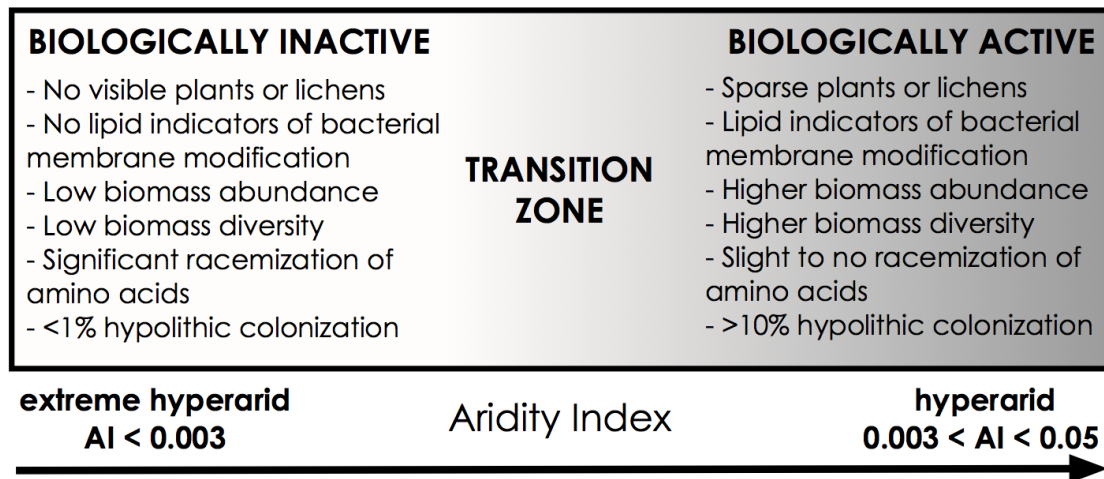


Figure 2.7: **Conceptual Figure Showing Differences in Biomarker Content of Soils Under Increasingly Dry Conditions.** Key differences are observed in soils biomarker content along the Atacama's aridity transect including lipids, amino acid racemization, and peptides (this paper), and hypolithic colonization (Warren-Rhodes et al., 2006) that suggest that biological activity may not be occurring or negligible in the driest soils. In light of these differences, we propose a new ecoregion demarcation (Olson et al., 2001) and suggest that it's warranted to reflect the biological inactivity of soils that is imposed by extreme hyperaridity.

CHAPTER 3

XEROPRESERVATION OF FUNCTIONALIZED LIPID BIOMARKERS IN HYPERARID SOILS IN THE ATACAMA DESERT

3.1 Introduction

Understanding taphonomic processes and the conditions conducive to long term preservation of organic matter has been critical for reconstructing the evolutionary history of life on Earth (Peters et al., 2005) and in developing strategies to search for evidence of life elsewhere (Eigenbrode, 2008; Summons et al., 2011). Microbial processes mediate the majority of organic matter decomposition (Skopintsev, 1981; Petsch et al., 2001; Kuzyakov, 2010), with only approximately 0.1% of the global net primary production preserved in the sediment record (Holser et al., 1988; Des Marais, 2001). This limits the quantity and quality of molecular fossils (a.k.a. biomarkers) that become preserved after organisms die.

Long-term preservation of biomarkers is enhanced when fast sedimentation or mineral encapsulation impede or mitigate microbial attack (Van Veen and Kuikman, 1990; Farmer and Des Marais, 1999), or under environmental conditions that limit microbial activity and retard organic degradation, such as low temperature and humidity (Rethemeyer et al., 2010). In this chapter, we focus on the preservation of biomolecules in an environment that has been extremely dry (i.e. hyperarid, aridity index <0.05) over geologic timescales. While hyperarid deserts represent 7.5% of the Earth's continental landmass (UNEP definition) and fossils are known to be preserved in them (Pyenson et al., 2014), biomarker degradation and taphonomic processes over geological timescales in a hyperarid environments has not been previously investigated. We hypothesized that typical pathways of organic matter degradation

would be inhibited in long-lived hyperarid regions where low water activity suspends microbial activity and greatly reduces enzyme action (de Gomez-Puyou and Gomez-Puyou, 1998).

The accumulation and degree of preservation of biomolecules is investigated in million-year-old hyperarid soils in the Atacama Desert, the oldest, continuously dry desert on Earth (Clarke, 2006). Lipids were investigated in particular because they have functional groups that are susceptible to microbial attack, but also contain recalcitrant hydrocarbon cores that can be preserved over geologic time scales, recording the presence and activity of organisms living millions to billions of years ago as well as the history of diagenetic conditions since the time of deposition (Peters et al., 2005; Eigenbrode, 2008).

3.1.1 Study Site

The Yungay region of the Atacama Desert experiences <2 mm of precipitation annually (McKay et al., 2003), with rain events often interspaced by a decade or more. The Aridity Index value, which is defined as the ratio of mean annual precipitation to potential evapotranspiration, is approximately 0.001 in this region. This value is 30-100 times more arid than the Mojave or Gobi Deserts (Davila and Schulze-Makuch, 2016).

Surface soils in the Yungay region primarily experience water activities that range from 0.01-0.52 over the course of a diurnal cycle (Connon et al., 2007), well below 0.6, the threshold for microbial growth (Grant et al., 2004). The extreme aridity causes an absolute lack of habitation by plants or animals and can only support a sparse microbial population in surface soils that are primarily derived from atmospheric inputs (Warren-Rhodes et al., 2006; Connon et al., 2007; Lester et al., 2007, Chapter 2). This region has been arid to semiarid since the late Jurassic (150 million years), and has experienced continuous hyperaridity for the last ~ 2 million years (Hartley and

Chong, 2002; Hartley et al., 2005; Jordan et al., 2014). Fluvial incision and deposition ceased at Yungay near the Plio-Pleistocene boundary coinciding with transition to hyperarid climatic conditions within the region. Subsequent to drying, landforms have retained and accumulated the aeolian deposits of atmospheric salts and dust in the upper meter of the soil column (Ewing et al., 2006).

A 2.5 m stratigraphic sequence in a soil pit that was previously dug (Sutter et al., 2007) was sampled, and can be generally categorized into three major units (Fig. 3.1A): (i) gypsiferous soils in the top 90 cm; (ii) clay-rich units below 90 cm depth; and (iii) a 10 cm thick well-cemented, massive halite unit that interrupts the clay units at 140-150 cm depth. Within the top 2 meters of soil, 87% of the NaCl is located in this massive halite unit (Ewing et al., 2006). Sparse plant material is found in the clay units below the massive halite unit (Ewing et al., 2008; Fig. 3.6).

Landform ages in this region are ~ 2 million years based on cosmogenic radionuclide concentrations in surface boulders and Ar isotopes in interbedded volcanic ash deposits (Ewing et al., 2008). During this time, atmospheric salts have been vertically redistributed in the top ~ 1.5 meters of unaltered fluvial deposit and dust derived silicate matrix due to episodic wetting events Ewing et al. (2006; 2008). Small rain events (1 mm or less) do not saturate the surface soil in Yungay, nor are able to percolate past the gypsic crusts at 10-20 cm depth (Davis et al., 2010). These gypsic crusts act as a strong barrier to the diffusion of moisture into the soil (Davis et al., 2010). For larger rain events that are able to percolate down past the gypsic crust, according to (Ewing et al., 2006; 2008), the massive, well-cemented halite unit at 140-150 cm signals the maximum depth of rainwater percolation and salt distillation over the last 2 million years. This is further supported by the low concentrations of soluble ions, including chloride, in layers below the halite. Hence, the massive, well-cemented halite unit has acted as an aquiclude, preventing clay layers beneath from being exposed to rainwater and other modern surficial processes (Ewing et al., 2006).

Consequently, organic matter in the deeper clay layers is of fossil origin, possibly older than 2 million years but at least $>40,000$ years because it is “radiocarbon dead” (Ewing et al., 2008), and represents a rare opportunity to investigate the degradation of functionalized lipid biomarkers over geological timescales in the absence of water.

3.2 Methods

3.2.1 Sample Collection

Seven samples were collected from the soil pit in Yungay. Samples were collected in September 2014, before the decennial rain event that occurred in March 2015. Due to the extremely low inventory of biomass in Atacama soils (Ewing et al., 2006), samples were collected by scientists wearing full-body, sterile, clean-room suits (<1 colony forming unit per 10,000 garments), masks, glasses, and gloves to minimize the introduction of emitted anthropogenic biological contaminants (Meadow et al., 2015) during sampling. To remove surface contamination and expose fresh faces of the different soil horizons, approximately 20 cm of the pit wall was removed using a solvent-cleaned chisel. Samples were then collected in the soil pit from the bottom up using a unique solvent-cleaned drill bit to loosen the material. A unique solvent-cleaned spoon was used to scoop samples into glass jars that had been heated to 500°C for greater than 8 hours. Each sample was collected using a unique drill bit and spoon to minimize cross contamination. Surface soils and sulfate-rich sample from 10 cm depth were collected about 50-100 m away from soil pit where there was no visible foot traffic. Samples were kept frozen until being returned to NASA Goddard Space Flight Center for storage at -20°C .

Before sampling, glass jars (Qorpak 8oz clear straight sided round with green polypropylene cap and PTFE disc attached, cleaned and certified for semi-volatiles) were washed in Method Smarty soap, rinsed three times with tap water, then rinsed three times with distilled water (18.3 Mohm), dried overnight, then ashed at 500

degrees C overnight (>8 hr). Lids were wiped with a Kimwipe soaked in methanol to remove dust. Then lid was attached to clean jar and shaken with methanol, acetone, then hexanes. Lids never came into contact with the sample; ashed ultra high vacuum aluminum foil (All-Foils Inc.) was placed over ashed glass jars before lid was attached. Sampling spoons were scrubbed with a brush with Simple Green detergent. They were then rinsed three times with tap water, three times with distilled water, methanol, acetone, and hexanes. Drill bits and chisels were put into a dishwasher with Method Smarty Soap. They were heavily scrubbed with Simple Green detergent, then rinsed in tap water and distilled water. They were sonicated in a methanol bath for 15 minutes, and then were then rinsed with methanol immediately after being pulled from the bath. They were then rinsed three times with methanol, acetone, then hexanes.

3.2.2 Lipid Analyses

Glass jars containing samples were removed from the -20°C freezer and were kept for 30 minutes to 1 hour at room temperature to prevent condensation of moisture onto soil directly. Soils were not lyophilized, in order to reduce the exposure time to the laboratory environment to minimize contamination risk and due to the extremely low water content in the hyperarid soils. Preliminary samples that were lyophilized to estimate water content in soil showed only 1.4% reduction in mass due to water loss.

For each unique sample, approximately 100 g of soil was homogeneously powdered with a solvent washed and ashed ceramic mortar and pestle. Soil samples were extracted using a modified Bligh and Dyer protocol (Bligh and Dyer, 1959; Jahnke et al., 1992). The protocol was modified primarily to minimize transfer steps and thus minimize loss from these organically lean soils. Three extractions were then performed on 70-90g of a powdered sample, 40 mL of HPLC-grade H₂O, 100 mL of methanol, and of 50 mL of methylene chloride. After addition of solvents, the resultant slurry

was sonicated and stirred. The mixture was then left to settle until solvent became mostly clear. Clear solvent was poured into a new flask. The monophasic extraction mixture of HPLC-grade water, methanol, and methylene chloride was split by further addition of methylene chloride and water to a final volume ratio of 1:1:0.9. This mixture was gravimetrically separated. Solvent extracts were added to separatory funnel with 180 mL of extract and 47 mL of methylene chloride and inverted two times to mix. Water (47 mL) was then added to drive methanol into the aqueous phase. The methylene chloride layer was slowly drained into a new flask. The methanol and water phase was discarded. The resulting extract was evaporated under a stream of N₂ and transferred into smaller vials until 100 μ L remained. Care was taken to minimize the number of containers used in the evaporation process and to thoroughly rinse and sonicate the sides of all vessels after draining to recover any lipid left behind. 10% of the total lipid extract was set aside for LC-MS (1/100 of 10% of the total lipid extract was injected on the LC-MS).

Thirty percent of the total lipid extract was subjected to a medium acid methanolysis (Kates, 1989) to cleave ester-linked membrane fatty acids and to methylate free fatty acids (FFA) through reaction with commercial methanolic HCl 0.5N (Supelco, LC08137B) following the Kates, 1986 procedure. This simultaneously adds a methyl group to free fatty acids, and also tranesterifies complex lipids (phospholipids, triacylglycerols, steryl esters). This breaks the ester bond liberating the previously esterified fatty acids and then methylates them. Acid methanolysis gives a “total” solvent-extractable fatty acid pool, and thus produced a total fatty acid methyl ester (FAME). One microliter of a 1 microgram per microliter 5 α -cholestan-3 β -ol standard was then added. The derivatized portion was silylated with bis-(trimethylsilyl) trifluoroacetamide (BSTFA) (Fluka, Lot number BCBL7513V). This step silylated OH groups on hydroxyl FAMEs, remaining FFA, and should have also silylated any other hydroxyl lipids (sterols, alkanols) had they present. The final volume was 40 μ L,

which contained 30% of the derivatized total lipid extract. 1/40th of this volume was then injected into the GC-MS. This aliquot of the derivatized TLE (30% of total) was analyzed on an Agilent 5975C gas chromatograph-mass spectrometer (GC-MS).

GC-MS was performed on an Agilent 5975C inert XL MSD system equipped with an Agilent DB-5MS column (60 m x 250 μ m x 0.25 μ m, Agilent, Santa Clara, CA, USA) with helium as carrier at 1mL/min. We separated lipids by the following protocol: the oven temperature was held at 70°C for 2 min and then increased from 70°C to 130°C at 10°C per min, then increased to 310°C at 4°C per min and held at this temperature for 37 min.

The lipids were quantified relative to an internal standard (5 α -cholestanol, 12.5 ng on column). A portion of each TLE (10% of total) was also analyzed for glycerol di- and tetraethers on a 1260 Infinity series liquid chromatograph-mass spectrometer (LC-MS). Following a LC-MS version of the tandem column protocol (Becker et al., 2013), lipid analyses were performed on an Agilent 1260 Infinity series liquid chromatography system coupled to a 6130 quadrupole mass spectrometer via APCI interface. Separation of compounds was achieved with two ACQUITY UPLC BEH HILIC Amide columns (2.1 x 150 mm, 1.7 μ m, Waters, Eschborn, Germany) maintained at 50°C. The solvent gradient program used a constant flow rate of 0.5 mL/min and: 1. a linear change from 3% B to 20% B in 20 minutes; 2. a linear increase to 50% B at 35 minutes; 3. a linear increase to 100% B at 45 minutes, holding for 6 minutes; and 4. a decrease to 3% B for 9 minutes to re-equilibrate the column, where A was n-hexane and B was n-hexane/isopropanol (90:10). APCI source conditions were positive ion mode, drying gas (N₂) temperature 350°C, vaporizer temperature 380°C, drying gas flow rate 6 L/min, nebulizer gas (N₂) pressure 30 psi, capillary voltage 2000 V, corona current 5 μ A. Glycerol di- and tetraethers were detected by both full scans and selected ion monitoring. Lipids were identified on the basis of accurate mass (better than 1 ppm), retention time, and diagnostic fragments, and

quantified by $[M+H]^+$, with an extraction window of individual ion chromatograms being ± 0.01 m/z units. We used C46 GTGT as injection standard to determine the concentration of glycerol ether lipids.

3.2.3 Anion Analysis

Samples were sieved to obtain a <2 mm fraction. This fraction was then thoroughly ground with a mortar and pestle. One g of crushed soil fraction was then extracted with 20 g of Milli-Q water and diluted an additional 10 times. Samples were spiked with 12.5 μ L of 1 mg/L $^{35}\text{Cl}^{18}\text{O}_4$ as the internal standard.

The ion chromatography-mass spectrometry-mass spectrometry (IC-MS-MS) analysis protocol used an IC-25 isocratic pump with an EG40 electrochemical eluent generator, 2 mm bore AG21/AS21 guard and separation column sets housed in a LC30 temperature controlled oven (30°C), ASRS-Ultra II anion suppressor in external water mode, and a CD-25 conductivity detector, all from ThermoFisher/Dionex. Around the elution window of perchlorate ($t_R \sim 45$ min), 40 min after injection, a diverter valve directed the CD25 effluent to a tandem mass spectrometer (Thermo Scientific Quantum Discovery Max with a heated ESI probe and enhanced mass resolution). Electrochemically generated high purity KOH eluent was used in gradient mode at a concentration of 5 mM to 80 mM and a flow rate of 0.35 mL/min. Eluent generation, sample injection (5 μ L), electrochemical suppression, autoranging conductivity detection and data acquisition were all conducted under Excalibur/Chromeleon software control. Perchlorate was quantified by the -99 to -83 Th (m/z) transition ratioed to the -107 to -89 Th internal standard transition. All data were interpreted in terms of a 5-point calibration with check standards run daily. Any sample falling outside the calibration range was reanalyzed after appropriate dilution. All samples were minimally analyzed in triplicate.

3.3 Results

The abundance and diversity of functionalized lipid groups increased with depth throughout the profile (Figs. 3.1b and 3.2). The most abundant class of lipids detected were FAMES, which are formed through the transesterification of esterified fatty acids (e.g., complex membrane-bound polar lipids, acylglycerols, sterol esters) as well as methylation of FFAs (Ichihara et al., 1996). Between 20 and 62 unique FAMES were detected in each sample with alkyl chain lengths between 13 and 34 carbons, including methyl-branched FAMES (terminal branched and mid-chain). The FAME profile composition was markedly different between horizons (Fig. 3.2), with diversity and abundance increasing with depth (Figs. 3.1b and 3.2). FAMES were particularly abundant in the clay layers, with a maximum concentration in the deepest layer analyzed (215 cm) of 742 ng/g soil, comprised of 62 unique FAMES. The abundance of FAMES in the gypsiferous soil was lower by a factor of 4 or more. Deeper clay layers contained FAMES with unsaturated bonds in their alkyl chains (Fig. 3.2). Small amounts of silylated fatty acids were also detected in soils 100 cm and below, reflecting free fatty acids not methylated during our acid methanolysis procedure (Table 3.1). Additionally, α - and β - monohydroxy monocarboxylic fatty acids were detected that contain a hydroxyl (OH) group exposed to the external environment and available to be chemically altered. Based on the diagnostic fragment ions at m/z 175 and 159, α -hydroxy fatty acids were the more abundant member.

The upper gypsiferous soils were dominated by n -C_{16:0} and n -C_{18:0} FAMES, and contained both iso and antiso FAMES (Fig. 3.2). N -alkanes were also present in these units and had an unusual, slight even-over-odd chain length preference in the C₂₅-C₃₃ range (Fig. 3.3). Contamination from petroleum can be excluded by the absence of phenanthrene and other polycyclic aromatic hydrocarbons in the samples (Volkman, 2006). Hydroxy fatty acids were not detected in the gypsiferous soils, with the sole

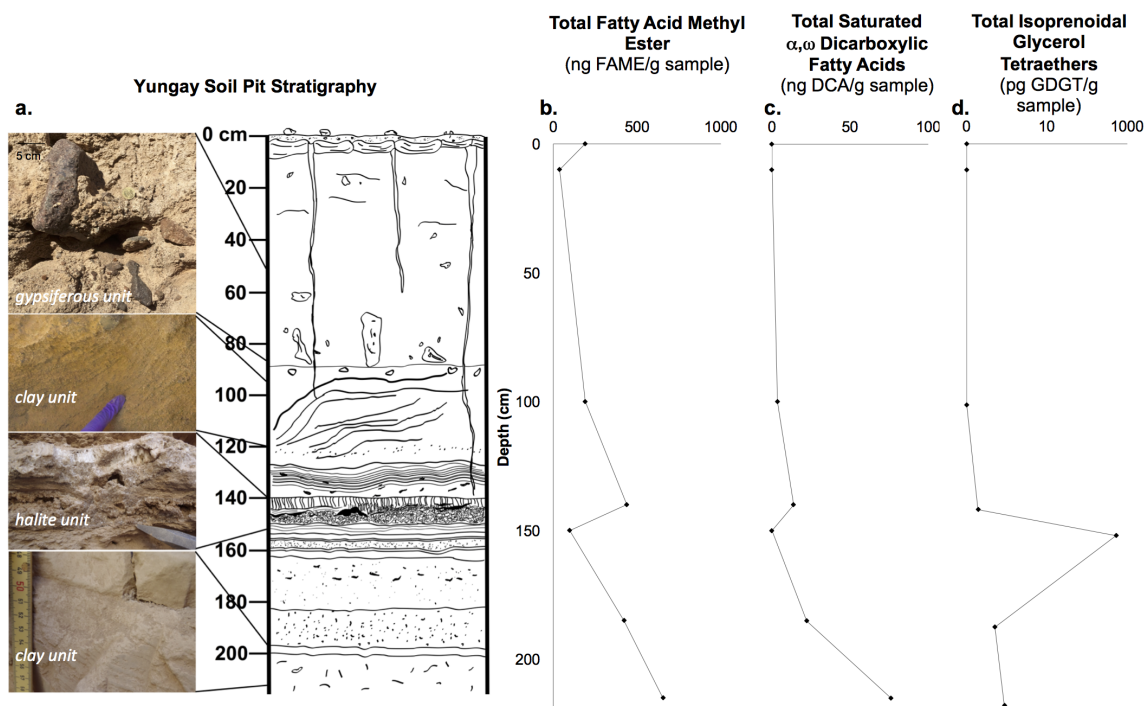


Figure 3.1: Yungay Soil Pit Stratigraphy and Key Lipid Abundances: a) The soil pit contains three major units: gypsiferous soils (0-90 cm depth), clay-rich units (> 90 cm depth), and a 10 cm-thick halite unit that interrupts clay units at 150 cm depth. Gypsiferous soils are matrix-supported and contain angular lithics. A clay unit at 100 cm depth contains centimeter-sized laminations composed of coarse sand. A clay unit at 140 cm depth contains fine sub-cm sized laminations (Fig. 3.6). The massive, well-cemented halite unit (~140-150 cm) has two major morphologies: vertical, crystalline structures and mottled halite. Beneath are alternating bands of well-sorted clay units and contain fibrous plant fragments (cm-size) that become more concentrated with depth. A more detailed description of the stratigraphic profile is provided by (Ewing et al., 2006; 2008). b, c, d) Total abundances of FAME, DCA, and Isoprenoidal GDGT were found to increase with depth with the exception of the halite unit (150 cm). Isoprenoidal GDGT and DCA were absent from upper gypsiferous soil. Isoprenoidal GDGTs are plotted on a logarithmic scale due to the presence of a high relative abundance of Archaeol in the halite unit.

Table 3.1: Free Fatty Acids in Yungay Pit Soils Detected through Derivatization with a Silylation Agent (ng free fatty acid/ g of sample): Note these values do not represent the total amount of free fatty acid present in the soils, but instead reflects free fatty acids that remained after acid methanolysis. Some of the FAME content is comprised of what were free fatty acids prior to analysis. N.d. is not detected.

Carbon Chain Length	100 cm depth (clay unit)	140 cm depth (clay unit)	150 cm depth (halite unit)	185 cm depth (clay unit)
12	n.d.	n.d.	0.10	n.d.
13	n.d.	0.08	n.d.	0.01
14	n.d.	0.32	0.03	0.04
15	0.12	0.29	n.d.	0.04
16	0.61	0.91	1.53	0.17
17	n.d.	0.62	n.d.	0.16
18	0.62	0.40	0.26	0.12
19	0.08	0.15	n.d.	0.11
20	0.02	0.16	n.d.	0.11
21	n.d.	n.d.	n.d.	0.80
22	0.31	0.41	n.d.	0.35
23	n.d.	n.d.	n.d.	n.d.
24	n.d.	n.d.	n.d.	1.43
25	n.d.	n.d.	n.d.	n.d.
26	0.38	n.d.	n.d.	n.d.
27	n.d.	n.d.	n.d.	n.d.
28	0.20	n.d.	n.d.	n.d.

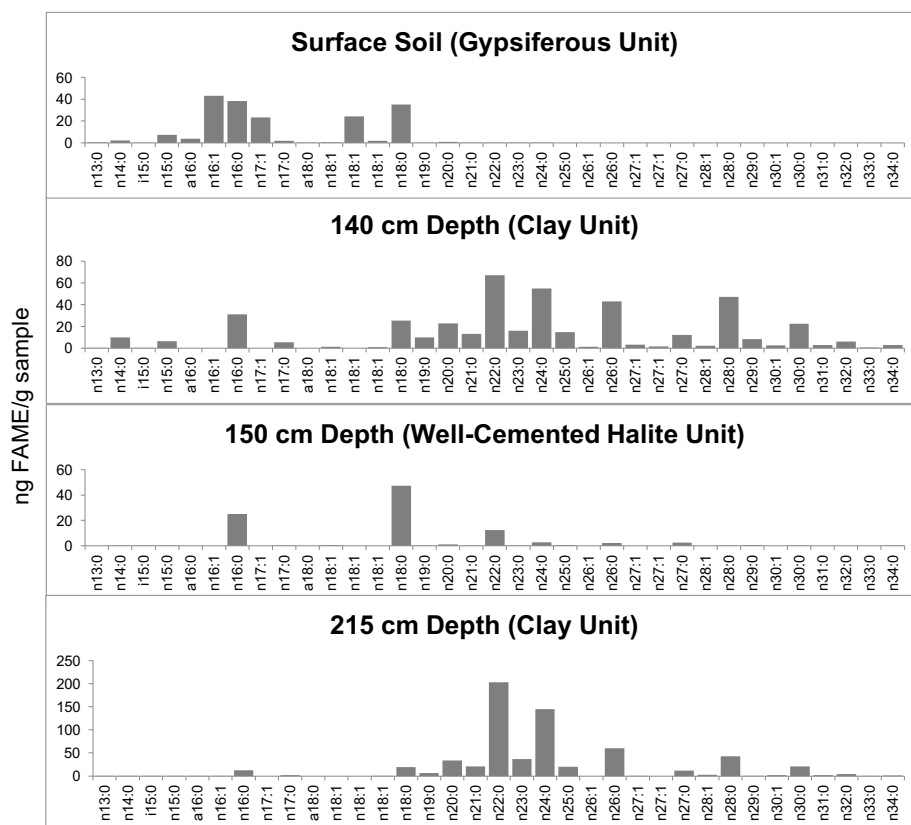


Figure 3.2: **Fatty Acid Methyl Ester (FAME) Profiles for Representative Yungay Pit Samples:** Upper gypsiferous soils were dominated by n -C_{16:0} and n -C_{18:0} FAMES. On the other hand, clay units were dominated by n -C_{22:0} and greater chain length FAMES and contain a greater diversity in FAME content. The deepest clay unit had the greatest total FAME abundance. The well-cemented halite unit was dominated by n -C_{16:0} and n -C_{18:0} FAMES. The vertical scale changes between plots.

Table 3.2: Monohydroxy Monocarboxylic Fatty Acids in Yungay Pit Soils in ng hydroxy fatty acid per g sample N.d. is not detected.

Carbon Chain Length	Surface Soil (gypsiferous unit)	100 cm depth (clay unit)	140 cm depth (clay unit)	150 cm depth (halite unit)	185 cm depth (clay unit)
15	n.d.	n.d.	n.d.	n.d.	0.02
16	0.95	0.32	n.d.	n.d.	0.22
17	n.d.	n.d.	0.09	n.d.	0.10
18	n.d.	0.16	0.12	0.09	0.18
19	n.d.	0.19	0.58	n.d.	0.08
20	n.d.	0.36	0.39	n.d.	0.51
21	n.d.	0.19	0.40	n.d.	0.84
22	n.d.	0.74	1.45	0.25	4.70
23	n.d.	0.77	1.50	0.07	7.37
24	n.d.	n.d.	n.d.	n.d.	32.94
25	n.d.	0.65	1.68	n.d.	8.29
26	n.d.	0.98	3.01	n.d.	11.37
27	n.d.	0.18	0.54	n.d.	1.98
28	n.d.	0.56	1.15	n.d.	3.19
29	n.d.	0.09	0.31	n.d.	1.38
30	n.d.	n.d.	0.30	n.d.	1.81
31	n.d.	n.d.	0.19	n.d.	0.50
32	n.d.	n.d.	0.14	n.d.	0.78
33	n.d.	n.d.	n.d.	n.d.	0.49

exception of a single chain length class (n -C_{16:0}) found in the surface soil (Table 3.2). Additionally, no archaeal lipids were detected within gypsiferous units.

Conversely, the clay-rich units below the aquiclude contained a higher abundance of lipids and included lipid classes that were not detected in the upper gypsiferous soils. The FAME profile in these units was dominated by n -C_{22:0} and n -C_{24:0} FAMES (Fig. 3.2). Dimethyl esters of saturated, -dicarboxylic fatty acids (DCA) were detected in all samples below 100 cm depth, with abundance and chain length ranges increasing with depth. The deepest clay unit below the aquiclude had the largest

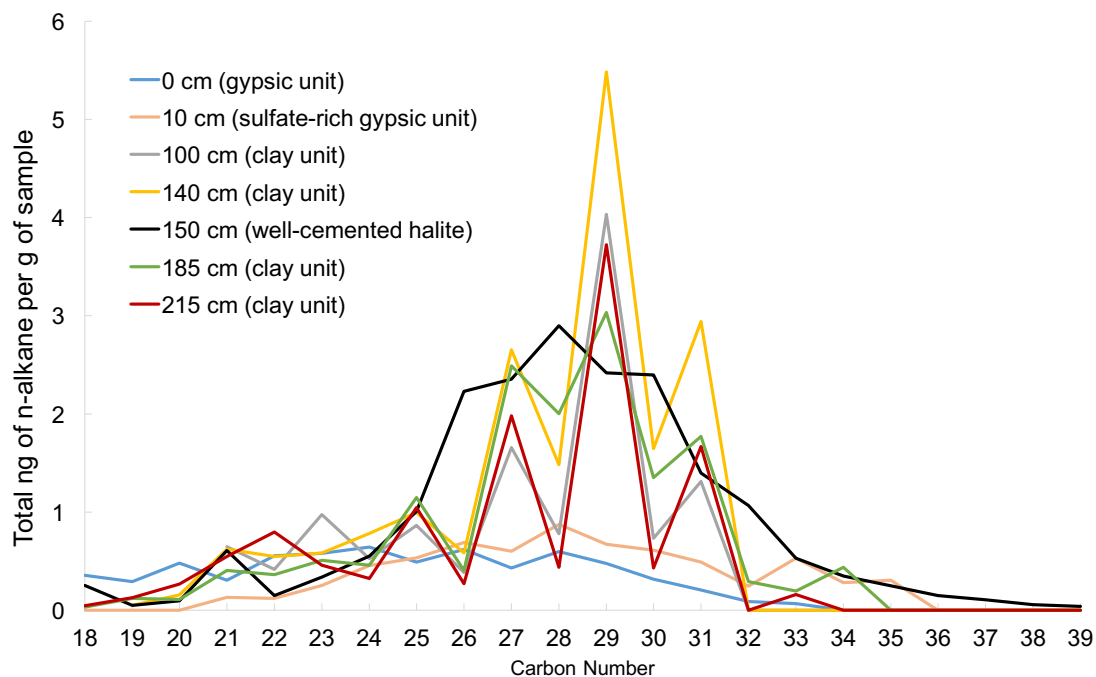


Figure 3.3: ***n*-Alkane Content in Yungay Pit Soils:** The straight chain *n*-alkane content of Yungay soils reveals two distinct patterns. Clay rich units exhibit an odd-over-even chain length preference. Conversely, gypsiferous soils and the halite unit exhibit a slight even-over-odd chain length preference.

abundance, and also the largest range in chain length (C9-C31) (Fig. 3.1c; Table 3.3), while only trace amounts of C22 DCA was observed in the halite unit. α - and β -monohydroxy monocarboxylic acids were also present in clay units with a relatively high abundance of *n*-C_{24:0}. A clay-rich sample at 185 cm depth had the highest total abundance of this lipid class as well as the greatest diversity, with chain lengths that ranged from C15 to C33. *N*-alkanes in these clay units contained an odd-over-even chain length preference (Fig. 3.3).

Isoprenoidal glycerol dialkyl glycerol tetraethers (GDGTs) (Fig. 3.1d) and non-isoprenoidal, branched GDGTs were detected in clay-rich layers below 100 cm depth (Table 3.4), but not in the upper gypsiferous soils. An isoprenoidal GDGT (GDGT-0) was extracted from a clay-rich unit at 140 cm depth, and three additional isoprenoidal GDGTs (GDGT-1, GDGT-2, and crenarchaeol) along with five non-isoprenoidal GDGTs were identified in the clay-rich units at 185 cm and 215 cm depth respectively (Fig. 3.4 and Table 3.4). Branched GDGTs were found in greater abundance than isoprenoidal GDGTs.

Significantly, the well-cemented halite unit at 140-150 cm depth contained a GDGT profile distinctive from both the gypsiferous and clay-rich units. It was characterized by a relatively high abundance of isoprenoidal glycerol diether, archaeol (481 pg/g of soil), a lesser abundance of isoprenoidal GDGT-0, and the halophilic archaeal biomarker, C20-C25 extended archaeol (Table 3.4).

Chloride, perchlorate, nitrate and sulfate anions were interrogated via IC and perchlorate anions through IC/MS-MS (Fig. 3.5). Of these, sulfate and chloride were the predominant species. Sulfate is the least soluble of the anions and is maximally present at the surface with penetration down to 100 cm where there is a significant drop in concentration. The more soluble chloride anion is present in all samples except the surface, showing a primary maximum at 150 cm (the halite layer) and a smaller secondary maximum at 100 cm. Despite being more soluble than chloride, nitrate

Table 3.3: Saturated α - ω - Dicarboxylic Fatty Acids in Yungay Pit Soils in ng DCA per g sample N.d. is not detected. DCAs not detected in samples analyzed from units above 100 cm

Carbon Chain Length	100 cm depth (clay unit)	140 cm depth (clay unit)	150 cm depth (halite unit)	185 cm depth (clay unit)	215 cm depth (clay unit)
9	n.d.	n.d.	n.d.	n.d.	0.19
10	n.d.	n.d.	n.d.	n.d.	0.08
11	n.d.	n.d.	n.d.	0.06	0.10
12	n.d.	n.d.	n.d.	0.08	0.12
13	n.d.	n.d.	n.d.	0.05	0.15
14	n.d.	0.06	n.d.	0.17	0.25
15	n.d.	n.d.	n.d.	n.d.	0.72
16	n.d.	n.d.	n.d.	0.81	6.68
17	n.d.	1.51	n.d.	0.32	0.80
18	0.20	0.52	n.d.	0.84	4.67
19	n.d.	0.48	n.d.	0.55	2.67
20	0.22	0.68	n.d.	1.08	n.d.
21	0.62	n.d.	n.d.	1.24	0.12
22	0.91	2.06	0.01	3.74	19.47
23	n.d.	n.d.	n.d.	3.35	8.24
24	0.45	1.23	n.d.	3.26	11.37
25	0.27	1.45	n.d.	1.77	3.65
26	n.d.	n.d.	n.d.	0.32	6.49
27	0.31	1.50	n.d.	2.99	3.06
28	0.64	2.17	n.d.	n.d.	4.16
29	n.d.	1.02	n.d.	0.80	1.39
30	n.d.	0.85	n.d.	0.89	1.35
31	n.d.	0.36	n.d.	n.d.	0.33

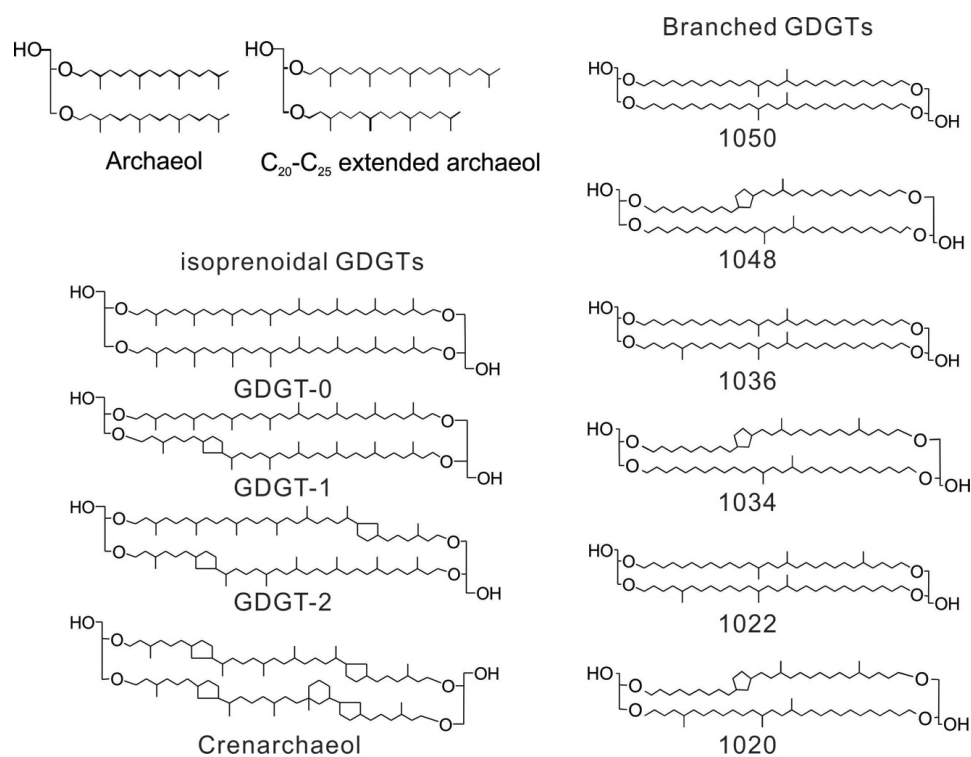


Figure 3.4: **Glycerol Ether Lipids Detected in Atacama Samples:** Glycerol ether lipids detected in the Atacama samples. Archaeol and C₂₀-C₂₅ extended archaeol are archaeal diethers. Isoprenoidal and branched GDGTs are archaeal and bacterial tetraethers, respectively.

Table 3.4: The occurrence of glycerol tetraethers (GDGTs) in Yungay Pit Soils (pg GDGT per g sample).

	Structure	Surface Soil (gypsif- erous unit)	10 cm depth (gypsif- erous unit)	100 cm depth (clay unit)	140 cm depth (clay unit)	150 cm depth (halite unit)	185 cm depth (clay unit)	215 cm depth (clay unit)
isoprenoidal GDGTs	Archaeol	n.d.	n.d.	n.d.	n.d.	481	n.d.	n.d.
	C20-325 extended	n.d.	n.d.	n.d.	n.d.	2.66	n.d.	n.d.
	Archaeol							
	GTGT-0	n.d.	n.d.	n.d.	n.d.	0.69	n.d.	n.d.
	GDGT-0	n.d.	n.d.	n.d.	0.19	39.04	0.2	0.27
	GDGT-1	n.d.	n.d.	n.d.	n.d.	n.d.	0.09	0.08
branched GDGTs	GDGT-2	n.d.	n.d.	n.d.	n.d.	n.d.	n.d.	0.22
	Crenarchaeol	n.d.	n.d.	n.d.	n.d.	n.d.	0.21	0.3
	1050	n.d.	n.d.	n.d.	0.24	n.d.	1.06	0.96
	1048	n.d.	n.d.	n.d.	n.d.	n.d.	n.d.	0.4
	1036	n.d.	n.d.	n.d.	n.d.	n.d.	0.82	0.7
	1034	n.d.	n.d.	n.d.	n.d.	n.d.	0.28	0.47
	1022	n.d.	n.d.	n.d.	n.d.	n.d.	0.28	0.39
	1020	n.d.	n.d.	n.d.	n.d.	n.d.	0.1	0.21

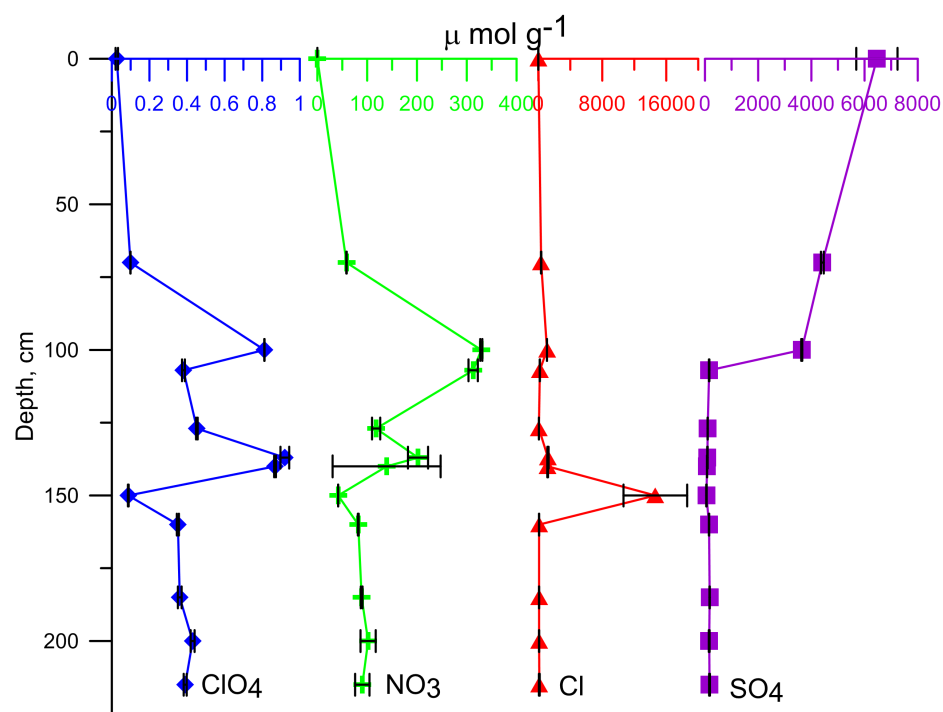


Figure 3.5: **Anion Profiles in the Yungay Soil Column:** Anion profiles of chloride, perchlorate, nitrate and sulfate with depth in the Yungay. The point at 150 cm was taken from the massive, well-cemented halite unit.

is found only in relatively small quantities in the massive, well-cemented halite unit, with maxima at 100 and 137 cm. Similarly, perchlorate has two maxima at 100 and 137 cm.

3.4 Discussion

3.4.1 Anion Distribution with Depth in Yungay

Chloride concentration significantly decreases below 150 cm, while the nitrate and perchlorate anions slightly increase and stabilize in concentration (Fig. 3.5). This reaffirms that 150 cm is the depth of maximum percolation as previously proposed (Ewing et al., 2006; 2008) as percolating rainfall would have solubilized and subsequently carried chloride to the clay layers below. There are also relative maxima in the perchlorate, nitrate, and chloride profiles at 100 cm. It is possible that this depth represents percolation from smaller rain events. The changes in the anion chemistry throughout the soil profile likely do not necessarily represent the percolation depth throughout its history, but instead represent the percolation depth at and after the establishment of the chloride-rich layer that acts to inhibit the flow of water downward at 2 Ma or earlier.

Significantly, the relative maxima in nitrate and perchlorate at 137 cm depth are offset from the chloride maximum at 150 cm. Given nitrate is more soluble than chloride, it is unexpected that these maxima are offset, and that only a relatively small quantity of nitrate is detected in the halite unit. This discrepancy gives additional credence to the idea that the halite unit may have originally formed by a process different than the previously proposed “wash down” model. It is likely that some of the chloride present in this unit was derived through the solubilizing of atmospherically-derived halite that was deposited by wind and subsequent washing down through the profile by wetting events. But, the undisrupted sub-cm laminations present in the layers above the halite unit (Fig. 3.6) and the anion concentration

profiles point to an alternative formation mechanism for the halite unit.

3.4.2 Biomarker Preservation Under Prolonged Hyperarid Conditions

Fatty acids are rapidly destroyed by biological degradation such as aerobic and anaerobic respiration, fermentation, and photoheterotrophy (Brocks and Summons, 2004; Kuzyakov, 2010), and incubation experiments with phytoplankton have demonstrated complete degradation over the course of a few weeks (Sun et al., 1997). Hence, in most environments, the presence of labile lipids such as FFAs and FAMEs is indicative of extant communities or of recent biogenesis (Simoneit et al., 1998). Surprisingly, the concentration of FAMEs (Fig. 3.1b and 3.2) and FFAs (Table 3.1) in Yungay soils was not only found to increase with depth in the soil sequence, but FFAs and FAMEs retained labile features such as unsaturated bonds in the alkyl chains within the deeper, sealed-off clay units. In addition, α - and β - monohydroxy monocarboxylic acids were primarily found in clay-rich units below 1 m depth (Table 3.2), despite this class of fatty acid's susceptibility to rapid diagenesis (Volkman, 2006) and hydroxyl group loss (e.g., Bordenave, 1993).

Given the short residence time of labile fatty acids in most environments, their detection throughout the soil profile suggests that they either represent extant biomass, or exceptionally well-preserved functionalized fossil lipids. We considered evidence for both scenarios. The Yungay region is one of the driest areas in the Atacama Desert. The water activity in the surface soils is well below the threshold for metabolic growth and enzymatic activity (Connon et al., 2007), and should remain very low and constant below a depth of 1 m (Azua-Bustos et al., 2015). The extremely dry conditions are reflected in the low biomass (10^3 - 10^5 cells cm^{-3}) in surface soils (e.g., Navarro-Gonzalez et al., 2003; Connon et al., 2007; and Crits-Christoph et al., 2013), and low organic carbon content (<102 ppm) (Connon et al., 2007 and Ewing et al., 2006), which is “radiocarbon dead” (older than 40,000 years) below a depth of 100 cm (Ew-



Figure 3.6: **Finely Laminated Soil Unit at 140 cm depth:** Image of a perchlorate and nitrate-rich soil unit located at 140 cm depth, 10 cm above the massive, well-cemented halite unit. This unit is comprised of silt to fine sand-sized particles that form undisturbed, fine sub-cm sized laminations and contains cm-sized voids. Such laminations are diagnostic of quiescent deposition in a sustained aqueous environment, such as a perennial pond.

ing et al., 2008). In addition, the D/L ratio of aspartic acid in the top cm of soil indicates significant racemization of biologically produced amino acids, and yields ages of 10^3 to 10^5 years (Skelley et al., 2007). Together, these data argue against substantial biological activity or recent biogenesis of lipids, even in the topmost gypsiferous soils. Instead, functionalized lipids in the top 1 m of soil likely represent relatively modern atmospheric inputs, a conclusion supported by the fact that the majority of cultivable isolates found in these soils are root-associated microbes in an environment where there has not been plant growth in millions of years (Lester et al., 2007).

On the other hand, the deeper clay layers that contain the highest concentration and diversity of lipids including plant lipids, have been isolated from rainwater as well as modern surface inputs for a period of hundreds of thousands to a few-million years by the massive halite unit at 140-150 cm depth. This halite unit is a marker of maximum water percolation (Ewing et al., 2006) and has acted as an aquiclude. Soluble ion distribution in the soil profile (Fig. 3.5) reaffirms that there has been little or no percolation of rainwater through this halite unit (see below). Therefore, we argue that the functionalized lipids in the deeper clay units, and especially the archaeal and plant lipids found to be absent from the upper gypsiferous and surface soils, are fossils of organisms in an excellent state of chemical and structural preservation since their time of deposition.

The remarkable degree of preservation of functionalized fatty acids and other lipids over tens of thousands to a few million years in hyperarid soils can be explained by the extremely low water activity, a taphonomic process that we term xeropreservation (preservation by drying). Low water activity in soils arrests biological activity (e.g., both the synthesis and degradation of lipids) and suspends or greatly reduces chemical degradation, inhibiting modification of a cell's own lipid membrane as well as the action of heterotrophs. In particular, low water activity can inactivate or slow

the reaction rate of the cell's own lytic enzymes, or those of heterotrophs, that degrade organic moieties upon cell death (e.g., de Gomez-Puyou and Gomez-Puyou, 1998). By halting aerobic or anaerobic metabolic activity, labile lipids such as fatty acids can be preserved. Such excellent lipid biomarker preservation is comparable to other geological samples that have been subjected to rapid dehydration, such as in polymerized resins like amber (Bada et al., 1999; Schweitzer, 2004), and opens the possibility for extreme longevity of other labile biomarkers such as ancient DNA. Additionally, the structural and chemical integrity of labile lipids throughout the soil profile suggests that chemical oxidation of these biomolecules has been limited despite the photochemical formation and accumulation of reactive oxidant species in these hyperarid soils (Georgiou, 2015). Again, this is likely due to the extremely low water availability in these soils, a factor exacerbated with depth, which limits soil organic oxidant chemistry.

Additionally, there are a number of abiotic conditions known to increase preservation of organic matter. Clay minerals present in the soil, which include smectite and kaolinite, may play a role enhancing the preservation of organics (e.g., polar lipids) through interaction with charged mineral surfaces (Farmer and Des Marais, 1999; Eigenbrode, 2008; Summons et al., 2011). Entombment by chemical precipitates is another mechanism of microbial fossilization (Farmer and Des Marais, 1999; Melendez et al., 2013; Williams et al., 2015). The many salts observed at Yungay could have served a similar function by encasing microorganisms or organic matter, thereby leading to increased chance of long-term preservation. It is also possible that the environmental conditions microorganisms were exposed to prior to drying had some effect on the degree of preservation of intracellular biomolecules. Stress (e.g., osmotic stress, decreases in pH, and starvation) has been shown to induce a number of survival strategies including modifications in cell membrane fatty acid composition, which afford protections to microorganisms that increase recovery after drying (Morgan et

al., 2006 and references therein). The possibility that cellular modifications from environmental stressors before drying offer increased long-term preservation should be investigated further.

3.4.3 Microbial Diversity and Paleoenvironmental Reconstruction Based on Lipid Biomarkers

Certain lipids have been used as taxonomic markers for particular groups of microorganisms (e.g., Summons and Lincoln, 2012). Some recent work has called into question the utility of this approach, specifically as it relates to methylated hopanoids (e.g., Rashby et al., 2007; Welander et al., 2010). However, ester-linked membrane fatty acids are commonly used to assess microbial diversity (e.g., White et al., 1993), since the fatty acid chain length, number and position of double bonds, cyclopropane rings, and position of methyl branches allow for distinction between aerobes, anaerobes, sulfate-reducing bacteria, cyanobacteria, actinomycetes, fungi, protozoa, plants, and green algae (Vestal and White, 1989 and references therein). The excellent preservation of the labile and refractory lipids allowed us to characterize taxonomic groups present in each stratigraphic unit, perform paleoenvironmental reconstructions based on known habitats of these groups, and assess environmental change over time. We broadly used FAMES, isoprenoidal glycerol ethers, DCAs, and alkanes to distinguish between bacteria, archaea, and higher organisms such as plants throughout the soil profile.

FAME profiles in the upper gypsiferous soils were indicative of a predominant bacterial source (Volkman, 1998; Kaneda, 1991). The slight even-over-odd carbon chain length preference in alkanes was unusual, and could indicate a distinctive microbial origin or alteration of algal detritus (Elias et al., 1997). The lack of archaeal lipids from the gypsiferous soils was consistent with previous work that noted an absence of archaeal groups based on 16S RNA analyses (Crits-Christoph et al., 2013). These

data support the idea that the Yungay region soils contain a population primarily consisting of bacteria.

On the other hand, clay-rich units below 100 cm depth contained lipid biomarkers not detected in the soils above, including lipids that are typically diagnostic of plants. The long-chain DCAs detected are likely derived from plant biopolymers such as suberin and cutin (Wakeham, 1999). The odd-over-even chain length preference seen in C24-C32 n-alkanes is a common biosignature of terrestrial plants (e.g., Wakeham, 1999; Volkman, 2006). The finding of plant-derived lipids in clay-rich units is consistent with the finding of cm-long fragments of fibrous plant material in samples at 185 cm and 215 cm depth (Ewing et al., 2006, Fig. 3.7). Plant-derived DCAs identified in units beneath the aquiclude especially supports the argument for preservation of labile lipids under hyperarid conditions as the plant material is certainly no longer living, and hasn't been since burial (>40,000 years ago).

The presence of α - and β -monohydroxy monocarboxylic acids almost exclusively in the clay units also points to past inputs of biological lipids. While monohydroxy monocarboxylic acids can form from the decomposition of FAMES, the profile of α - and β -monohydroxy monocarboxylic acids in the clays differs from that of the FAME profiles and is suggestive of a unique source instead of a diagenetic product. This class of lipid is common in soil, marine, and lacustrine sediments (Volkman et al., 1998; Volkman, 2006 and references therein), and occurs in a wide range of taxonomic groups, or can be produced as intermediates in the α - and β oxidation of monocarboxylic acids, so their exact source is difficult to determine, although the most abundant monohydroxy monocarboxylic acid found (n -C_{24:0}) is known to occur in certain seagrass species (Wakeham, 1999).

Isoprenoidal GDGTs, a class of membrane lipids diagnostic for archaea (Pearson and Ingalls, 2013; Schouten et al., 2013) were also found in the clay units, along with branched GDGTs that are sourced from bacteria (Weiher et al., 2006). Non-



Figure 3.7: Centimeter-Sized Fragments of Fibrous Plant Material Found at 215 cm Depth: An image taken of sample collected from the unit at 215 cm. The arrow points to one of the fibrous cm-sized plant fragments present interspersed throughout this unit, and a likely source for some of the plant lipid biomarkers detected.

isoprenoidal, branched GDGTs are proposed bacterial lipids (Weihers et al., 2006). Their greater abundance versus isoprenoidal GDGTs in the lower clay units is consistent with a dominant bacterial signal. Furthermore, this signal is inconsistent with offshore marine sources (e.g., Schouten et al., 2013) which argues against atmospheric sources. This, along with the absence of GDGTs in the upper gypsiferous soils suggests that both bacterial and archaeal GDGTs are syngenetic to the host clay unit. Together with the evidence for plant biomarkers, the presence of bacterial and archaeal GDGTs towards the bottom of the soil profile indicates a past wetter environment that was once capable of supporting a more diverse ecosystem than that what exists under the current hyperarid environmental conditions.

Finally, the well-cemented halite unit at approximately 140-150 cm depth contained a GDGT profile distinct from both the gypsiferous and clay-rich units. The relatively high abundance of archaeol; a lesser abundance of isoprenoidal GDGT-0; and the presence of the biomarker C20-C25 extended archaeol (Table 3.4) are all diagnostic of halophilic archaea (Kates, 1978; Koga, 2005; Jahnke et al., 2008; Birgel et al., 2014). The occurrence of the halite unit between two layered clay units (Figs. 3.1 and 3.6) and the halophilic archaeal lipid biomarkers found within the halite unit are consistent with formation in a small-scale evaporitic environment under a wetter climate regime. In this scenario, the buried halite layer could represent a paleo-surface horizon formed during a period of intense evaporation. This is in contrast to the proposed “wash-down” origin of the halite layer, whereby the salt-rich horizon formed from the episodic vertical transport of atmospheric salt during infrequent rain events and subsequent reprecipitation (Ewing et al., 2006; 2008). The presence of diagnostic archaeal lipids found only in the halite unit, and the presence of undisrupted fine laminations in the clay unit immediately above (Fig. 3.6), both suggest that rainwater percolation might not be the sole mechanism responsible for the formation of the halite unit. However, soluble ion concentrations (Fig. 3.1) do indicate that

atmospherically-derived salts have been solubilized by rainwater and reprecipitated for the most part above the halite unit (at 100 and 137 cm depth, Fig. 3.5). Thus, the halite unit still marks the maximum depth for percolation of rainwater as suggested by (Ewing et al., 2006; 2008).

The wetter climate regime in the Yungay region inferred from the lipid biomarkers in the clay and halite units could be related to permanent El Niño-like conditions inferred for the central Atacama 5.6-4.7 million years (Wang et al., 2015), or with short, punctuated wet climate intervals during the last ~5 million years (Jordan et al., 2014), a timing that is consistent with the estimated age of the soil profile (> 2 million years).

In summary, extreme and prolonged dryness has been responsible for the preservation of labile biomarkers in hyperarid Atacama soils. This is likely due to the low water activity in the soils, which prevents any significant microbial activity or chemical degradation of organic compounds. The exceptional preservation of functionalized and more fragile or labile lipids, especially at the bottom of the soil profile that has been sealed-off from rainwater over a tens-of-thousands to a few million-years time scale, is comparable to the preservation of other labile biomarkers in deep-frozen permafrost or in polymerized resins like amber, and allows us to reconstruct significant taxonomic changes that may point to a shift in the hydrologic regime > 2 million years ago.

CHAPTER 4

DETECTABILITY OF LIPID BIOMARKERS IN ATACAMA SOILS BY MARS FLIGHT INSTRUMENTATION: RAMAN SPECTROSCOPY AND EVOLVED GAS ANALYSIS

The previous two chapters have detailed the lipid content of Atacama soils, both surface soils across the aridity gradient and soils collected with depth in one of the driest regions of the desert. Lipids comprise roughly 10% of the dry weight of cellular material (Cooper, 2000), and serve a number of critical functions within a cell, such as energy storage, signaling, and composing cell membranes, making them a required biomolecule for terrestrial life. Lipids and their degradation byproducts are also some of the best preserved molecular biomarkers in the fossil record (Eigenbrode, 2008). For these two reasons, lipids will be a target for future planetary missions searching for extant or ancient life, both on Mars (e.g. Report of the Mars 2020 Science Definition Team, 2013) and in the outer Solar System (e.g. Europa Lander Report, 2016). Thus, it is critical to understand the detectability of lipid biomolecules contained in samples from key terrestrial “analog” sites such as the Atacama by flight or flight-like instruments. Natural samples can offer insight into flight instrument performance in response to common organic detection challenges such as low biomass concentration, organic complexity, and organic interactions with inorganic material such as oxidants or mineral encapsulation. Analyzing such samples with flight instruments provides critical data that advances the science readiness of the instruments and the missions broadly.

The search for organic carbon and biomarkers continues to be a high priority goal in the exploration of Mars. Understanding and interpreting a positive or negative result in an extraterrestrial “life detection” experiment rests on the ability to con-

textualize it with a range of naturally-occurring terrestrial samples, both in terms of age and mineralogy. Thus, the goal of the following section is to use knowledge of the biomolecular content of Atacama soils acquired through standard laboratory techniques to assess the detection capability of current and future Mars mission flight-instrumentation. The following sections focus on two flight instrument organic characterization techniques: Raman laser spectroscopy, slated to fly on both ESA and NASA Mars rovers in 2020 and recommended by the Europa Lander Report (2016), and Evolved Gas Analysis, a technique currently being employed on the martian surface by the Mars Science Laboratory and previously employed by the Viking and Phoenix Landers.

4.1 Critical Assessment of Biomarker Detection with Raman Laser Spectroscopy on Biomass-Poor Soils

4.1.1 Introduction

The Mars2020 and ExoMars rovers will each carry a Raman Spectrometer to Mars to identify and characterize minerals and organic compounds and search for biomarkers. Raman spectrometers offer operational simplicity. Samples are analyzed at a distance, non-destructively, and with minimal or no sample handling, minimizing the risk of contamination (Summons et al., 2014). They are expected to serve as useful “survey” instruments, providing mineralogy and structural information of targets, in addition to critical information about the presence of carbon aggregates on the surface of samples. For the Mars2020 mission, Raman instruments will be used in part to provide information about organic content of surface samples to a parts-per-million (ppm) level (Beegle et al., 2014; Maurice et al, 2015), and will be key in determining whether a sample should be cached for later return to Earth (Report of the Mars 2020 Science Definition Team, 2013).

However, operational simplicity comes at a performance cost. Raman spectrom-

eters have much lower limits of detection (LOD) than other analytical systems used for organic characterization, such as GC-MS. Additionally, they are often unable to detect individual carbon molecules in complex mixtures (Summons et al., 2014), are susceptible to topographic and matrix effects (Report of the Mars 2020 Science Definition Team, 2013) and fluorescence of organics and minerals, especially iron bearing minerals (Sobron et al., 2014). These challenges could make it difficult to establish the source of a carbon signal (exogenous, biogenic, or contamination), and perhaps even prevent the detection of carbon altogether, especially in samples that have low carbon abundance, as is expected near the surface of Mars (Freissinet et al., 2015). It is therefore paramount to test the performance of Raman Spectrometers when analyzing complex natural samples with very low organic and biomass contents to understand the significance of a negative result, particularly when evaluating samples for caching a selection for future return to Earth.

Results from prior martian missions constrain the expected abundance of organic carbon in sediments on Mars. The Viking 1 lander detected the release of 15 parts per billion (ppb) of methyl chloride and 1 to 50 ppb fluoroethers from soil samples upon heating (Biemann et al., 1976). The Phoenix Lander searched for organics with the Thermal and Evolved-Gas Analyzer (TEGA). No organic fragments were identified at ppb levels (Ming et al., 2010). Mars Science Laboratory detected chlorobenzene (150-325 ppb) and C2 to C4 dichloroalkanes (up to 70 ppb) in multiple portions of fines from the Cumberland drill hole in the Sheepbed mudstone at Yellowknife Bay (Freissinet et al., 2015). Together, these results suggest that the amount of organics in Martian materials will likely be lower than ppm range. If present, biomarkers would be expected to represent only a fraction of the total organic composition, likely at ppb or lower concentrations. Given the detection of hydrocarbons in multiple martian samples, and the propensity for preservation of biological lipid biomolecules in geologic settings, understanding the detectability of lipids is paramount to understanding

organic carbon content and the search for molecular biosignatures on Mars.

The capability of the ExoMars Raman Laser Spectrometer (RLS) for organic and biomarker detection was tested using biomass-poor soils from the Atacama Desert. Organic compounds in these soils are tens of thousands (surface) to millions of years old (ca. 2 meters depth) (Skelley et al., 2007; Ewing et al., 2008; Chapter 2, 3). As such, there has been ample time for complex mineral-organic interactions to occur, a critical determinant in organic carbon detectability in natural samples. Soils are well characterized for the abundance and identity of organics using traditional laboratory techniques to a ppt level, including their lipid (Chapter 2, 3), protein/peptide and amino acid (Skelley et al., 2007; Chapter 2), DNA (Connon et al., 2007; Lester et al., 2007; Crits-Christoph et al., 2013), and TOC content (Ewing et al., 2008). Organic carbon is present in soils at 100-200 ppm levels (Ewing et al., 2008) and lipids are present at hundreds-of-ppb levels (Chapter 3). Surface soils are known to contain viable organisms at concentrations 10^3 - 10^5 cells per gram (Crits-Christoph et al., 2013), and soils at 2 m depth contain preserved lipids from dead organisms, including fatty acids, at 1 ppm level (Ewing et al., 2008; Chapter 3). However, modern or ancient DNA has yet to be detected (J. DiRuggiero, personal communication; R. Nichols and B. Shapiro, personal communication).

Atacama soils were analyzed to assess the capability of the RLS to detect extant lipid biomarkers in soils with very low cell abundance (Yungay surface soils), and fossil lipid biomarkers in subsurface soils at low ppm abundance, near the LOD of the instrument.

4.1.2 Methods

Analysis of Analytical-Grade Standards

Analytical-grade standards of short-chain and cyclic hydrocarbons and common lipid biomarkers were analyzed with RLS. Standards were used to build a library of Raman

spectral features to identify similar organic molecules in the natural soil samples. Standards that were suspended in a solvent were dried under a stream of N₂ at room temperature onto the bottom of a flat, 2 mL combusted (550°C for 12 hours) glass vial. Standards that were powdered were also loaded into combusted glass vials.

There were four fatty acid standards analyzed. These included the two most common membrane fatty acids, *n*-C_{16:0} and *n*-C_{18:0} (Sigma-Aldrich, 76119), which were also the most abundant lipids detected in Atacama soil samples (Chapter 3). An unsaturated fatty acid (*n*-C_{16:1}) was also included to look at any effect of double bonds in the hydrocarbon chain (Sigma-Aldrich, 76169). Finally, a bacterial fatty acid methyl ester mix (Sigma-Aldrich, 47080-U Supelco) was analyzed which contained a mixture of fatty acids of various chain lengths including some with hydroxyl groups and methyl branches.

Two geolipids were analyzed including the C₂₀ isoprenoid hydrocarbon phytane (Sigma-Aldrich, 80165), a fossil derivative of phytol side chain of chlorophyll (Powell and McKirdy, 1973) that has also been found in membranes of thermophilic Archaea (King et al., 1998), and 17 β , 21 β -hopane (Sigma-Aldrich, 07562), a polycyclic isoprenoid similar in structure to the hopane biomarkers that are the oldest probably syngenetic biomarkers detected in billion-year-old fossils on Earth (Brocks and Summons, 2004). Three alkane (straight-chain normal hydrocarbons) standards were analyzed including a C₂₈H₅₈ octacosane standard (Sigma-Aldrich, O504), a mixture of saturated alkanes of chain lengths 7 carbons in length to 30 (Sigma-Aldrich, 49451-U), and a mixture of alkanes that only contained even numbers of carbon between 10 and 40 carbons (Sigma-Aldrich, 68281), a potential biosignature. An even-over-odd preference in carbon chain length was also detected in Atacama soil samples (Chapter 3).

Finally, five polycyclic aromatic hydrocarbon (PAH) standards were analyzed with varying numbers of rings and bay regions: naphthalene (2-ring PAH), anthracene (3-

ring PAH), phenanthrene (3-ring PAH with one bay region), pyrene (4-ring PAH), and chrysene (4-ring PAH with two bay regions) (Sigma-Aldrich, 147141, A89200, P11409, 185515, 48565 respectively). PAHs are found to commonly occur exogenously (Becker et al., 1997), but also can be created through the degradation of biogenic compounds (Shuttleworth et al., 1995). The analysis of the PAH standards was meant to provide an “abiotic counterpoint” to the hopane standard which is also aromatic but a derivative of biogenic compounds.

Analysis of Atacama Soil Samples

Atacama samples were pulverized in a solvent-rinsed and combusted (550°C, 12 hours) mortar and pestle. No other further processing was done to samples. All Atacama samples analyzed were collected and stored utilizing extremely clean protocols to avoid introducing contamination into the biomass-poor soils (Chapter 2, 3).

Analyses with the ExoMars RLS Simulator

To be as mission relevant as possible, analytical standards and bulk soils were analyzed using the same protocols planned for the ExoMars mission using an ExoMars RLS Simulator prototype at the Unidad Asociada Universidad de Valladolid-Centro de Astrobiología (CAB), the lead institution for the RLS investigation, run under conditions similar to those to be used by the RLS on the ExoMars rover (Lopez-Reyes et al., 2014). Powdered soil samples were placed on a refillable container similar to ExoMars’ sample distribution carousel serving the RLS, which can be emptied and reused for new analyses just as during mission operations. The RLS, in its automatic mode, then analyzed a set of at least 10 points in each sample, with a 50 micron spot size and an irradiance level of 0.6-1.2 kW cm⁻² with a 532 nm continuous wave (CW) laser (Rull et al., 2011). RLS instrument data products were analyzed using a statistical procedure previously applied in macro techniques, such as XRD and FT-Raman

(Kontoyannis et al., 1997; Kontoyannis and Vagenas, 2000; Vagenas and Kontoyannis, 2003). A detailed point-by-point analysis procedure is provided in Lopez-Reyes et al. (2014). In the case of the up to ~2 Ma soil samples collected from 215 cm depth in Yungay, 157 RLS Simulator spectra were taken of this sample in order to evaluate the frequency with which carbon was detected.

4.1.3 Results and Discussion

Raman Spectroscopy of Analytical-Grade Standards

Raman spectra of lipids contain a few characteristic bands (Majzner et al., 2014). These include peaks at 1400-1500 cm^{-1} from the scissoring and ~1300 cm^{-1} from the twisting vibrations of the CH_2 and CH_3 groups in the hydrocarbon chain, in the 1050-1200 cm^{-1} region are attributed to C-C stretching vibrations, at ~1600 cm^{-1} from the C=C stretching vibration, and an intense group of bands from 2800 to ~3100 cm^{-1} due to the C-H stretching modes (Majzner et al., 2014). There are a number of factors that can alter lipid spectra including temperature, pressure, and crystallization conditions, as well as the presence of additional functional groups (Kobayashi et al., 1984; Majzner et al., 2014). RLS Simulator spectra of lipid and hydrocarbon standards revealed a number of these characteristic features. Features observed in the fatty acid standards with are generally consistent with fatty acid spectra observed using a confocal Raman spectrometer with a 532 nm laser (Majzner et al., 2014), with a few exceptions for a few standards at lower wavenumbers.

The Raman spectra of major bacterial fatty acids $n\text{-C}_{16:0}$ and $n\text{-C}_{18:0}$ were nearly indistinguishable, although the spectral envelope of the C=C stretching region (2800-3100 cm^{-1}) in $n\text{-C}_{18:0}$ shows a blue shift, likely due to a longer chain molecular arrangement (Fig. 4.1). The most intense band observed in individual fatty acid standard Raman spectra was centered at approximately 2800 cm^{-1} . The complex mixture of bacterial fatty acids did not produce strong bands relative to the pure compounds.

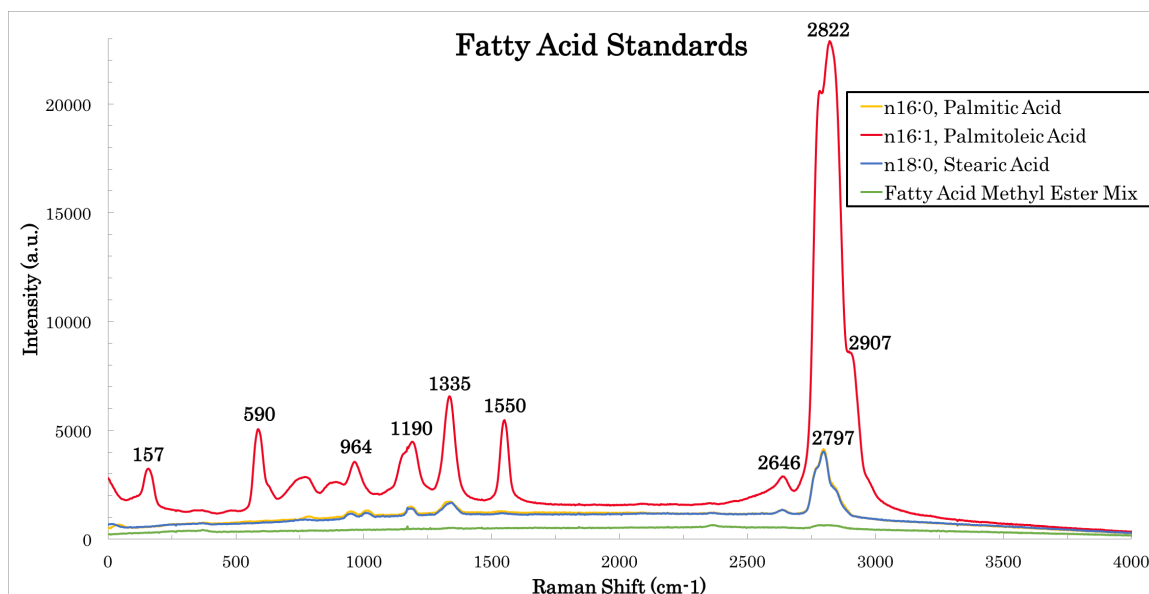


Figure 4.1: RLS spectra of four fatty acid standards.

With respect to previously published Raman spectra, there were slight discrepancies of maximum intensity wavenumber values at lower wavenumbers ($<1600\text{ cm}^{-1}$), likely due to sample processing and experimental conditions, but generally the pattern of bands was similar for both palmitic acid and palmitoleic acid (Majzner et al., 2014). Unsaturated and saturated fatty acids showed similar sets of features to one another except for the 1550 cm^{-1} band (seen in palitoleic acid), which is likely due to the C=C stretching vibration (Fig. 4.1).

The RLS spectrum of selected geolipid standards can be seen in Figure 4.2. The spectrum of phytane resembled that of the saturated fatty acids with the exception of the small peak centered at 1045 cm^{-1} , a shift in the peak in the $900\text{-}1500\text{ cm}^{-1}$ region, and peak at 707 cm^{-1} . The differences in the Raman spectra between isoprenoidal membrane lipids versus fatty acids were relatively minor. As such, in a field sample, it may be difficult distinguish microorganisms with distinct membrane lipids at their most basic level (i.e., bacteria versus archaea). The hopane standard was featureless. This class of compounds that are generally long-lived in the fossil record unfortunately does not seem to produce a strong RLS response.

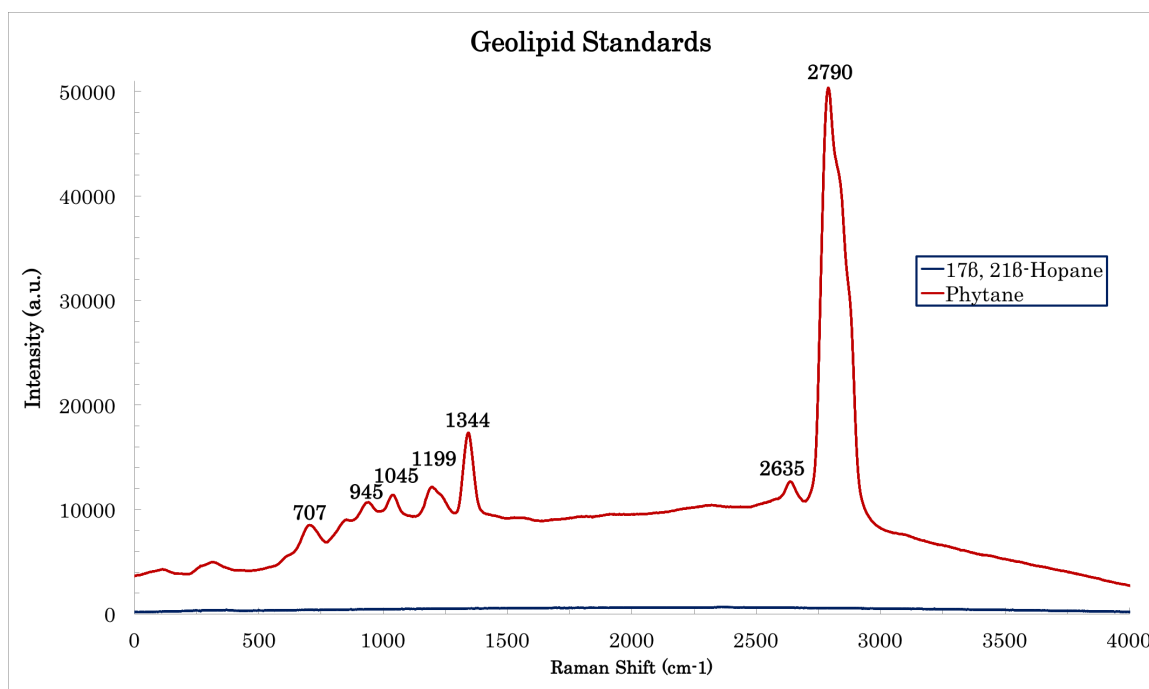


Figure 4.2: RLS spectra of two geolipid standards.

Alkane standards analyzed (Fig. 4.3) were similar to one another, with a higher background fluorescence signal from the mixtures of alkanes versus the standards. The even-only alkane mixture produced a set of peaks nearly indistinguishable spectrally from a mixture of all chain lengths. Carbon chain length preference is a widely used signature of biogenicity of alkanes. This implies that a biogenic hydrocarbon pattern would be difficult to identify using Raman laser spectroscopy.

Aromatic standards RLS spectra were generally strongly fluorescent (Fig. 4.4), with a few relatively small carbon-related bands visible in the phenanthrene and naphthalene structures. Aromatic species similar in structure to these standards are ubiquitous exogenously and would be expected to be present on Mars (Benner et al., 2000). The highly fluorescent nature of these compounds would make identification of these species difficult using 532 nm as excitation for Raman analysis (RLS and SuperCam on Mars 2020). Fortunately, Mars 2020 also includes a deep-UV Raman spectrometer, SHERLOC, which is able to unambiguously identify aromatic standards

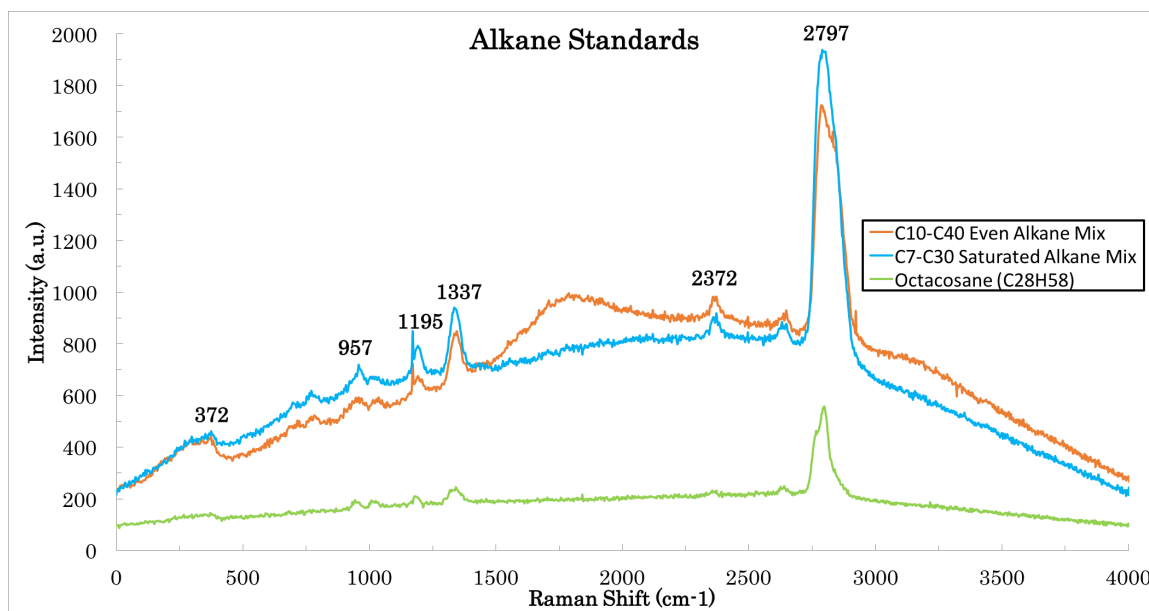


Figure 4.3: RLS spectra of one pure alkane and two alkane mixtures.

in spiked laboratory-simulated samples (Abbey et al., 2017).

Standards did not have a straightforward response in the Raman RLS simulator. In short, pure, straight-chain aliphatic compounds such as phytane, alkanes, and single methyl-fatty acid standards had distinguishable and strong bands in spectra obtained with flight-like Raman instruments. Aromatic species, including the biogenic species, hopane, and simple two to four ring PAHs, were either largely fluorescent, or had relatively small peaks. Biosignatures in alkane mixtures were not distinguishable from abiogenic counterparts, and complex mixtures of bacterial fatty acids had a very low overall signal. The analysis of these few standards was not meant to be an exhaustive list. Instead, it demonstrates the variety of responses observable in common lipid and hydrocarbon standards using a flight-like RLS. Other techniques such as time-gated detection may be required in future developments based on RLS in order to improve the signal.

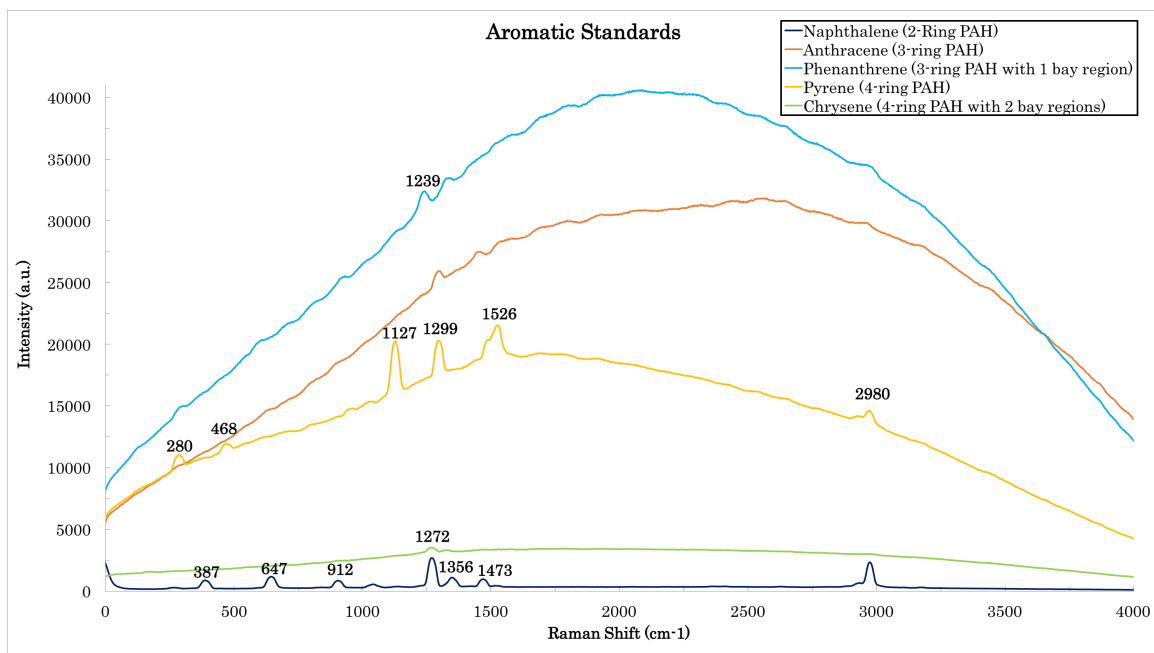


Figure 4.4: RLS spectra of five polycyclic aromatic hydrocarbon standards with various configurations and number of rings.

ExoMars RLS Simulator Spectra of Atacama Bulk Soils

The ExoMars RLS Simulator instrument detected carbon bands in over half of the measurement points taken on all soil samples analyzed from the hyperarid core of the Atacama Desert. However, the instrument failed to identify the most abundant lipid and hydrocarbon biomarkers (e.g., $n\text{-C}_{16:0}$ and $n\text{-C}_{18:0}$ fatty acids) known to be present in the same soil samples at ppb-ppm concentrations, despite the distinct Raman spectral peaks observed in the fatty acid standards (Fig. 4.1). The detection limit requirement of the instrument is < 800 ppm (Hutchinson et al., 2014). However, because individual compounds were not present at ppm levels- a common characteristic of most organics from most natural samples- individual organic species were not identifiable with Raman spectroscopy. Additionally, the lack of individual organic species detection could be due to the fact that organics in the samples were a complex mixture, which is known generally to reduce the overall Raman signal that is generated, or induce a large background fluorescence response that is not specific

to any one type of compound.

Surface soil sample with extant lipid biomarkers: Only two carbon-related bands were detected from Yungay surface soils wavelengths ~ 1300 and 1600 cm^{-1} (Fig. 4.5), which are carbon disordered “D” and graphitic “G” bands (Brolly et al., 2016). These bands were apparent in 4 out of 10 sampling points (Fig. 4.5). The G band at 1600 cm^{-1} is due to the in-plane vibration of aromatic carbons, and the 1300 cm^{-1} band is an intense and broad band seen in poorly ordered carbon (Brolly et al., 2016). The D and G bands detected in Atacama soil samples were low-intensity relative to the other inorganic bands.

The soil RLS spectra did not contain other diagnostic bands specific to any one class of organic compound including the strong 2800 cm^{-1} band observed in lipid standards (Figs. 4.1-4.4). Instead, they contained relatively small peaks that only indicate the presence of poorly-ordered carbon. These bands are commonly observed in non-biologic carbon-bearing samples such as graphene, and are not necessarily indicative of biogenic carbon.

The instrument did return an excellent mineralogical snapshot compared with data that has been returned using XRD techniques. These soils contain a number of minerals and salts such as gypsum, anhydrite, clays, perchlorate, nitrate, and halite (Ewing et al., 2006). In this soil, 10 points in the soil aliquot were measured (Fig. 4.5). The ExoMars RLS detected a number of minerals reported previously using XRD from these soils (Ewing et al., 2006) including gypsum, carbonate, and clays including kaolinite (Fig. 4.5).

Subsurface soil sample with fossil lipid biomarkers: In this soil sample collected at 215 cm depth, both fatty acid and alkane biomarkers are known to be present at ppm and ppb concentrations, respectively (Chapter 3), and the the TOC is twice as high at this depth as in surface soils (Ewing et al., 2008). Figure 4.6 shows 10 representative RLS spectra from this unit (out of 157 spectra collected).

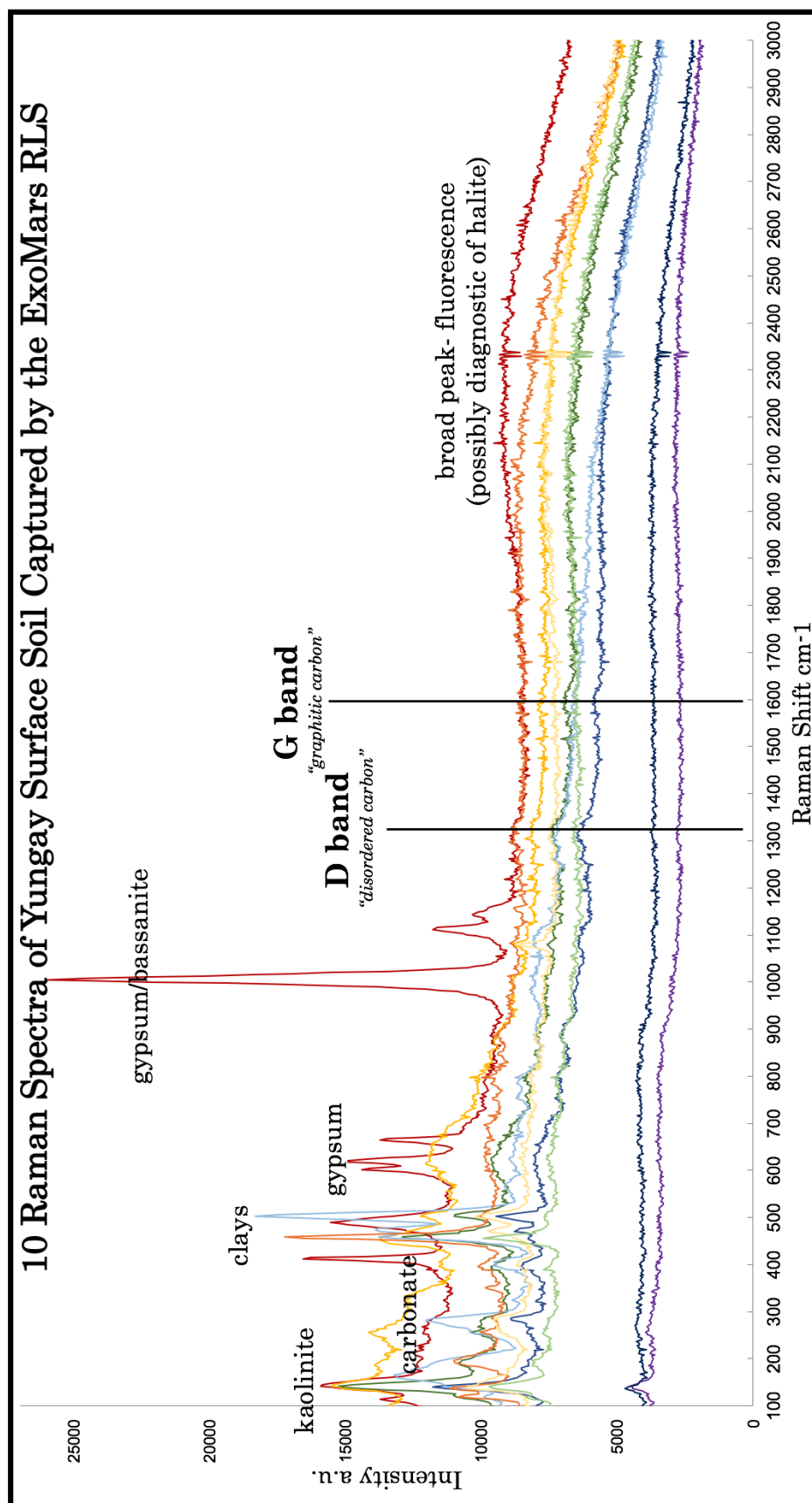


Figure 4.5: RLS spectra of 10 points along a surface soil sample from the Yungay region. Mineral and organic peaks are labeled.

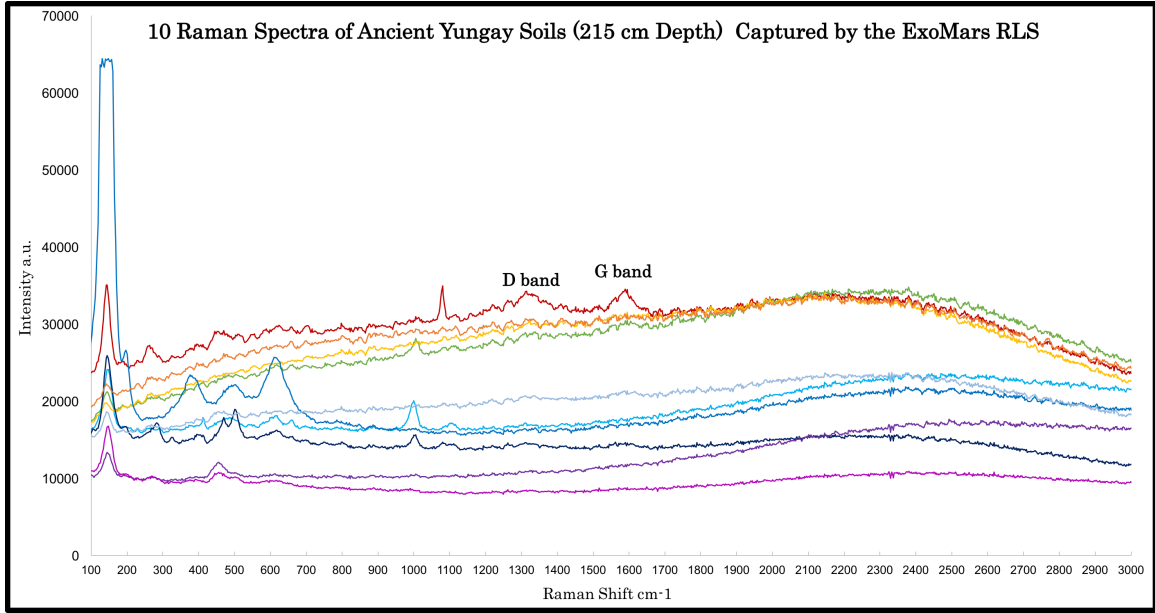


Figure 4.6: RLS spectra of 10 points along an ancient clay-rich soil from 215 cm depth in Yungay. The two peaks indicative of carbon are labeled.

Spectral bands of organic material from this deeper soil closely resembled those of the surface soil despite increased abundance of fatty acids and TOC: the only carbon bands that were detected were at 1300 and 1600 cm^{-1} . 101 out of 137 RLS Simulator spectra contained these D and G bands, a 74% rate of detection of carbon in these biomass-poor soils. This may indicate that carbonaceous material is not distributed homogeneously across a micron-sized area. Heterogeneity is a widely observed phenomenon at many scales in desert soils (Crits-Christoph et al., 2013). This analysis indicates that using a measurement technique that analyzes 10 points along a particular sample is an effective way of getting a representative snapshot of the soil in biomass-poor Atacama samples. Results are being used by the RLS team to explore adaptive concepts of operation to maximize the detectability of biomass during the mission (Sobron, personal communication).

4.1.4 Conclusion

Raman spectroscopy was not able to identify the most abundant biogenic lipid or hydrocarbon compounds contained in biomass-poor Yungay soils. Raman spectroscopy could be a suitable diagnostic tool for the general presence of carbon compounds in natural samples. However, current prototypes might not be capable of detecting specific compounds in complex samples (soils, sediments, regolith), if present at concentrations equivalent to or lower than those found in the biologically leanest environments on Earth. Raman spectroscopy alone may not be sufficient to assess carbon content of a complex natural sample in martian samples that are not rich in organic compounds. Therefore, this may have implications for selection of samples to cache on Mars 2020 if more information is required than whether a sample bears carbon or not at a ppm level.

4.2 Organic Ions Detected in Yungay Soils through Evolved Gas Analysis (EGA) Despite Low Biomass Abundance and Perchlorate Presence

4.2.1 Introduction

Evolved Gas Analysis (EGA) is a “survey” type measurement (Summons et al., 2014) that can be used to understand the carbon content of a sample through slow heating to high temperature with continuous mass spectrometry typically under the presence of helium. Organics are liberated through thermal desorption, thermal decomposition (i.e., pyrolysis), and combustion in the presence of O₂ released from minerals. Additionally, other gases will evolve from heated minerals. EGA is a useful technique to probe the gross structure of organics, associations between organics and minerals, as well as the mineralogy of a sample (McAdam et al., 2015). This technique is currently being employed by the Sample Analysis at Mars (SAM) instrument aboard the Mars Science Laboratory (MSL) (Mahaffy et al., 2012). Thermal volatilization-mass spec-

troscopy techniques were previously employed on Mars by the Phoenix (Smith, 2004) and Viking Landers (Biemann et al., 1976). MSL EGA data has revealed refractory organic matter such as C1-C5 alkyl hydrocarbons, single-ring aromatic hydrocarbons, chlorinated alkyl and aromatic hydrocarbons, sulfur-bearing alkyl and aromatic hydrocarbons to be present in eolian sediments and some lacustrine mudstones in Gale Crater on Mars, although the source is unknown (Eigenbrode et al., 2015; Freissinet et al., 2015). It is also worth noting that the majority of the EGA temperature range (0-600°C) within the SAM instrument has a high background of organic compounds due to an on-board derivatization agent, resulting in lower confidence in indigenous organic signals contained in this range.

Although EGA flight-instruments have a greater mass, volume, and energy requirements, and are operationally more complex than a Raman flight instrument due to sample handling requirements, the degree of sample processing is simple when compared to other techniques used in biomarker detection (e.g., wet chemistry or solvent extraction is not required). On the other hand, because thermal energy is used to dissociate polymers for detection, macromolecular structural information is lost in the creation of smaller, volatile organics detectable by EGA. However, a single EGA “run” can generate a significant amount of molecular information about the general organic content of a sample, down to ppb levels for a single molecular species in the case of the SAM instrument (Mahaffy et al., 2012). It can also indicate how organic compounds relate to sample mineralogy. Typically, information about the relationship between organic and inorganic material is lost in most other types of standard biomarker analyses such as solvent extraction-GC-MS.

EGA is a way to assess which general classes of organics may be present in a sample. It is not useful for determining the exact compound identity, but instead the general groups of organics present that are degraded and released by slow heating. In the absence of minerals, biochemical compounds are known to have predictable

Table 4.1: Table of organic byproducts released via EGA and typical m/z values from common biomolecules based off of Valdivia-Silva et al., (2009); Navarro-González et al. (2003); Simmonds et al., (1969), but is not an exhaustive list of byproducts.

Biomolecule Class	Expected EGA Byproducts (example m/z)
Proteins, Peptides, and Amino Acids	Carboxylic Acids (60), Saturated Nitriles, Saturated and Unsaturated Aromatic Hydrocarbons (50, 78, 127, 178)
Carbohydrates	Aliphatic Aldehydes (29), Ketones (58), Carboxylic Acids (60), Aromatics (50, 78, 127, 178), Furans (81)
Fatty Acids	Alkanes (43), Alkenes (103), Aromatic Compounds (50, 78, 127, 178), Short Chain Carboxylic Acids (60)
Porphyrins	Pyrroles (67, 80)
Nucleic Acid Bases	Unsaturated Nitriles, Substituted Furans (85, 95)

byproducts (4.1), which would be expected if cells were present in a sample. For example, if mass fragments consistent with carboxylic acids, alkanes, alkenes, and aromatic compounds were found in conjunction with one another (i.e., had similar evolution temperatures and peak shapes), the data would be perhaps suggestive of the presence of fatty acids. If the EGA data suggested fatty acids, proteins, and nucleic acids were present in a sample, it would then be possible that cellular components could be responsible for the signature.

Previous studies that used a Phoenix-like thermal and evolved gas analysis technique to search for organics in soils from the hyperarid Pampas de La Joya region in the Atacama, which contain <30 ppm of organic C and a non-biological oxidant were unable to identify organic ions (Valdivia-Silva et al., 2009). Even when these Atacama soils were doped with cells, oxidative activity of matrix soil was thought to eliminate diagnostic organic fragments during thermal processing (Valdivia-Silva et al., 2009). On Mars, where perchlorate is abundant (~1000 ppm) and organics

are scarce (a few ppm), perchlorate is thought to have obfuscated the organic signal in both Viking and Phoenix experiments by promoting combustion during pyrolysis (Biemann, 2007; Hecht et al., 2009; Navarro-González et al., 2010). Some have argued against using pyrolytic techniques on Mars for this reason (Navarro-Gonzalez et al., 2006, 2009, 2010).

The goals of this study are 1) to assess the detectability of organic carbon in biomass-poor, perchlorate-rich Yungay soils through SAM-like EGA in three distinct horizons (surface soils, perchlorate-rich, and ancient buried soils), and 2) to determine whether organic ions, if detected, could be potentially diagnostic of the presence of microorganisms.

4.2.2 Methods

Three samples were selected for EGA analysis from the major distinct soil horizons in Yungay (Chapter 3). These samples include surface soil (8 ppm perchlorate), the massive halite unit at 150 cm depth in containing unusual archaeal lipid biomarkers in a salt-rich matrix with approximately 75 ppm of perchlorate, and a clay-rich unit containing fossil plant fragments and the highest relative abundance of lipid biomarkers in the soil column (40 ppm perchlorate).

Soil samples were pulverized in a combusted mortar and pestle. About 20 mg of sample was loaded into previously combusted cups (500°C for 8 hr) and loaded onto a carousel of a modified commercial benchtop pyrolyzer-mass spectrometer instrument (Frontier Lab Pyrolyzer/Agilent 7890A GC/5975C inert XL MSD) modified for low-fidelity, SAM-like EGA experiments. Samples were then automatically dropped into an oven. Helium was used as a carrier gas at a pressure of 1 bar, and a flow rate of 1.8 mL/min. The following heating protocol was used: hold at 50°C for 10 minutes, ramp at the rate of 35°C/min to 1050°C, hold at 1050°C for 6 min. Gas processing line temperature was set to 300°C. The mass spectrometer was in “scan” mode for

masses 10-550 Da. The inlet mode was split and had a split ratio of 10:1 Two to three “clean up” runs with a 100:1 split were run in between each sample, and blank runs with empty cups were run before and after each sequence to monitor any possible background contamination. Data was background subtracted and smoothed.

4.2.3 Results and Discussion

Major ions detected in SAM-like EGA are shown in Figures 4.7, 4.8, and 4.9. In these figures, blue tones were used to represent major inorganic gases, red tones for straight-chain organics (alkyl, aldehydes, esters, ketones), and green tones for aromatic compounds. EGA data can be difficult to interpret due to the fact that m/z traces can have contributions from multiple compounds. In natural samples, the source of an m/z signal as well as its state can be unknown, both from minerals (e.g., water can be adsorbed, interstitial, or connate, and many minerals could contain water) and organics (e.g., species can be free in a sample, in polymers within a cell, or bound externally or internally with a mineral). Additionally, reactions can take place between evolved gases within the instrument during analysis (Xie and Pan, 2001), including the halogenation of functionalized aromatics (Miller et al., 2015). Species interpretations of m/z values presented in this section are based on what is known to be commonly abundant, as well as other co-eluting masses with similar peak shapes also associated with a compound. Sources of various masses will also be speculated on based upon known mineralogy and organic content of samples described previously (Ewing et al., 2006; Ewing et al., 2008; Crits-Christoph et al., 2013; Chapter 3).

Water (m/z 18) and CO_2 (m/z 44) dominated the EGA signal of all soils analyzed. Water was primarily released from water bound in minerals contained within the soil such as clays. Carbon dioxide has a number of potential sources including oxidation of organic matter and breakdown of carbonates at temperatures $<500^\circ\text{C}$ (McAdam et al., 2011). Other major inorganic gases are present in varying amounts from sample

to sample, with changing peak shapes. Oxygen (m/z 32) has a surprisingly flat shape at low temperature in the clay rich soils from the surface and 215 cm depth. In the halite unit, O_2 peaks correspond with the NO (m/z 30) peak at about 600°C, and SO_2 (m/z 64) peaks at about 450°C, 750°C, and 850°C correspond with O_2 peaks in the halite unit. These four major releases of oxygen in the halite unit may indicate the breakdown of oxygen-rich salts contained within the sample such as sulfate or nitrate. HCl (m/z 36) may be sourced from perchlorate salts, known to be present in this unit at a concentration of about 75 ppm, or from the abundant halite (Chapter 3).

Organic ion release temperature and abundance were significantly different in the three samples analyzed. This is likely due to a combination of factors including the abundance and diversity of organics contained within the samples as well as the different mineralogical content of the soils. Yungay surface soils had two major releases of organics: straight chain fragments evolved between 150°C and 600°C with a maximum release temperature at 200°C, and aromatic fragments evolved between 200°C and 450°C with a maximum at about 350°C (Fig. 4.7). The major release of straight chain organics includes aldehydes (m/z 29), C2 hydrocarbons (m/z 43), methyl ketones or dialkyl ketones (m/z 58), and methyl esters (m/z 59). The release of saturated alkane fragments along with ketones and methyl esters may be suggestive of the breakdown of fatty acids, or lipid membranes. The major release of aromatics includes pyrroles (m/z 67), benzene (m/z 78), and pyridine (m/z 79). While it is unclear exactly which biomolecule classes are contributing to this signal, fragments could be suggestive of the breakdown of porphyrins, proteins, and/or carbohydrates, perhaps the more abundant biomolecules contained within a cell. The evolution of potential fatty-acid fragments before aromatic fragments may indicate that cells in the surface soil are largely intact, which is consistent with prior studies of the microbial content of these soils including their viability (Connon et al., 2007; Lester

et al., 2007; Crits-Christoph et al., 2013). Additionally, it is possible that once the bacterial cell membrane is destroyed through heating, the cell contents such as proteins, porphyrins, and carbohydrates are then released, hence the discrepancy in peak shape and evolution temperatures as observed through SAM-like EGA.

The EGA signal of organic ions released from the buried clay unit at 215 cm depth (Fig. 4.8) differed greatly from surface soil. Firstly, the straight-chain alkyl major release is missing. Instead, there are two large organic releases at about 270°C and 550°C that contain a mixture of alkanes, aromatics, and esters. This unit is known to contain about double the abundance of fatty acids as the surface soil (Chapter 3), macroscopic plant fragments (Ewing et al., 2008), and a lack of DNA (Nichols, personal communication). Ethyl and methyl esters (m/z 73 and 74) along with alkene fragments (m/z 103) could be sourced from the breakdown fatty acids. The abundance of aromatic fragments, with up to three-ring polycyclic aromatic hydrocarbons including benzene (m/z 78), naphthyl ions (m/z 127), methyl naphthalene (m/z 142), biphenyl (m/z 154), and phenanthrene (m/z 178), could be evolving from the pyrolysis of plant material with a maximum at 600°C. The releases of the methyl and ethyl esters along with the aromatics, especially at 600°C, may indicate that organics are bound in a different way than the original cellular state as was indicated in the surface soil. Additionally, chlorobenzene (m/z 112) is present, perhaps indicating that chlorination of aromatics is occurring within the instrument, as in martian soils (Miller et al., 2015, Freissinet et al., 2015). The difference in organic ion evolution between surface soils and older soils at 2 m depth shows that aged organic material, which has had significant time to degrade and interact with minerals, can dramatically change the organic ion content, temperature of release, and peak shape in EGA data.

Finally, the halite unit from 1.5 m depth in Yungay had an EGA signal different from the two clay-rich samples (Fig. 4.9). Firstly, there is significant evidence for halogenation of alkyl and aromatic fragments occurring at high (<700°C) temperature

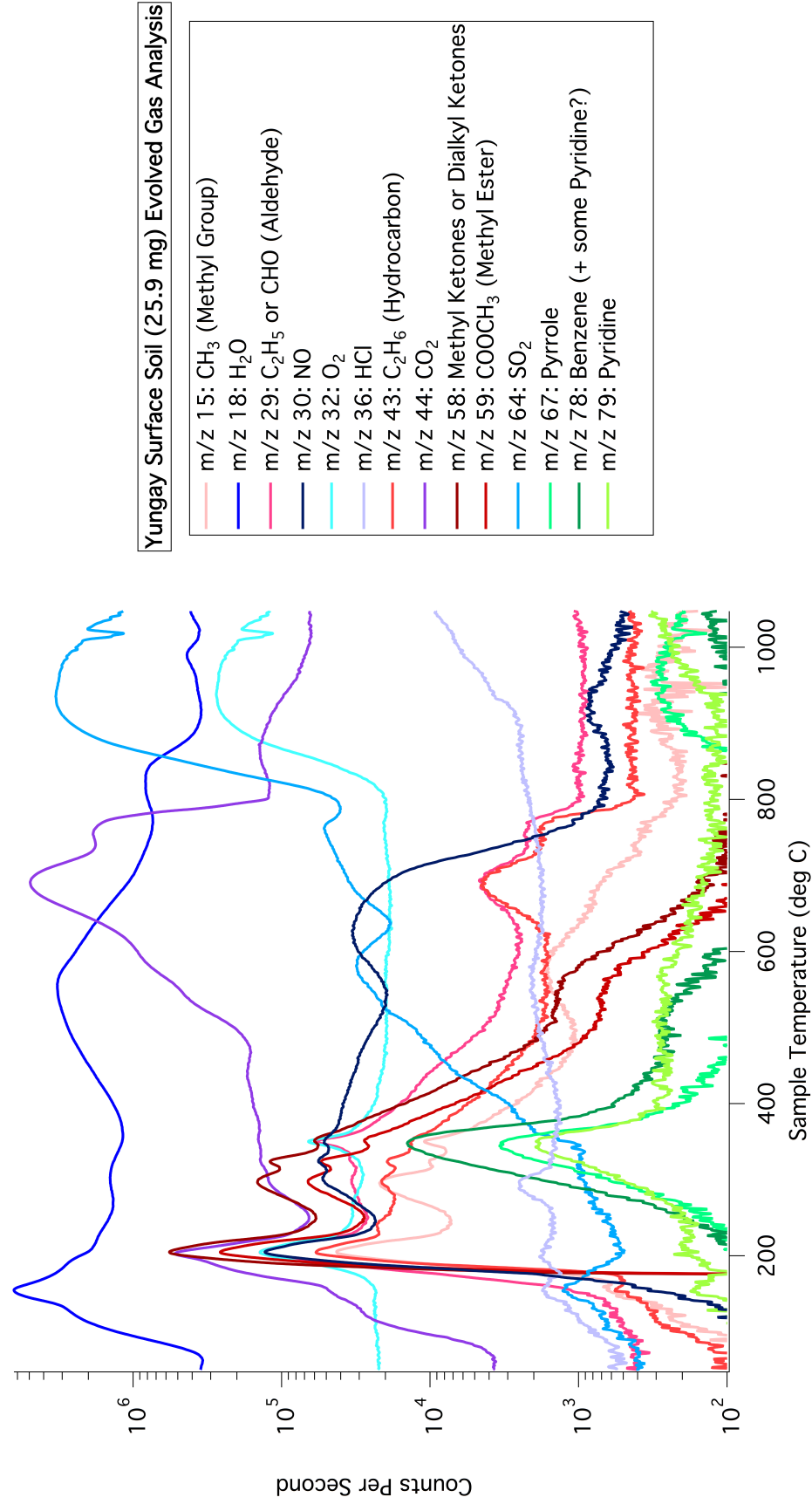


Figure 4.7: SAM-like EGA of Yungay surface soil. Red traces are organic m/z values may indicate the breakdown of a lipid membrane followed by green traces of organic m/z values that may be sourced from breakdown of sugars and nucleobases.

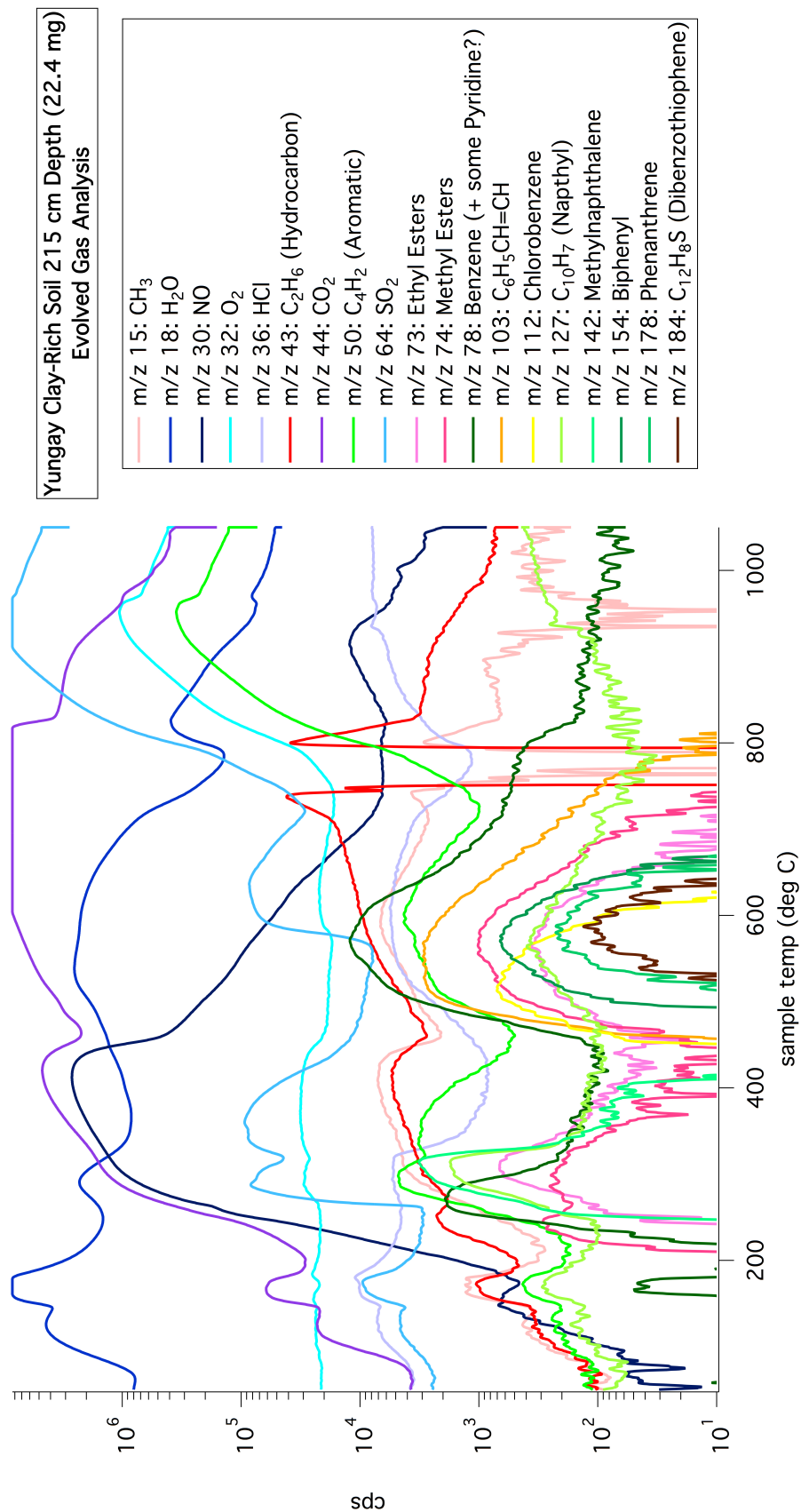


Figure 4.8: SAM-like EGA of clay-rich soil from 215 cm depth in Yungay. Traces of organic ions are suggestive of the presence of fatty acids bound in a different way than the original cellular state as was indicated in the surface soil.

due to the presence of HCl and potentially HBr (m/z 80). This includes unusual ions such as alkyl bromide (m/z 133), hexachlorobenzene (m/z 163), and a chlorinated aromatic (m/z 270). While there is a release of organic ions at between ~ 350 - 660°C including C_2 and C_8 straight-chain hydrocarbons (m/z 43 and 105), simple one ring aromatics (m/z 50 and 78), and carboxylic acids (m/z 60), the overall signal is not suggestive of a large biogenic component despite the presence of known presence of fatty acids and archaeal lipids in the halite (Chapter 3). However, the sharp releases at 850 - 900°C that can be observed in many ions including water, carbon dioxide, C_2 hydrocarbon, C_4 aromatic, and carboxylic acid may indicate the presence of organics contained in water inclusions within the halite crystals, given that the melting point of halite is at about that temperature.

4.2.4 Conclusion

In summary, organic ions were detectable in all three samples analyzed: modern clay-rich soil, ancient clay-rich soil, and a halite and perchlorate-rich unit despite the presence of oxidizers and low organic carbon abundances. The ion content, peak shape, temperature evolution, and intensity were different in all three samples. The organics released in surface soils had perhaps the strongest indication of biogenicity. However, even the buried clays still contained the EGA “fingerprints” of an ancient hydrocarbon producing environment. Perchlorate-rich samples produce a distinct, complex EGA signal in which there might be evidence for chlorination and bromination of organics occurring within the instrument, likely obscuring the *in situ* organic speciation at least partially. Yet, EGA of this sample revealed that the halite may harbor water-rich inclusions that bear organics, a finding that would be difficult to make using with other techniques.

EGA of Yungay soils indicate that this technique can be useful for a preliminary analysis of the organic content of an organically-complex, salt-rich, and biomass-poor

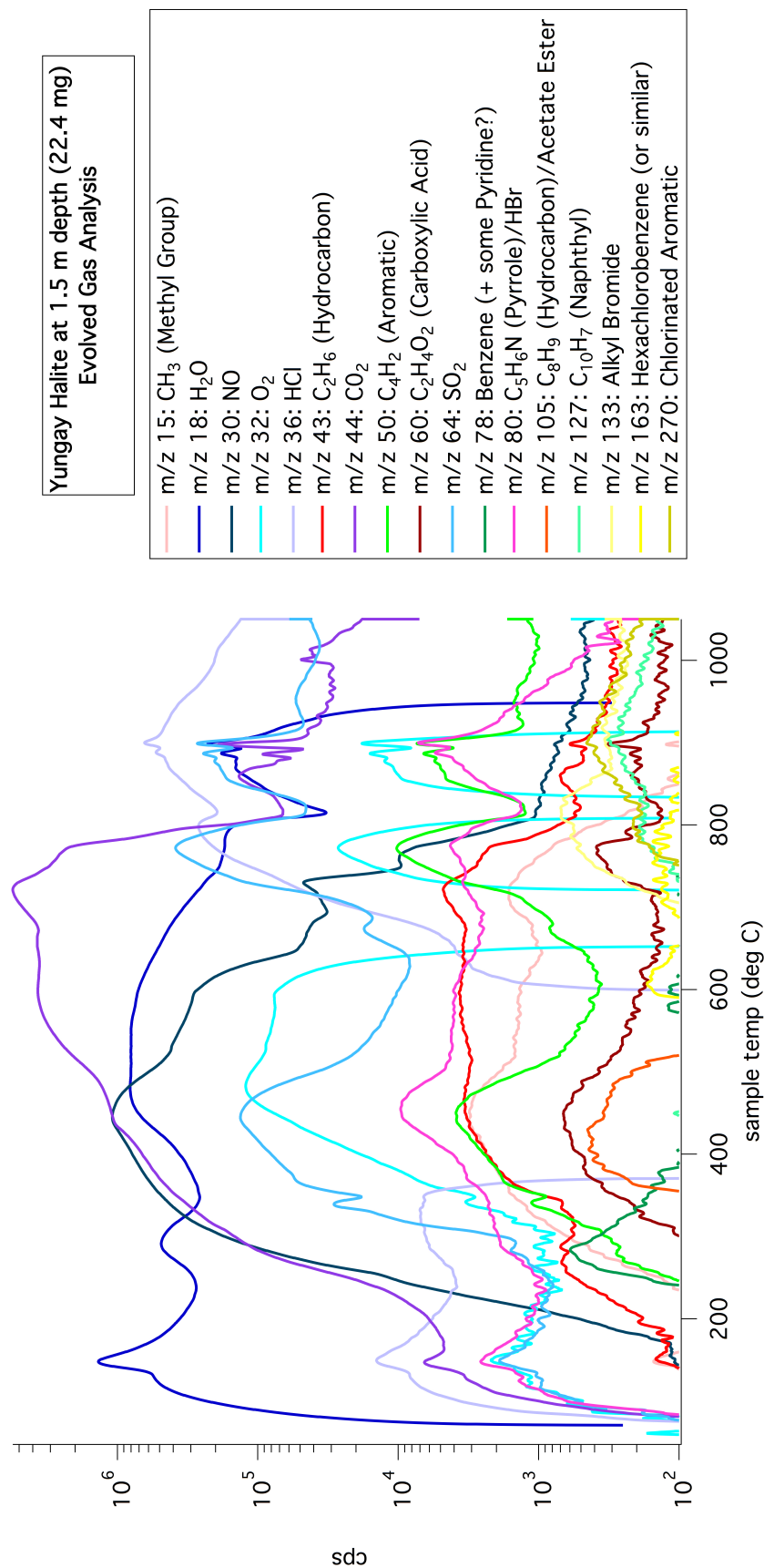


Figure 4.9: SAM-like EGA of halite and perchlorate-rich sample from 1.5 m depth in Yungay may show evidence of halogen-chemistry occurring within the instrument. Potential fluid inclusions bearing organics in the halite (sharp peaks) are released at 850-900°C.

natural sample. Although detailed information about the exact nature of organic molecules (i.e., larger polymers) is obscured in EGA data, the general presence of major classes of biomolecules such as fatty acids was suggested by the data, even in the presence of perchlorates. Given the relative operational simplicity of this technique and the amount of information retrieved by just one run, especially regarding the relationship between organics and inorganics, this technique would still be a useful addition on future Mars rover or lander missions. However, the information about organic presence obtained through EGA would be more useful with comparison and verification from instruments capable of measuring organic material with more specificity (i.e., targeted analysis of specific biomolecule classes and biosignatures).

CHAPTER 5

CONCLUSIONS AND IMPLICATIONS FOR MARS

Functionalized lipid biomarkers are preserved in clays and salts under extreme hyper-arid conditions for tens-of-thousands to a few million years or more. This is likely due in large part to the suspension degradation due to the activity of microorganisms. Xeropreservation (preservation by drying) of biomolecules represents an important, unexplored source of paleo-biological and paleo-environmental information in the hyperarid core of the Atacama Desert. Biomarkers in a soil profile in the Yungay region point to past wetter conditions that supported a larger diversity of organisms and metabolic processes than under the current climate.

The preservation of biomolecules under extreme dryness provides a tool to investigate trends in metabolic activity as a function of aridity. The absence of biomarkers diagnostic of active metabolism in soils in the driest parts of the Atacama Desert suggests that the dry limit of habitability might have been crossed in these hyperarid soils. Organisms in the driest parts of the desert do not seem to be better adapted to the physicochemical conditions. The dry limit of habitability might also have been crossed on the surface of Mars, which is 100-1000 times drier than the driest parts of the Atacama. If the small, decadal rain events in the extreme hyperarid region of the Atacama are not enough to sustain soil organisms, then we might expect soils on Mars—where water may be even more sporadically present in surface soils (Ojha. et al., 2015) if at all—to be similarly uninhabitable.

While extreme dryness in the Atacama Desert might not support metabolic activity, which leads to soils with very low biomass, the resulting fossil remains are well preserved and contain diagnostic biomarkers, detectable with current technologies. If life existed on Mars in the past, under similarly dry conditions, then the extreme

hyperarid environment could have been conducive to biomarker preservation, however low in concentration if organics are not degraded by other processes such as radiation. Those molecules could still carry some of the molecular “hallmarks” needed to identify their biogenicity (e.g., homochirality of amino acids; fatty acid even-over-odd chain length preferences; complexity in structure).

Sample acquisition and handling which includes sample preparation, while requiring increased complexity in instrument design, leads to increased information about organic content. While operational simplicity in flight instruments is beneficial from an engineering perspective, it can impede the production of data that is most useful for scientific questions of interest (e.g. search for evidence of life). Certainly, greater characterization of the organic material contained in ancient or modern martian sediments will be one of the the most important astrobiological advancements of the next few decades.

Instead of addressing habitability from an abstract perspective of, “ancient Mars would have been able to support life,” detailed characterization of organic material and the identification of putative molecular biomarkers could lead to answering of the more direct question, “did ancient Mars ever support life?” In examining case studies such as the martian meteorite ALH84001 or the purported body fossils in the Apex Chert as examples, physical biosignatures and/or the presence of non-specific carbon signals alone may not be enough to definitively identify the signs of life in ancient martian sediments because of the high probability that those signals could have been generated by an abiotic process. Instead, molecular biomarkers are information-rich, meaning that they not only contain information about not only presence, but also the activity of organisms through the specificity in their structure that connects them to a biological process. A great deal of information about organic material will be required to understand whether a sediment once harbored life. Understanding the preservation, degradation, and alteration of biomarkers as well as perfecting the

techniques of detecting them will be crucial for the search for life in the coming decades.

5.1 Future Work

In Yungay, future investigations should extend studies of biomarker preservation in buried, older soils to other more fragile biomarkers such as proteins, peptides, amino acids, and DNA. Differences in abundance and degree of preservation between these different biomolecule classes could be an avenue to investigate interactions occurring in the mineral matrix, biological degradation activity, and other abiotic degradation factors such as irradiation that could lead to differences. Additional studies should also look at the activity of enzymes under the extreme hyperarid climatic conditions. Better understanding of the preservation pathways of molecular biosignatures in hyperarid environments informs potential for success of NASA missions.

Follow-up investigations should also test the hypotheses presented here in other extremely dry terrestrial settings, especially in the Antarctic, where dryness is linked to cold temperatures. The high elevation (>1000m) region of the McMurdo Dry Valleys is an obvious target. This region hosts the coldest and driest permafrost soils on Earth, where snow accumulation is less than 10 millimeters per year (Doran, 2002; Marchant and Head, 2007), air temperatures rarely exceed 0°C, and most of the region is often or permanently shadowed due to surrounding topography. Lipid biomarker preservation “quality” in the high elevation McMurdo Dry Valleys ought to be similar to or better than in Yungay. Additionally, soil microbial communities would be exposed to similar levels of desiccation, so a lack of biomarkers linked to ongoing microbial activity is also expected.

Finally, it would be valuable to test biomarker detectability in million-year-old, biomass-poor, salt-rich Atacama soils using other Mars flight-instrumentation such as the Deep UV resonance Raman and fluorescence spectrometer slated to fly on

NASA's Mars 2020 rover, and SAM-like GC-MS with derivatization (MTBSTFA and TMAH). Testing of flight instrumentation with a suite of natural samples with Mars-like properties is crucial for instrument and technique development and interpretation of future positive or negative biomolecule detections in martian samples.

REFERENCES

- [1] W. J. Abbey, R. Bhartia, L. W. Beegle, L. DeFlores, V. Paez, K. Sijapati, S. Sijapati, K. Williford, M. Tuite, W. Hug, *et al.*, “Deep uv raman spectroscopy for planetary exploration: The search for in situ organics,” *Icarus*, vol. 290, pp. 201–214, 2017.
- [2] M. E. Allentoft, M. Collins, D. Harker, J. Haile, C. L. Oskam, M. L. Hale, P. F. Campos, J. A. Samaniego, M. T. P. Gilbert, E. Willerslev, *et al.*, “The half-life of dna in bone: Measuring decay kinetics in 158 dated fossils,” *Proceedings of the Royal Society of London B: Biological Sciences*, rspb20121745, 2012.
- [3] P. Alpert, *The limits and frontiers of desiccation-tolerant life*, 2005.
- [4] B. A. Annous, M. F. Kozempel, and M. J. Kurantz, “Changes in membrane fatty acid composition of *pediococcus* sp. strain nr1 b-2354 in response to growth conditions and its effect on thermal resistance,” *Applied and environmental microbiology*, vol. 65, no. 7, pp. 2857–2862, 1999.
- [5] A. Azua-Bustos, L. Caro-Lara, and R. Vicuña, “Discovery and microbial content of the driest site of the hyperarid atacama desert, chile,” *Environmental microbiology reports*, vol. 7, no. 3, pp. 388–394, 2015.
- [6] J. L. Bada and E. A. Hoopes, “Alanine enantiomeric ratio in the combined amino acid fraction in seawater,” *Nature*, vol. 282, no. 5741, pp. 822–823, 1979.
- [7] J. L. Bada and G. D. McDonald, “Amino acid racemization on mars: Implications for the preservation of biomolecules from an extinct martian biota,” *Icarus*, vol. 114, no. 1, pp. 139–143, 1995.
- [8] J. L. Bada, X. S. Wang, and H. Hamilton, “Preservation of key biomolecules in the fossil record: Current knowledge and future challenges,” *Philosophical Transactions of the Royal Society of London B: Biological Sciences*, vol. 354, no. 1379, pp. 77–87, 1999.
- [9] L. Becker, D. P. Glavin, and J. L. Bada, “Polycyclic aromatic hydrocarbons (pahs) in antarctic martian meteorites, carbonaceous chondrites, and polar ice,” *Geochimica et Cosmochimica Acta*, vol. 61, no. 2, pp. 475–481, 1997.
- [10] L. Beegle, R. Bhartia, L. DeFlores, S. Asher, A. Burton, S. Clegg, P. Conrad, K. Edgett, B. Ehlmann, F. Langenhorst, *et al.*, “Sherloc: Scanning habitable

environments with raman & luminescence for organics & chemicals, an investigation for 2020,” in *AGU Fall Meeting Abstracts*, vol. 1, 2014, p. 06.

- [11] S. A. Benner, K. G. Devine, L. N. Matveeva, and D. H. Powell, “The missing organic molecules on mars,” *Proceedings of the National Academy of Sciences*, vol. 97, no. 6, pp. 2425–2430, 2000.
- [12] K. Biemann, “On the ability of the viking gas chromatograph–mass spectrometer to detect organic matter,” *Proceedings of the National Academy of Sciences*, vol. 104, no. 25, pp. 10 310–10 313, 2007.
- [13] K. Biemann, J. Oro, P. Toulmin, L. Orgel, A. Nier, D. Anderson, P. Simmonds, D. Flory, A. Diaz, D. Rushneck, *et al.*, “Search for organic and volatile inorganic compounds in two surface samples from the chryse planitia region of mars,” *Science*, vol. 194, no. 4260, pp. 72–76, 1976.
- [14] D. Birgel, A. Guido, X. Liu, K.-U. Hinrichs, S. Gier, and J. Peckmann, “Hyper-saline conditions during deposition of the calcare di base revealed from archaeal di-and tetraether inventories,” *Organic Geochemistry*, vol. 77, pp. 11–21, 2014.
- [15] Y. Blanco, M. Moreno-Paz, and V. Parro, “Experimental protocol for detecting cyanobacteria in liquid and solid samples with an antibody microarray chip,” *JoVE (Journal of Visualized Experiments)*, no. 120, e54994–e54994, 2017.
- [16] E. G. Bligh and W. J. Dyer, “A rapid method of total lipid extraction and purification,” *Canadian journal of biochemistry and physiology*, vol. 37, no. 8, pp. 911–917, 1959.
- [17] M. Bordenave, “The sedimentation of organic matter,” *Applied Petroleum Geochemistry, Éditions Technip, Paris*, pp. 15–76, 1993.
- [18] O. BORGEL, “The coastal desert of chile,” 1973.
- [19] J. Brocks and R. Summons, “Sedimentary hydrocarbons, biomarkers for early life-10.3,”
- [20] —, “Biomarkers for early life,” *Biogeochemistry*, vol. 8, pp. 63–115, 2003.
- [21] C. Broly, J. Parnell, and S. Bowden, “Raman spectroscopy: Caution when interpreting organic carbon from oxidising environments,” *Planetary and Space Science*, vol. 121, pp. 53–59, 2016.
- [22] A. T. Bull, J. A. Asenjo, M. Goodfellow, and B. Gómez-Silva, “The atacama desert: Technical resources and the growing importance of novel microbial diversity,” *Annual Review of Microbiology*, vol. 70, pp. 215–234, 2016.

- [23] D. J. Burdige, “Preservation of organic matter in marine sediments: Controls, mechanisms, and an imbalance in sediment organic carbon budgets?” *Chemical reviews*, vol. 107, no. 2, pp. 467–485, 2007.
- [24] A. S. Burton, J. C. Stern, J. E. Elsila, D. P. Glavin, and J. P. Dworkin, “Understanding prebiotic chemistry through the analysis of extraterrestrial amino acids and nucleobases in meteorites,” *Chemical Society Reviews*, vol. 41, no. 16, pp. 5459–5472, 2012.
- [25] L. Cáceres, B. Gómez-Silva, X. Garró, V. Rodríguez, V. Monardes, and C. P. McKay, “Relative humidity patterns and fog water precipitation in the atacama desert and biological implications,” *Journal of Geophysical Research: Biogeosciences*, vol. 112, no. G4, 2007.
- [26] M. Chen and T. S. Bibby, “Photosynthetic apparatus of antenna-reaction centres supercomplexes in oxyphotobacteria: Insight through significance of pcb/isia proteins,” *Photosynthesis research*, vol. 86, no. 1, pp. 165–173, 2005.
- [27] Y. Y. Chen and M. G. Gänzle, “Influence of cyclopropane fatty acids on heat, high pressure, acid and oxidative resistance in escherichia coli,” *International journal of food microbiology*, vol. 222, pp. 16–22, 2016.
- [28] J. D. Clarke, “Antiquity of aridity in the chilean atacama desert,” *Geomorphology*, vol. 73, no. 1, pp. 101–114, 2006.
- [29] A. K. Cobb and R. E. Pudritz, “Nature’s starships. i. observed abundances and relative frequencies of amino acids in meteorites,” *The Astrophysical Journal*, vol. 783, no. 2, p. 140, 2014.
- [30] M. J. Collins and M. S. Riley, “11. amino acid racemization in biominerals: The impact of protein degradation and loss,” *Perspectives in Amino Acid and Protein Geochemistry*, p. 120, 2000.
- [31] C. A. Conley, G. Ishkhanova, C. P. Mckay, and K. Cullings, “A preliminary survey of non-lichenized fungi cultured from the hyperarid atacama desert of chile,” *Astrobiology*, vol. 6, no. 4, pp. 521–526, 2006.
- [32] S. A. Cannon, E. D. Lester, H. S. Shafaat, D. C. Obenhuber, and A. Ponce, “Bacterial diversity in hyperarid atacama desert soils,” *Journal of Geophysical Research: Biogeosciences*, vol. 112, no. G4, 2007.
- [33] M. J. Coolen, G. Muyzer, W. I. C. Rijpstra, S. Schouten, J. K. Volkman, and J. S. S. Damsté, “Combined dna and lipid analyses of sediments reveal changes in holocene haptophyte and diatom populations in an antarctic lake,” *Earth and Planetary Science Letters*, vol. 223, no. 1, pp. 225–239, 2004.

- [34] G. Cooper, *The cell: A molecular approach, 2nd edn. the cell: A molecular approach. sunderland, ma*, 2000.
- [35] A. Crits-Christoph, C. K. Robinson, T. Barnum, W. F. Fricke, A. F. Davila, B. Jedynak, C. P. McKay, and J. DiRuggiero, “Colonization patterns of soil microbial communities in the atacama desert,” *Microbiome*, vol. 1, no. 1, p. 28, 2013.
- [36] K. Czamara, K. Majzner, M. Z. Pacia, K. Kochan, A. Kaczor, and M. Baranska, “Raman spectroscopy of lipids: A review,” *Journal of Raman Spectroscopy*, vol. 46, no. 1, pp. 4–20, 2015.
- [37] A. F. Davila and D. Schulze-Makuch, “The last possible outposts for life on mars,” *Astrobiology*, vol. 16, no. 2, pp. 159–168, 2016.
- [38] W. L. Davis, I. de Pater, and C. P. McKay, “Rain infiltration and crust formation in the extreme arid zone of the atacama desert, chile,” *Planetary and Space Science*, vol. 58, no. 4, pp. 616–622, 2010.
- [39] D. J. Des Marais, “Isotopic evolution of the biogeochemical carbon cycle during the precambrian,” *Reviews in Mineralogy and Geochemistry*, vol. 43, no. 1, pp. 555–578, 2001.
- [40] P. T. Doran, C. P. McKay, G. D. Clow, G. L. Dana, A. G. Fountain, T. Nylen, and W. B. Lyons, “Valley floor climate observations from the mcmurdo dry valleys, antarctica, 1986–2000,” *Journal of Geophysical Research: Atmospheres*, vol. 107, no. D24, 2002.
- [41] A. Dorfman, *Desert Memories: Journeys through the Chilean North*. National Geographic Society, 2004.
- [42] G. Eglinton, G. A. Logan, R. Ambler, J. Boon, and W. Perizonius, “Molecular preservation [and discussion],” *Philosophical Transactions of the Royal Society B: Biological Sciences*, vol. 333, no. 1268, pp. 315–328, 1991.
- [43] B. L. Ehlmann, J. F. Mustard, S. L. Murchie, J.-P. Bibring, A. Meunier, A. A. Fraeman, and Y. Langevin, “Subsurface water and clay mineral formation during the early history of mars,” *Nature*, vol. 479, no. 7371, pp. 53–60, 2011.
- [44] J. L. Eigenbrode, “Fossil lipids for life-detection: A case study from the early earth record,” in *Strategies of Life Detection*, Springer, 2008, pp. 161–185.
- [45] J. Eigenbrode, A. Steele, R. Summons, B. Sutter, A. McAdam, H. Franz, P. Mahaffy, P. Conrad, C. Freissinet, D. Glavin, *et al.*, “Evidence of refractory

organic matter preserved in the mudstones of yellowknife bay and the murray formations,” in *AGU Fall Meeting Abstracts*, 2015.

- [46] V. O. Elias, B. R. Simoneit, and J. N. Cardoso, “Even n-alkane predominances on the amazon shelf and a northeast pacific hydrothermal system,” *Naturwissenschaften*, vol. 84, no. 9, pp. 415–420, 1997.
- [47] S. Ewing, J. Macalady, K. Warren-Rhodes, C. McKay, and R. Amundson, “Changes in the soil c cycle at the arid-hyperarid transition in the atacama desert,” *Journal of Geophysical Research: Biogeosciences*, vol. 113, no. G2, 2008.
- [48] S. A. Ewing, B. Sutter, J. Owen, K. Nishiizumi, W. Sharp, S. S. Cliff, K. Perry, W. Dietrich, C. P. McKay, and R. Amundson, “A threshold in soil formation at earth’s arid–hyperarid transition,” *Geochimica et Cosmochimica Acta*, vol. 70, no. 21, pp. 5293–5322, 2006.
- [49] J. D. Farmer and D. J. Des Marais, “Exploring for a record of ancient martian life,” *Journal of Geophysical Research: Planets*, vol. 104, no. E11, pp. 26 977–26 995, 1999.
- [50] C. Freissinet, D. Glavin, P. R. Mahaffy, K. Miller, J. Eigenbrode, R. Summons, A. Brunner, A. Buch, C. Szopa, P. Archer, *et al.*, “Organic molecules in the sheepbed mudstone, gale crater, mars,” *Journal of Geophysical Research: Planets*, vol. 120, no. 3, pp. 495–514, 2015.
- [51] R. D. Garreaud, A. Molina, and M. Farias, “Andean uplift, ocean cooling and atacama hyperaridity: A climate modeling perspective,” *Earth and Planetary Science Letters*, vol. 292, no. 1, pp. 39–50, 2010.
- [52] C. D. Georgiou, H. J. Sun, C. P. McKay, K. Grintzalis, I. Papapostolou, D. Zisimopoulos, K. Panagiotidis, G. Zhang, E. Koutsopoulou, G. E. Christidis, *et al.*, “Evidence for photochemical production of reactive oxygen species in desert soils,” *Nature communications*, vol. 6, 2015.
- [53] M. T. de Gomez-Puyou and A. Gomez-Puyou, “Enzymes in low water systems,” *Critical reviews in biochemistry and molecular biology*, vol. 33, no. 1, pp. 53–89, 1998.
- [54] J. Goordial, A. Davila, D. Lacelle, W. Pollard, M. M. Marinova, C. W. Greer, J. DiRuggiero, C. P. McKay, and L. G. Whyte, “Nearing the cold-arid limits of microbial life in permafrost of an upper dry valley, antarctica,” *The ISME journal*, vol. 10, no. 7, pp. 1613–1624, 2016.

- [55] J. H. Graham, N. C. Hodge, and J. B. Morton, "Fatty acid methyl ester profiles for characterization of glomalean fungi and their endomycorrhizae," *Applied and environmental microbiology*, vol. 61, no. 1, pp. 58–64, 1995.
- [56] W. Grant, "Life at low water activity," *Philosophical Transactions of the Royal Society B: Biological Sciences*, vol. 359, no. 1448, pp. 1249–1267, 2004.
- [57] D. W. Grogan and J. E. Cronan, "Cyclopropane ring formation in membrane lipids of bacteria," *Microbiology and Molecular Biology Reviews*, vol. 61, no. 4, pp. 429–441, 1997.
- [58] J. P. Grotzinger, J. Crisp, A. R. Vasavada, R. C. Anderson, C. J. Baker, R. Barry, D. F. Blake, P. Conrad, K. S. Edgett, B. Ferdowski, *et al.*, "Mars science laboratory mission and science investigation," *Space science reviews*, vol. 170, no. 1-4, pp. 5–56, 2012.
- [59] J. P. Grotzinger, D. Y. Sumner, L. Kah, K Stack, S Gupta, L Edgar, D Rubin, K Lewis, J Schieber, N Mangold, *et al.*, "A habitable fluvio-lacustrine environment at yellowknife bay, gale crater, mars," *Science*, vol. 343, no. 6169, p. 1 242 777, 2014.
- [60] J. Grotzinger, S Gupta, M. Malin, D. Rubin, J Schieber, K Siebach, D. Sumner, K. Stack, A. Vasavada, R. Arvidson, *et al.*, "Deposition, exhumation, and paleoclimate of an ancient lake deposit, gale crater, mars," *Science*, vol. 350, no. 6257, aac7575, 2015.
- [61] J. Guckert, M. Hood, and D. White, "Phospholipid ester-linked fatty acid profile changes during nutrient deprivation of vibrio cholerae: Increases in the trans/cis ratio and proportions of cyclopropyl fatty acids," *Applied and environmental microbiology*, vol. 52, no. 4, pp. 794–801, 1986.
- [62] A. J. Hartley and G. Chong, "Late pliocene age for the atacama desert: Implications for the desertification of western south america," *Geology*, vol. 30, no. 1, pp. 43–46, 2002.
- [63] A. J. Hartley, G. Chong, J. Houston, and A. E. Mather, "150 million years of climatic stability: Evidence from the atacama desert, northern chile," *Journal of the Geological Society*, vol. 162, no. 3, pp. 421–424, 2005.
- [64] M. Hecht, S. Kounaves, R. Quinn, S. West, S. Young, D. Ming, D. Catling, B. Clark, W. Boynton, J Hoffman, *et al.*, "Detection of perchlorate and the soluble chemistry of martian soil at the phoenix lander site," *Science*, vol. 325, no. 5936, pp. 64–67, 2009.

- [65] H. J. Heipieper, B. Loffeld, H. Keweloh, and J. A. de Bont, "The cis/trans isomerisation of unsaturated fatty acids in pseudomonas putida s12: An indicator for environmental stress due to organic compounds," *Chemosphere*, vol. 30, no. 6, pp. 1041–1051, 1995.
- [66] H. J. Heipieper, F. Meinhardt, and A. Segura, "The cis–trans isomerase of unsaturated fatty acids in pseudomonas and vibrio: Biochemistry, molecular biology and physiological function of a unique stress adaptive mechanism," *FEMS microbiology letters*, vol. 229, no. 1, pp. 1–7, 2003.
- [67] H. J. Heipieper, G. Meulenbeld, Q. van Oirschot, and J. De Bont, "Effect of environmental factors on the trans/cis ratio of unsaturated fatty acids in pseudomonas putida s12.," *Applied and Environmental Microbiology*, vol. 62, no. 8, pp. 2773–2777, 1996.
- [68] W. Holser, M. Schidlowski, F. Mackenzie, and J. Maynard, "Geochemical cycles of carbon and sulfur," *Chemical Cycles in the Evolution of the Earth*, pp. 105–173, 1988.
- [69] M. M. Hossain and H. Nakamoto, "Htpg plays a role in cold acclimation in cyanobacteria," *Current microbiology*, vol. 44, no. 4, pp. 291–296, 2002.
- [70] ———, "Role for the cyanobacterial htpg in protection from oxidative stress," *Current microbiology*, vol. 46, no. 1, pp. 0070–0076, 2003.
- [71] J. Houston and A. J. Hartley, "The central andean west-slope rainshadow and its potential contribution to the origin of hyper-aridity in the atacama desert," *International Journal of Climatology*, vol. 23, no. 12, pp. 1453–1464, 2003.
- [72] I. B. Hutchinson, J. Parnell, H. G. Edwards, J. Jehlicka, C. P. Marshall, L. V. Harris, and R. Ingley, "Potential for analysis of carbonaceous matter on mars using raman spectroscopy," *Planetary and Space Science*, vol. 103, pp. 184–190, 2014.
- [73] K. Ichihara, A. Shibahara, K. Yamamoto, and T. Nakayama, "An improved method for rapid analysis of the fatty acids of glycerolipids," *Lipids*, vol. 31, no. 5, pp. 535–539, 1996.
- [74] L. L. Jahnke, H. Stan-Lotter, K. Kato, and L. I. Hochstein, "Presence of methyl sterol and bacteriohopanepolyol in an outer-membrane preparation from methylococcus capsulatus (bath)," *Microbiology*, vol. 138, no. 8, pp. 1759–1766, 1992.
- [75] L. Jahnke, V. Orphan, T. Embaye, K. Turk, M. Kubo, R. Summons, and D. Des Marais, "Lipid biomarker and phylogenetic analyses to reveal archaeal

biodiversity and distribution in hypersaline microbial mat and underlying sediment,” *Geobiology*, vol. 6, no. 4, pp. 394–410, 2008.

- [76] T. E. Jordan, N. E. Kirk-Lawlor, N. P. Blanco, J. A. Rech, and N. J. Cosentino, “Landscape modification in response to repeated onset of hyperarid paleoclimate states since 14 ma, atacama desert, chile,” *Geological Society of America Bulletin*, vol. 126, no. 7-8, pp. 1016–1046, 2014.
- [77] T. Kaneda, “Iso-and anteiso-fatty acids in bacteria: Biosynthesis, function, and taxonomic significance,” *Microbiological reviews*, vol. 55, no. 2, pp. 288–302, 1991.
- [78] M Kates, “Isolation, analysis and identification of lipids,” *Techniques in Lipidology. Elsevier, Amsterdam*, pp. 268–618, 1972.
- [79] ———, “The phytanyl ether-linked polar lipids and isoprenoid neutral lipids of extremely halophilic bacteria,” *Progress in the chemistry of fats and other lipids*, vol. 15, no. 4, pp. 301–342, 1977.
- [80] M KATES, M de Rosa, A Gambacorta, and J. Bu’Lock, “On and analysis of complex polar lipids of methanospirillum hungatei references and notes,” *Biophys. Res. Commun*, vol. 82, p. 716, 1978.
- [81] R. Keil and L. Mayer, “12.12-mineral matrices and organic matter,” 2014.
- [82] L. L. King, T. K. Pease, and S. G. Wakeham, “Archaea in black sea water column particulate matter and sediments—evidence from ether lipid derivatives,” *Organic Geochemistry*, vol. 28, no. 11, pp. 677–688, 1998.
- [83] A. H. Knoll, R. E. Summons, J. R. Waldbauer, and J. E. Zumberge, “The geological succession of primary producers in the oceans,” *Evolution of Primary Producers in the Sea*, pp. 133–163, 2007.
- [84] M. Kobayashi, T. Kobayashi, Y. Itoh, and K. Sato, “Polytypism in n-fatty acids and low-frequency raman spectra: Stearic acid b form,” *The Journal of chemical physics*, vol. 80, no. 6, pp. 2897–2903, 1984.
- [85] Y. Koga and H. Morii, “Recent advances in structural research on ether lipids from archaea including comparative and physiological aspects,” *Bioscience, biotechnology, and biochemistry*, vol. 69, no. 11, pp. 2019–2034, 2005.
- [86] C. Kontoyannis and N. Vagenas, “Ft-raman spectroscopy: A tool for monitoring the demineralization of bones,” *Applied Spectroscopy*, vol. 54, no. 11, pp. 1605–1609, 2000.

- [87] C. G. Kontoyannis and N. V. Vagenas, "Calcium carbonate phase analysis using xrd and ft-raman spectroscopy," *Analyst*, vol. 125, no. 2, pp. 251–255, 2000.
- [88] P. Krishna and G. Gloor, "The hsp90 family of proteins in arabidopsis thaliana," *Cell stress & chaperones*, vol. 6, no. 3, pp. 238–246, 2001.
- [89] Y. Kuzyakov, "Priming effects: Interactions between living and dead organic matter," *Soil Biology and Biochemistry*, vol. 42, no. 9, pp. 1363–1371, 2010.
- [90] P. H. Lebre, P. De Maayer, and D. A. Cowan, "Xerotolerant bacteria: Surviving through a dry spell," *Nature Reviews Microbiology*, vol. 15, no. 5, pp. 285–296, 2017.
- [91] E. D. Lester, M. Satomi, and A. Ponce, "Microflora of extreme arid atacama desert soils," *Soil Biology and Biochemistry*, vol. 39, no. 2, pp. 704–708, 2007.
- [92] G. Lopez-Reyes, F. Rull, G. Venegas, F. Westall, F. Foucher, N. Bost, A. Sanz, A. Catalá-Espí, A. Vegas, I. Hermosilla, *et al.*, "Analysis of the scientific capabilities of the exomars raman laser spectrometer instrument," *European Journal of Mineralogy*, vol. 25, no. 5, pp. 721–733, 2013.
- [93] G. Lopez-Reyes, P. Sobron, C. Lefebvre, and F. Rull, "Multivariate analysis of raman spectra for the identification of sulfates: Implications for exomars," *American Mineralogist*, vol. 99, no. 8-9, pp. 1570–1579, 2014.
- [94] R Madan, C Pankhurst, B Hawke, and S Smith, "Use of fatty acids for identification of am fungi and estimation of the biomass of am spores in soil," *Soil Biology and Biochemistry*, vol. 34, no. 1, pp. 125–128, 2002.
- [95] P. R. Mahaffy, C. R. Webster, M. Cabane, P. G. Conrad, P. Coll, S. K. Atreya, R. Arvey, M. Barciniak, M. Benna, L. Bleacher, *et al.*, "The sample analysis at mars investigation and instrument suite," *Space Science Reviews*, vol. 170, no. 1-4, pp. 401–478, 2012.
- [96] D. R. Marchant and J. W. Head, "Antarctic dry valleys: Microclimate zonation, variable geomorphic processes, and implications for assessing climate change on mars," *Icarus*, vol. 192, no. 1, pp. 187–222, 2007.
- [97] L. M. Markillie, S. M. Varnum, P. Hradecky, and K.-K. Wong, "Targeted mutagenesis by duplication insertion in the radioresistant bacterium deinococcus radiodurans: Radiation sensitivities of catalase (kata) and superoxide dismutase (soda) mutants," *Journal of bacteriology*, vol. 181, no. 2, pp. 666–669, 1999.

- [98] A. G. Marr and J. L. Ingraham, "Effect of temperature on the composition of fatty acids in escherichia coli," *Journal of Bacteriology*, vol. 84, no. 6, pp. 1260–1267, 1962.
- [99] S. Maurice, R. C. Wiens, S. Le Mouélic, R. Anderson, O. Beyssac, L. Bonal, S. Clegg, L. DeFlores, G. Dromart, W. Fischer, *et al.*, "The supercam instrument for the mars2020 rover," in *European Planetary Science Congress 2015, held 27 September-2 October, 2015 in Nantes, France, Online at <http://meetingorganizer.copernicus.org/EPSC2015>, id. EPSC2015-185*, vol. 10, 2015, p. 185.
- [100] A. McAdam, P. Archer Jr, B Sutter, H. Franz, J. Eigenbrode, D. Ming, R. Morris, P. Niles, J. Stern, C Freissinet, *et al.*, "Major volatiles from msl sam evolved gas analyses: Yellowknife bay through lower mount sharp," 2015.
- [101] A. McAdam, I. Ten Kate, J. Stern, P. Mahaffy, D. Blake, R. Morris, A Steele, and H. Amundson, "Field characterization of the mineralogy and organic chemistry of carbonates from the 2010 arctic mars analog svalbard expedition by evolved gas analysis," 2011.
- [102] M. D. McCarthy, J. I. Hedges, and R. Benner, "Major bacterial contribution to marine dissolved organic nitrogen," *Science*, vol. 281, no. 5374, pp. 231–234, 1998.
- [103] C. P. McKay, E. I. Friedmann, B. Gómez-Silva, L. Cáceres-Villanueva, D. T. Andersen, and R. Landheim, "Temperature and moisture conditions for life in the extreme arid region of the atacama desert: Four years of observations including the el nino of 1997–1998," *Astrobiology*, vol. 3, no. 2, pp. 393–406, 2003.
- [104] J. F. Meadow, A. E. Altrichter, A. C. Bateman, J. Stenson, G. Brown, J. L. Green, and B. J. Bohannon, "Humans differ in their personal microbial cloud," *PeerJ*, vol. 3, e1258, 2015.
- [105] I. Melendez, K. Grice, and L. Schwark, "Exceptional preservation of palaeozoic steroids in a diagenetic continuum," *Scientific reports*, vol. 3, p. 2768, 2013.
- [106] P. A. Meyers and R. Ishiwatari, "Lacustrine organic geochemistry—an overview of indicators of organic matter sources and diagenesis in lake sediments," *Organic geochemistry*, vol. 20, no. 7, pp. 867–900, 1993.
- [107] G. H. Miller, C. P. Hart, E. B. Roark, and B. J. Johnson, "13. isoleucine epimerization in eggshells of (the (lightless australian birds genyomis and dro-maius)," *Perspectives in Amino Acid and Protein Geochemistry*, p. 161, 2000.

- [108] K. E. Miller, B. Kotrc, R. E. Summons, I. Belmahdi, A. Buch, J. L. Eigenbrode, C. Freissinet, D. P. Glavin, and C. Szopa, “Evaluation of the tenax trap in the sample analysis at mars instrument suite on the curiosity rover as a potential hydrocarbon source for chlorinated organics detected in gale crater,” *Journal of Geophysical Research: Planets*, vol. 120, no. 8, pp. 1446–1459, 2015.
- [109] D. Ming, H. Lauer, P. Archer, B Sutter, D. Golden, R. Morris, P. Niles, and W. Boynton, “Combustion of organic molecules by the thermal decomposition of perchlorate salts: Implications for organics at the mars phoenix scout landing site,” in *Lunar and Planetary Science Conference*, vol. 40, 2009, p. 2241.
- [110] C. A. Morgan, N Herman, P. White, and G Vesey, “Preservation of micro-organisms by drying; a review,” *Journal of microbiological methods*, vol. 66, no. 2, pp. 183–193, 2006.
- [111] J. Muñoz-Rojas, P. Bernal, E. Duque, P. Godoy, A. Segura, and J.-L. Ramos, “Involvement of cyclopropane fatty acids in the response of pseudomonas putida kt2440 to freeze-drying,” *Applied and Environmental Microbiology*, vol. 72, no. 1, pp. 472–477, 2006.
- [112] J. Mustard, M Adler, A Allwood, D. Bass, D. Beaty, J. Bell III, W. Brinckerhoff, M Carr, D. Des Marais, B Drake, *et al.*, *Report of the mars 2020 science definition team, posted july 2013 by the mars exploration program analysis group (mepag)*, 2013.
- [113] G. Muyzer, P. Sandberg, M. H. Knapen, C. Vermeer, M. Collins, and P. Westbroek, “Preservation of the bone protein osteocalcin in dinosaurs,” *Geology*, vol. 20, no. 10, pp. 871–874, 1992.
- [114] R. Navarro-González, E. Iniguez, J. d. l. Rosa, and C. P. McKay, “Characterization of organics, microorganisms, desert soils, and mars-like soils by thermal volatilization coupled to mass spectrometry and their implications for the search for organics on mars by phoenix and future space missions,” *Astrobiology*, vol. 9, no. 8, pp. 703–715, 2009.
- [115] R. Navarro-González, K. F. Navarro, J. de la Rosa, E. Iñiguez, P. Molina, L. D. Miranda, P. Morales, E. Cienfuegos, P. Coll, F. Raulin, *et al.*, “The limitations on organic detection in mars-like soils by thermal volatilization–gas chromatography–ms and their implications for the viking results,” *Proceedings of the National Academy of Sciences*, vol. 103, no. 44, pp. 16 089–16 094, 2006.
- [116] R. Navarro-González, F. A. Rainey, P. Molina, D. R. Bagaley, B. J. Hollen, J. de la Rosa, A. M. Small, R. C. Quinn, F. J. Grunthaner, L. Cáceres, *et al.*, “Mars-like soils in the atacama desert, chile, and the dry limit of microbial life,” *Science*, vol. 302, no. 5647, pp. 1018–1021, 2003.

- [117] R. Navarro-González, E. Vargas, J. de La Rosa, A. C. Raga, and C. P. McKay, “Reanalysis of the viking results suggests perchlorate and organics at midlatitudes on mars,” *Journal of Geophysical Research: Planets*, vol. 115, no. E12, 2010.
- [118] I. Noy-Meir, “Desert ecosystems: Environment and producers,” *Annual review of ecology and systematics*, vol. 4, no. 1, pp. 25–51, 1973.
- [119] L. Ojha, M. B. Wilhelm, S. L. Murchie, A. S. McEwen, J. J. Wray, J. Hanley, M. Massé, and M. Chojnacki, “Spectral evidence for hydrated salts in recurring slope lineae on mars,” *Nature Geoscience*, vol. 8, no. 11, pp. 829–832, 2015.
- [120] H. Okuyama, N. Okajima, S. Sasaki, S. Higashi, and N. Murata, “The cis/trans isomerization of the double bond of a fatty acid as a strategy for adaptation to changes in ambient temperature in the psychrophilic bacterium, vibrio sp. strain abe-1,” *Biochimica et Biophysica Acta (BBA)-Lipids and Lipid Metabolism*, vol. 1084, no. 1, pp. 13–20, 1991.
- [121] D. M. Olson, E. Dinerstein, E. D. Wikramanayake, N. D. Burgess, G. V. Powell, E. C. Underwood, J. A. D’amico, I. Itoua, H. E. Strand, J. C. Morrison, *et al.*, “Terrestrial ecoregions of the world: A new map of life on earth: A new global map of terrestrial ecoregions provides an innovative tool for conserving biodiversity,” *BioScience*, vol. 51, no. 11, pp. 933–938, 2001.
- [122] M. N. Parenteau, L. L. Jahnke, J. D. Farmer, and S. L. Cady, “Production and early preservation of lipid biomarkers in iron hot springs,” *Astrobiology*, vol. 14, no. 6, pp. 502–521, 2014.
- [123] V. Parro, Y. Blanco, F. Puente-Sánchez, L. A. Rivas, M. Moreno-Paz, A. Echeverría, G. Chong-Díaz, C. Demergasso, and N. A. Cabrol, “Biomarkers and metabolic patterns in the sediments of evolving glacial lakes as a proxy for planetary lake exploration,” *Astrobiology*, 2016.
- [124] V. Parro, G. de Diego-Castilla, M. Moreno-Paz, Y. Blanco, P. Cruz-Gil, J. A. Rodríguez-Manfredi, D. Fernández-Remolar, F. Gómez, M. J. Gómez, L. A. Rivas, *et al.*, “A microbial oasis in the hypersaline atacama subsurface discovered by a life detector chip: Implications for the search for life on mars,” *Astrobiology*, vol. 11, no. 10, pp. 969–996, 2011.
- [125] D. J. Patzelt, L. Hodač, T. Friedl, N. Pietrasiak, and J. R. Johansen, “Biodiversity of soil cyanobacteria in the hyper-arid atacama desert, chile,” *Journal of phycology*, vol. 50, no. 4, pp. 698–710, 2014.

- [126] A. Pavlov, G Vasilyev, V. Ostryakov, A. Pavlov, and P Mahaffy, "Degradation of the organic molecules in the shallow subsurface of mars due to irradiation by cosmic rays," *Geophysical research letters*, vol. 39, no. 13, 2012.
- [127] A. Pearson and A. E. Ingalls, "Assessing the use of archaeal lipids as marine environmental proxies," *Annual Review of Earth and Planetary Sciences*, vol. 41, pp. 359–384, 2013.
- [128] K. E. Penkman, R. C. Preece, D. R. Bridgland, D. H. Keen, T. Meijer, S. A. Parfitt, T. S. White, and M. J. Collins, "A chronological framework for the british quaternary based on bithynia opercula," *Nature*, vol. 476, no. 7361, pp. 446–449, 2011.
- [129] K. E. Peters, C. C. Walters, and J. M. Moldowan, *The biomarker guide*. Cambridge University Press, 2005, vol. 1.
- [130] S. Petsch, T. Eglinton, and K. Edwards, "14c-dead living biomass: Evidence for microbial assimilation of ancient organic carbon during shale weathering," *Science*, vol. 292, no. 5519, pp. 1127–1131, 2001.
- [131] D. Poger and A. E. Mark, "A ring to rule them all: The effect of cyclopropane fatty acids on the fluidity of lipid bilayers," *The journal of physical chemistry B*, vol. 119, no. 17, pp. 5487–5495, 2015.
- [132] H. N. Poinar, M. Hoss, J. L. Bada, and S. Paabo, "Amino acid racemization and the preservation of ancient dna," *Science*, vol. 272, no. 5263, p. 864, 1996.
- [133] S. B. Pointing and J. Belnap, "Microbial colonization and controls in dryland systems," *Nature Reviews Microbiology*, vol. 10, no. 8, pp. 551–562, 2012.
- [134] M. Potts, "Desiccation tolerance of prokaryotes.," *Microbiological reviews*, vol. 58, no. 4, pp. 755–805, 1994.
- [135] T. Powell and D. McKirdy, "Relationship between ratio of pristane to phytane, crude oil composition and geological environment in australia," *Nature*, vol. 243, no. 124, pp. 37–39, 1973.
- [136] M. C. Proctor, M. J. Oliver, A. J. Wood, P. Alpert, L. R. Stark, N. L. Cleavitt, and B. D. Mishler, "Desiccation-tolerance in bryophytes: A review," *The Bryologist*, vol. 110, no. 4, pp. 595–621, 2007.
- [137] J. Quade, P. Reiners, C. Placzek, A. Matmon, M. Pepper, L. Ojha, and K. Murray, "Seismicity and the strange rubbing boulders of the atacama desert, northern chile," *Geology*, vol. 40, no. 9, pp. 851–854, 2012.

- [138] S. E. Rashby, A. L. Sessions, R. E. Summons, and D. K. Newman, “Biosynthesis of 2-methylbacteriohopanepolyols by an anoxygenic phototroph,” *Proceedings of the National Academy of Sciences*, vol. 104, no. 38, pp. 15 099–15 104, 2007.
- [139] J. Rethemeyer, F. Schubotz, H. M. Talbot, M. P. Cooke, K.-U. Hinrichs, and G. Mollenhauer, “Distribution of polar membrane lipids in permafrost soils and sediments of a small high arctic catchment,” *Organic Geochemistry*, vol. 41, no. 10, pp. 1130–1145, 2010.
- [140] L. A. Rivas, M. García-Villadangos, M. Moreno-Paz, P. Cruz-Gil, J. Gómez-Elvira, and V. Parro, “A 200-antibody microarray biochip for environmental monitoring: Searching for universal microbial biomarkers through immunoprofiling,” *Analytical chemistry*, vol. 80, no. 21, pp. 7970–7979, 2008.
- [141] J. Robie and D. White, “Lipid analysis in microbial ecology: Quantitative approaches to the study of microbial communities,” 1989.
- [142] L. Ruess, M. M. Häggblom, E. J. G. Zapata, and J. Dighton, “Fatty acids of fungi and nematodes—possible biomarkers in the soil food chain?” *Soil Biology and Biochemistry*, vol. 34, no. 6, pp. 745–756, 2002.
- [143] P. W. Rundel, M. O. Dillon, B. Palma, H. Mooney, S. Gulmon, and J. Ehleringer, “The phytogeography and ecology of the coastal atacama and peruvian deserts,” *Aliso: A Journal of Systematic and Evolutionary Botany*, vol. 13, no. 1, pp. 1–49, 1991.
- [144] L. Saavedra, J. Svensson, V. Carballo, D. Izmendi, B. Welin, and S. Vidal, “A dehydrin gene in *Physcomitrella patens* is required for salt and osmotic stress tolerance,” *The Plant Journal*, vol. 45, no. 2, pp. 237–249, 2006.
- [145] K. Sakamoto, T. Iijima, and R. Higuchi, “Use of specific phospholipid fatty acids for identifying and quantifying the external hyphae of the arbuscular mycorrhizal fungus *Gigaspora rosea*,” *Soil Biology and Biochemistry*, vol. 36, no. 11, pp. 1827–1834, 2004.
- [146] K. H. Schleifer and O. Kandler, “Peptidoglycan types of bacterial cell walls and their taxonomic implications,” *Bacteriological reviews*, vol. 36, no. 4, p. 407, 1972.
- [147] W. H. Schlesinger, *Biogeochemistry*. Gulf Professional Publishing, 2005, vol. 8.
- [148] S. Schouten, E. C. Hopmans, and J. S. S. Damsté, “The organic geochemistry of glycerol dialkyl glycerol tetraether lipids: A review,” *Organic geochemistry*, vol. 54, pp. 19–61, 2013.

- [149] M. H. Schweitzer, "Molecular paleontology: Some current advances and problems," in *Annales de paléontologie*, Elsevier, vol. 90, 2004, pp. 81–102.
- [150] B. Shirkey, D. P. Kovarcik, D. J. Wright, G. Wilmoth, T. F. Prickett, R. F. Helm, E. M. Gregory, and M. Potts, "Active fe-containing superoxide dismutase and abundant sodf mrna in nostoc commune (cyanobacteria) after years of desiccation," *Journal of bacteriology*, vol. 182, no. 1, pp. 189–197, 2000.
- [151] E. L. Shock and M. E. Holland, "Quantitative habitability," *Astrobiology*, vol. 7, no. 6, pp. 839–851, 2007.
- [152] K. L. Shuttleworth and E Cerniglia, "Environmental aspects of pah biodegradation," *Applied biochemistry and biotechnology*, vol. 54, no. 1, pp. 291–302, 1995.
- [153] B. R. Simoneit, R. Summons, and L. Jahnke, "Biomarkers as tracers for life on early earth and mars," *Origins of Life and Evolution of Biospheres*, vol. 28, no. 4, pp. 475–483, 1998.
- [154] A. M. Skelley, A. D. Aubrey, P. A. Willis, X. Amashukeli, P. Ehrenfreund, J. L. Bada, F. J. Grunthaner, and R. A. Mathies, "Organic amine biomarker detection in the yungay region of the atacama desert with the urey instrument," *Journal of Geophysical Research: Biogeosciences*, vol. 112, no. G4, 2007.
- [155] A. M. Skelley, J. R. Scherer, A. D. Aubrey, W. H. Grover, R. H. Ivester, P. Ehrenfreund, F. J. Grunthaner, J. L. Bada, and R. A. Mathies, "Development and evaluation of a microdevice for amino acid biomarker detection and analysis on mars," *Proceedings of the National Academy of Sciences of the United States of America*, vol. 102, no. 4, pp. 1041–1046, 2005.
- [156] B. Skopintsev, "Decomposition of organic matter of plankton, humification and hydrolysis," *Elsevier Oceanography Series*, vol. 31, pp. 125–177, 1981.
- [157] P. H. Smith, "The phoenix mission to mars," in *Aerospace Conference, 2004. Proceedings. 2004 IEEE*, IEEE, vol. 1, 2004.
- [158] P. Sobron, J. L. Bishop, D. F. Blake, B. Chen, and F. Rull, "Natural fe-bearing oxides and sulfates from the rio tinto mars analog site: Critical assessment of vnir reflectance spectroscopy, laser raman spectroscopy, and xrd as mineral identification tools," *American Mineralogist*, vol. 99, no. 7, pp. 1199–1205, 2014.
- [159] J Spence and C. Georgopoulos, "Purification and properties of the escherichia coli heat shock protein, htpg.," *Journal of Biological Chemistry*, vol. 264, no. 8, pp. 4398–4403, 1989.

- [160] F. Stevenson, "Organic forms of soil nitrogen," *Nitrogen in agricultural soils*, no. nitrogeninagrics, pp. 67–122, 1982.
- [161] R. Summons, A. Sessions, A. Allwood, H. Barton, D. Beaty, B. Blakkolb, J. Canham, B. Clark, J. Dworkin, Y. Lin, *et al.*, *Planning considerations related to the organic contamination of martian samples and implications for the mars 2020 rover*, 2014.
- [162] R. E. Summons, P. Albrecht, G. McDonald, and J. M. Moldowan, "Molecular biosignatures," *Space Science Reviews*, vol. 135, no. 1-4, pp. 133–159, 2008.
- [163] R. E. Summons, J. P. Amend, D. Bish, R. Buick, G. D. Cody, D. J. Des Marais, G. Dromart, J. L. Eigenbrode, A. H. Knoll, and D. Y. Sumner, *Preservation of martian organic and environmental records: Final report of the mars biosignature working group*, 2011.
- [164] R. E. Summons and S. A. Lincoln, "Biomarkers: Informative molecules for studies in geobiology," *Fundamentals of Geobiology*, pp. 269–296, 2012.
- [165] M.-Y. Sun, S. G. Wakeham, and C. Lee, "Rates and mechanisms of fatty acid degradation in oxic and anoxic coastal marine sediments of long island sound, new york, usa," *Geochimica et Cosmochimica Acta*, vol. 61, no. 2, pp. 341–355, 1997.
- [166] B. Sutter, J. Dalton, S. Ewing, R. Amundson, and C. McKay, "Terrestrial analogs for interpretation of infrared spectra from the martian surface and sub-surface: Sulfate, nitrate, carbonate, and phyllosilicate-bearing atacama desert soils," *Journal of Geophysical Research: Biogeosciences*, vol. 112, no. G4, 2007.
- [167] N. Vagenas, A. Gatsouli, and C. Kontoyannis, "Quantitative analysis of synthetic calcium carbonate polymorphs using ft-ir spectroscopy," *Talanta*, vol. 59, no. 4, pp. 831–836, 2003.
- [168] N. Vagenas and C. Kontoyannis, "A methodology for quantitative determination of minor components in minerals based on ft-raman spectroscopy: The case of calcite in dolomitic marble," *Vibrational spectroscopy*, vol. 32, no. 2, pp. 261–264, 2003.
- [169] J. Van Veen and P. Kuikman, "Soil structural aspects of decomposition of organic matter by micro-organisms," *Biogeochemistry*, vol. 11, no. 3, pp. 213–233, 1990.
- [170] J. K. Volkman, "Lipid markers for marine organic matter," in *Marine organic matter: Biomarkers, isotopes and DNA*, Springer, 2006, pp. 27–70.

- [171] J. K. Volkman, S. M. Barrett, S. I. Blackburn, M. P. Mansour, E. L. Sikes, and F. Gelin, "Microalgal biomarkers: A review of recent research developments," *Organic Geochemistry*, vol. 29, no. 5, pp. 1163–1179, 1998.
- [172] S. G. Wakeham, "Monocarboxylic, dicarboxylic and hydroxy acids released by sequential treatments of suspended particles and sediments of the black sea," *Organic Geochemistry*, vol. 30, no. 9, pp. 1059–1074, 1999.
- [173] F. Wang, G. Michalski, J.-H. Seo, D. E. Granger, N. Lifton, and M. Caffee, "Beryllium-10 concentrations in the hyper-arid soils in the atacama desert, chile: Implications for arid soil formation rates and el niño driven changes in pliocene precipitation," *Geochimica et Cosmochimica Acta*, vol. 160, pp. 227–242, 2015.
- [174] K. A. Warren-Rhodes, K. L. Rhodes, S. B. Pointing, S. A. Ewing, D. C. Lacap, B. Gómez-Silva, R. Amundson, E. I. Friedmann, and C. P. McKay, "Hypolith cyanobacteria, dry limit of photosynthesis, and microbial ecology in the hyperarid atacama desert," *Microbial Ecology*, vol. 52, no. 3, pp. 389–398, 2006.
- [175] J. W. Weijers, S. Schouten, E. C. Hopmans, J. A. Geenevasen, O. R. David, J. M. Coleman, R. D. Pancost, and J. S. Sinninghe Damsté, "Membrane lipids of mesophilic anaerobic bacteria thriving in peats have typical archaeal traits," *Environmental Microbiology*, vol. 8, no. 4, pp. 648–657, 2006.
- [176] P. V. Welander, M. L. Coleman, A. L. Sessions, R. E. Summons, and D. K. Newman, "Identification of a methylase required for 2-methylhopanoid production and implications for the interpretation of sedimentary hopanes," *Proceedings of the National Academy of Sciences*, vol. 107, no. 19, pp. 8537–8542, 2010.
- [177] D. C. White, P. Meadows, G. Eglinton, and M. Coleman, "In situ measurement of microbial biomass, community structure and nutritional status [and discussion]," *Philosophical Transactions of the Royal Society of London A: Mathematical, Physical and Engineering Sciences*, vol. 344, no. 1670, pp. 59–67, 1993.
- [178] J. Wierzchos, B. Cámara, A. de Los Ríos, A. Davila, I. Sánchez Almazo, O. Artieda, K. Wierzchos, B. GÓMEZ-SILVA, C. McKay, and C. Ascaso, "Microbial colonization of ca-sulfate crusts in the hyperarid core of the atacama desert: Implications for the search for life on mars," *Geobiology*, vol. 9, no. 1, pp. 44–60, 2011.
- [179] J. Wierzchos, A. de los Ríos, and C. Ascaso, "Microorganisms in desert rocks: The edge of life on earth," *International microbiology*, vol. 15, no. 4, pp. 172–182, 2013.

- [180] M. B. Wilhelm, A. F. Davila, J. L. Eigenbrode, M. N. Parenteau, L. L. Jahnke, X.-L. Liu, R. E. Summons, J. J. Wray, B. N. Stamos, S. S. O'Reilly, *et al.*, "Xeropreservation of functionalized lipid biomarkers in hyperarid soils in the atacama desert," *Organic Geochemistry*, vol. 103, pp. 97–104, 2017.
- [181] A. J. Williams, D. Y. Sumner, C. N. Alpers, S. Karunatilake, and B. A. Hofmann, "Preserved filamentous microbial biosignatures in the brick flat gossan, iron mountain, california," *Astrobiology*, vol. 15, no. 8, pp. 637–668, 2015.
- [182] A. Wilson, C. Boulay, A. Wilde, C. A. Kerfeld, and D. Kirilovsky, "Light-induced energy dissipation in iron-starved cyanobacteria: Roles of ocp and isia proteins," *The Plant Cell*, vol. 19, no. 2, pp. 656–672, 2007.
- [183] C. A. Wright and G. A. Beattie, "Pseudomonas syringae pv. tomato cells encounter inhibitory levels of water stress during the hypersensitive response of arabidopsis thaliana," *Proceedings of the National Academy of Sciences of the United States of America*, vol. 101, no. 9, pp. 3269–3274, 2004.
- [184] W Xie and W.-P. Pan, "Thermal characterization of materials using evolved gas analysis," *Journal of Thermal Analysis and Calorimetry*, vol. 65, no. 3, pp. 669–685, 2001.
- [185] K. Yamamoto, A. Shibahara, T. Nakayama, and G. Kajimoto, "Determination of double-bond positions in methylene-interrupted dienoic fatty acids by gc-ms as their dimethyl disulfide adducts," *Chemistry and Physics of Lipids*, vol. 60, no. 1, pp. 39–50, 1991.
- [186] Y.-M. Zhang and C. O. Rock, "Membrane lipid homeostasis in bacteria," *Nature Reviews Microbiology*, vol. 6, no. 3, pp. 222–233, 2008.

VITA

Mary Beth Wilhelm was born May 30, 1990 outside of Chicago, Illinois, but moved to Fremont, California in Silicon Valley during the dot-com boom in the late 1990s. As a child, she loved space and astronomy; her first grade science fair project was about the geology of Earth and Mars. When she grew older, her parents sent her to astronomy and space camps in the area. She then attended Saint Francis High School in Mountain View, learning everything she could about science, writing, and music. She began working as an intern at the nearby NASA Ames Research Center at age 16, studying gullies on Mars and analyzing data collected by the Spitzer Space Telescope with the most incredible mentors.

Drawn to the writings of Carl Sagan, Cornell University seemed like an obvious choice for undergraduate education. There she studied geological and planetary sciences (with a minor in dance). She participated in research projects from a variety of fields including astronomy, geology, and astrobiology. She worked on Cornell's Violet Satellite Project as the Science Team lead, made infrared astronomical observations of young solar systems using data she helped collect at Palomar Observatory, assisted in metamorphic petrological studies of mountains in New Mexico, lead three field trips to a Mars research station in the Utah Desert with other undergraduate students in science and engineering, and wrote an undergraduate thesis in astrobiology focused on the microbial community of a modern stromatolite. Summers were spent doing more research at NASA Ames and Johnson Space Center and field work in the Mojave Desert and Pavilion Lake in Canada. She was hired as a NASA Civil Servant through the Pathways program at age 19.

In 2012, she moved to Atlanta, Georgia for graduate studies at the Georgia Institute of Technology, spending time at multiple laboratories to accomplish her research

goals at NASA Goddard Space Flight Center, MIT, the Center for Astrobiology in Madrid, and NASA Ames. She was lucky enough to do field work in both the Atacama Desert, Chile, and Lake Untersee, Antarctica. In one five-month time period, she traveled to five continents. After completing her Ph.D., Mary Beth plans to continue her astrobiological research at NASA Ames Research Center as a Civil Servant in the Space Science and Astrobiology Division.